



# Guidelines for visualization and analysis of DC in tissues using multiparameter fluorescence microscopy imaging methods

*Felix Bayerl<sup>1</sup>, David A. Bejarano<sup>2</sup>, Giulia Bertacchi<sup>3</sup>, Anne-Claire Doffin<sup>4</sup>, Elisa Gobbini<sup>4</sup>, Margaux Hubert<sup>4</sup>, Lijian Li<sup>5,6,7</sup>, Philippa Meiser<sup>1</sup>, Anna-Marie Pedde<sup>1</sup>, Wilfried Posch<sup>3</sup>, Luise Rupp<sup>8</sup>, Andreas Schlitzer<sup>#2</sup>, Marc Schmitz<sup>#8,9,10</sup>, Barbara U. Schraml<sup>11,12</sup> , Stefan Uderhardt<sup>#5,6,7</sup>, Jenny Valladeau-Guilemond<sup>#4</sup>, Doris Wilflingseder<sup>#3</sup>, Viktoria Zaderer<sup>3</sup> and Jan P. Böttcher<sup>#1</sup> *

<sup>1</sup> Institute of Molecular Immunology, School of Medicine, Klinikum Rechts der Isar, Technical University of Munich (TUM), Ismaninger Str. 22, Munich, Germany

<sup>2</sup> Quantitative Systems Biology, Life and Medical Sciences (LIMES) Institute, University of Bonn, Germany

<sup>3</sup> Institute of Hygiene and Medical Microbiology, Medical University of Innsbruck, Innsbruck, Austria

<sup>4</sup> Cancer Research Center Lyon, UMR INSERM 1052 CNRS 5286, Centre Léon Bérard, 28 rue Laennec, Lyon, France

<sup>5</sup> Department of Internal Medicine 3 – Rheumatology and Immunology, Friedrich-Alexander University Erlangen-Nürnberg (FAU) and Universitätsklinikum Erlangen, Erlangen, Germany

<sup>6</sup> Deutsches Zentrum für Immuntherapie (DZI), Friedrich-Alexander University Erlangen-Nürnberg (FAU) and Universitätsklinikum Erlangen, Erlangen, Germany

<sup>7</sup> Exploratory Research Unit, Optical Imaging Centre Erlangen (OICE), Friedrich-Alexander University Erlangen-Nürnberg (FAU), Erlangen, Germany

<sup>8</sup> Institute of Immunology, Faculty of Medicine Carl Gustav Carus, TU Dresden, Dresden, Germany

<sup>9</sup> National Center for Tumor Diseases (NCT), Partner Site Dresden, Dresden, Germany

<sup>10</sup> German Cancer Consortium (DKTK), Partner Site Dresden, and German Cancer Research Center (DKFZ), Heidelberg, Germany

<sup>11</sup> Walter-Brendel-Centre of Experimental Medicine, University Hospital, LMU Munich, Planegg-Martinsried, Germany

<sup>12</sup> Biomedical Center, Institute for Cardiovascular Physiology and Pathophysiology, Faculty of Medicine, LMU Munich, Planegg-Martinsried, Germany

## Abstract

This article is part of the Dendritic Cell Guidelines article series, which provides a collection of state-of-the-art protocols for the preparation, phenotype analysis by flow cytometry, generation, fluorescence microscopy, and functional characterization of mouse and human dendritic cells (DC) from lymphoid organs and various non-lymphoid tissues. Here, we provide detailed procedures for a variety of multiparameter fluorescence microscopy imaging methods to explore the spatial organization of DC in tissues and to dissect how DC migrate, communicate, and mediate their multiple functional roles in immunity in a variety of tissue settings. The protocols presented here entail approaches to study DC dynamics and T cell cross-talk by intravital microscopy, large-scale visualization, identification, and quantitative analysis of DC subsets and their functions by multiparameter fluorescence microscopy of fixed tissue sections, and an approach to study DC interactions with tissue cells in a 3D cell culture model. While all protocols were

**Correspondence:** Jan P. Böttcher  
e-mail: j.boettcher@tum.de

<sup>#</sup>Section lead authors

written by experienced scientists who routinely use them in their work, this article was also peer-reviewed by leading experts and approved by all co-authors, making it an essential resource for basic and clinical DC immunologists.

## Contents

<b>Advantages of microscopy-based approaches for studying DC</b>	4
<b>1 Intravital imaging of DC-T cell interactions in mouse peripheral lymph nodes</b>	4
1.1 Introduction	4
1.2 Materials	5
1.2.1 Reagents	5
1.2.2 Animals	5
1.2.3 Equipment	5
1.2.4 Software	6
1.3 Step-by-step sample preparation	6
1.3.1 Isolation and transfer of DC from spleen	6
1.3.2 Isolation and transfer of TCR transgenic and wildtype T cells from lymph nodes	7
1.3.3 Cell staining protocol	7
1.3.4 Genetically encoded reporter mouse systems	7
1.3.5 Preparation of mouse popliteal lymph node for intravital imaging	7
1.4 Data analysis	9
1.5 Top tricks and pitfalls	9
<b>2 Visualization and identification of DC subsets in mouse tissues using Co-Detection by Indexing (CODEX)</b>	10
2.1 Introduction	10
2.2 Materials	11
2.2.1 Reagents	11
2.2.2 Equipment	11
2.2.3 Software	11
2.3 Step-by-step sample preparation	11
2.3.1 Organ preparation for CODEX multiplexed tissue staining	11
2.3.2 Preparation of cryosections for CODEX	14
2.3.3 CODEX staining of mouse fresh frozen sections	14
2.3.4 Remarks on antibody barcoding	15
2.3.5 CODEX imaging	16
2.4 Data processing and analysis	16
2.4.1 Data processing	16
2.4.2 Data analysis	17
<b>3 Detection of human DC subsets by multispectral imaging</b>	18
3.1 Introduction	18
3.2 Materials	20
3.2.1 Reagents	20
3.2.2 Equipment and software	21
3.3 Step-by-step sample preparation	21
3.3.1 Manual staining of a 7-color human DC subset panel	21
3.3.2 Automated staining of a 7-color human DC subset panel on a Ventana Discovery Ultra	21
3.3.3 Control slides for spectral library	22
3.4 Data analysis	22
3.5 Pitfalls	23
3.6 Top tricks	23
<b>4 Quantitative analysis and visualization of cDC1 in three-dimensional tissue volumes by high-resolution confocal microscopy</b>	24
4.1 Introduction	24
4.2 Materials	24
4.2.1 Reagents	24

4.2.2	Equipment	25
4.2.3	Software	25
4.3	<b>Step-by-step sample preparation</b>	25
4.3.1	Tissue preparation	25
4.3.2	Preparation of cryosections from mouse organs	26
4.3.3	Immunofluorescence staining of mouse cryosections	27
4.3.4	Preparation of vibratome sections of mouse tissues	27
4.3.5	Immunofluorescence staining of vibratome sections of mouse tissues	28
4.3.6	Visualization of cDC1 in mouse samples by immunofluorescence	28
4.3.7	Identification of cDC1 in human tissues	30
4.3.8	General remarks on confocal imaging of cDC1	30
4.3.9	Image processing	31
4.4	<b>Image data analysis</b>	32
4.4.1	Quantification of cell–cell interactions	32
4.4.2	Histocytometry population analysis	32
5	<b>Immunofluorescence microscopy of cDC1 in human tissues by coupling <i>in situ</i> hybridization with antibody staining</b>	33
5.1	<b>Introduction</b>	33
5.2	<b>Materials</b>	33
5.2.1	Reagents	33
5.2.2	Equipment	33
5.2.3	Software	33
5.3	<b>Step-by-step sample preparation</b>	33
5.3.1	Preparation of FFPE tumor section	33
5.3.2	Manual staining for <i>IFN<math>\lambda</math>-1</i> or <i>CD8A</i> and <i>CLEC9A</i> RNAscope staining followed by Cytokeratin immunofluorescent staining	34
5.3.3	Automated slide staining	36
5.4	<b>Data analysis</b>	38
6	<b>Quantitative image analysis of host–pathogen interactions in an <i>in vitro</i> 3D human lung/DC model</b>	38
6.1	<b>Introduction</b>	38
6.2	<b>Materials</b>	38
6.2.1	Reagents	38
6.2.2	Equipment	38
6.2.3	Software	40
6.3	<b>Step-by-step sample preparation</b>	40
6.3.1	Epithelial/DC co-cultures for immunofluorescence stainings	40
6.3.2	Isolation of monocytes and MoDC differentiation or optionally: Preparation of DC directly from human blood	42
6.3.3	Epithelial/DC co-cultures	42
6.3.4	Immunofluorescence (IF) staining of Epithelial/DC co-cultures and pathogens	43
6.3.5	Imaging of host-pathogen interactions using the Operetta CLS <sup>TM</sup>	43
6.4	<b>Combined Image and Data analysis using the Harmony software</b>	45
6.4.1	Discrimination of cells within co-cultures	47
6.4.2	Live/Dead cell analysis	47
6.4.3	XYZ- and 3D view of pathogen-DC interactions	47
6.4.4	Top tricks and pitfalls	48
6.4.5	Spot Analysis	48
6.4.6	Migration Analysis (RMS, Harmony software) of DC	49
	<b>Acknowledgements</b>	49
	<b>Conflict of interest</b>	49
	<b>Author contributions</b>	49
	<b>Data availability statement</b>	50
	<b>References</b>	50
	<b>Abbreviations</b>	52

## Advantages of microscopy-based approaches for studying DC

Microscopic imaging approaches allow to study the localization and spatial organization of dendritic cells (DC) in tissues, which is key for many of their functions in immunosurveillance and the initiation and regulation of immune responses.

The spatial information and high resolution provided by these methods allow for detailed and quantitative analysis of DC and their functions, and can be used to explore their spatial relationships with other cell types. Furthermore, intravital microscopic imaging allows to dynamically visualize and study fundamental aspects of DC behavior in real time.

An additional feature common to these different approaches is that they are performed without the need for cell isolation. DC form strong adhesive interactions with other cells and tissue elements and are difficult to extract from tissues, which can result in their erroneous quantification by isolation-based methods, such as flow cytometry and single-cell RNA sequencing. Cell isolation can further bias towards less adhesive DC states, posing the risk of inaccurate assessment of the functional composition of DC populations. These disadvantages do not apply to most microscopy-based analysis methods, which can therefore provide more accurate information about the actual abundance and cellular composition of DC in tissues.

## 1 Intravital imaging of DC-T cell interactions in mouse peripheral lymph nodes

### 1.1 Introduction

Intravital imaging allows us to capture the fascinating dynamics of the immune system. For a successful adaptive immune response, antigen-presenting DC and antigen-recognizing T cells must come together in a highly orchestrated and orderly fashion. This occurs in the peripheral lymph nodes, which provide the stage and setting for this assembly. DC, in particular the cells belonging to the cDC lineage (Box 1), take up and process antigens in peripheral tissues, mature, and migrate via the lymphatic vessels to the draining lymph nodes [1–4]. T cells circulate through the body, and enter lymphoid tissues via high-endothelial venules. Here, they must scan a large number of DC in search of their specific antigen in a short period of time before they undergo apoptosis. Once a naive T cell encounters its cognate antigen presented on a DC, this leads to a migration arrest and eventually to the formation of a stable immunological synapse. The initial scanning phase therefore represents a highly dynamic process that alternates between exploratory migration and sustained cell-cell interactions [5]. This process takes place deep in the parafollicular zone of the respective lymph node, which is not accessible to conventional microscopy. Here, 2-photon microscopy is used to penetrate deep into the tissue and visualize, record, and finally quantify such dynamic immune processes in an intact environ-

### Box 1. Imaging-based identification of DC subsets

DC are innate immune cells that act as sentinel leukocytes and fulfill essential roles in the initiation and regulation of immune responses. While some phenotypic and functional attributes are shared by the cells within the DC family, DC display substantial heterogeneity and can be parsed into different subsets. These subsets can be discriminated based on their ontogeny as well as their distinct gene expression profiles [1, 2], which together with external signals are key determinants of the functional capacities of an individual DC before and after its activation [3]. Therefore, the use of phenotypic markers in imaging experiments can help to determine DC subset affiliation and in part infer on functional specialization.

Of note, DC subset identity should not be confused with actual function, which needs to be addressed in additional experiments. Furthermore, many characteristic markers are shared among subsets and can further be expressed by some DC progenitors. Marker expression also varies drastically depending on the context, and can differ in specific organs, tumors, or inflammatory environments. The subset-specific expression of markers therefore needs to be carefully evaluated for individual experiments, e.g. by determining marker specificity by other methods such as flow cytometry and the loss of staining in models with subset-specific depletion [4].

Below, we provide a short summary on phenotypic markers currently used to identify the major subsets of cDC and other myeloid cells within the wider DC family. While in our protocols we mainly focus on the analysis of cDC and in particular cDC1, these protocols may be adapted to the analysis of other DC subsets, e.g. by incorporating an appropriate choice of the markers listed below. Within the individual sections, we further discuss additional markers and reporter models that allow a more detailed characterization and functional analyses of DC, where appropriate.

**cDC:** classical or conventional DC that are ontogenically distinct from other antigen-presenting cells (APC). cDC have a major role in the initiation of de novo T cell responses by presenting antigens to naive T cells in secondary lymphoid tissues ('T cell priming') and further regulate T cell proliferation and effector function. cDC express high levels of CD11c and MHCII in lymphoid and peripheral organs, however these markers are shared with many other cells within the DC family, especially under inflammatory conditions. cDC can further be identified by expression of CD24, CD26, and the transcription factor ZBTB46. cDC are further categorized in two distinct subsets, cDC type 1 (cDC1) and cDC type 2 (cDC2).

**cDC1:** are key for the regulation of cytotoxic CD8<sup>+</sup> T cell responses. cDC1 excel at the uptake of dead cell-associated

antigens and cross-presentation of acquired antigens on MHC class I molecules. In both mice and humans, all cDC1 express the chemokine receptor XCR1 and the C-type lectin receptor CLEC9A. cDC1 in lymphoid organs further express CD8 $\alpha$  while cDC1 in peripheral organs instead express the integrin  $\alpha$ E (CD103) in mice.

**cDC2:** can be distinguished from cDC1 by the absence of typical cDC1 markers such as XCR1 and CLEC9A expression and the preferential expression of CD11b and CD172a/Sirp1 $\alpha$  and in humans CD1c/BDCA-1 and CLEC10A. Of note, cDC2 are more heterogenous than cDC1 and can be further subdivided into different subsets, e.g. based on differential expression of the transcription factors T-bet and ROR $\gamma$ t that can be used to distinguish between cDC2A and cDC2B. Especially in humans, we are still lacking a general consensus on the reliable identification and classification of cDC2.

**Plasmacytoid DC (pDC):** characterized by the ability to produce type I interferons. Sometimes referred to as ‘plasmacytoid cells’ given their lymphoid origin and distinction from cDC. pDC commonly express low levels of MHCII, which is often used to discriminate these cells from cDC. Typical markers used to identify pDC are Siglec-H in mice and the IL-3 receptor  $\alpha$ /CD123 and CLEC4C/BDCA-2 in humans.

**Monocyte-derived DC (MoDC):** can act as APC and share some phenotypic markers with cDC such as CD11c and MHCII. In some tissues such as the spleen, CD64/FCGR1 can discriminate MoDC from cDC, however CD64 can also be expressed by cDC in some tissues such as kidney and lung and is upregulated on cDC by type I IFN signaling. Other markers used to discriminate MoDC from cDC are CD88, MERTK and CD14, which are shared with macrophages.

**Langerhans cells (LC):** APC found in the skin and skin-draining lymph nodes. LC have recently been re-classified as macrophages given their distinct gene expression profile and distinct development from fetal liver monocytes. LC express high levels of CD207/Langerin and CD172a/Sirp1 $\alpha$  as well as in humans CD1a.

ment at the single-cell level [6]. Different phases of cell-cell interactions between DC and T cells have been described [7]. Here, we describe a general intravital imaging protocol to study early, antigen-specific interactions between naive T cells and antigen-presenting DC using the transgenic CD4-TCR mouse strain 5C.C7 [8]. This protocol can easily be adapted to use different CD4-TCR system such as OT-II (CD4-TCR directed against OVA peptide 323–339 [9]) or SMARTA mice (CD4-TCR directed against LCMV glycoprotein 61–80 [10]) with their respective cognate antigen peptides. Of note, the basic surgical and experimental setup described in this section can be used not only for acute

Table 1. Reagents

Reagent	Cat. number	Supplier
Magnetic cell sorting kit for dendritic cells	130-125-835	Miltenyi Biotec
Magnetic cell sorting kit for naive T cells	130-104-453	
Hank's buffered saline (HBSS)	H4385	Sigma Aldrich
Phosphate buffered saline	10010023	Thermo Fisher
Pigeon cytochrome C peptide (sequence KAERADLIAYLKQATAK)	N.A.	CPC Scientific
Liberase DL	5401160001	Sigma Aldrich
RPMI-1640 Medium	R6504	Sigma Aldrich
Penicillin-Streptomycin	P4333	
L-Glutamine	G7513	
Fetal bovine serum	F7524	
Lipopolysaccharid from Escherichia coli O111:B4	L2630	Sigma Aldrich
CellTracker™ Blue CMAC Dye	C2110	Thermo Fisher
CellTracker™ Green CMFDA Dye	C2925	
CellTracker™ Red CMTPX Dye	C34552	

Table 2. Mice

Genotype	Strain ID	Source
B10.A-Rag2tm1Fwa H2-T18a Tg (Tcra5CC7,Tcrb5CC7) lwep	4094	Taconic
B10.A-H2a H2-T18a/SgSnJ	000469	The Jackson Laboratory

dynamic live imaging but also different down-stream application, including the specific in situ labeling of tissue compartments of interest using photo-activatable reporter systems (e.g., “NICHE-sequencing” [11, 12]).

1.2 Materials

1.2.1 Reagents

Necessary reagents are listed in Table 1.

1.2.2 Animals

Animal models referred to in this section are listed in Table 2.

1.2.3 Equipment

Necessary equipment is listed in Table 3.

**Table 3.** Equipment for animal anesthesia and imaging

Equipment	Model	Manufacturer
Laser-scanning microscope equipped with a motorized stage, a heating chamber, and external non-descanned detectors (NDDs)	LSM 710	Zeiss
Femtosecond-pulsed Ti:Sapphire two-photon laser	Chameleon	Coherent
Custom-made microscopy stage with manual 3-axis micromanipulator	M325	World Precision Instruments
Veterinary anesthesia vaporizer	VetFlo	Kent Scientific
Oxygen concentrator	Oxy Vet III	Eickemeyer

### 1.2.4 Software

Necessary software is listed in Table 4.

## 1.3 Step-by-step sample preparation

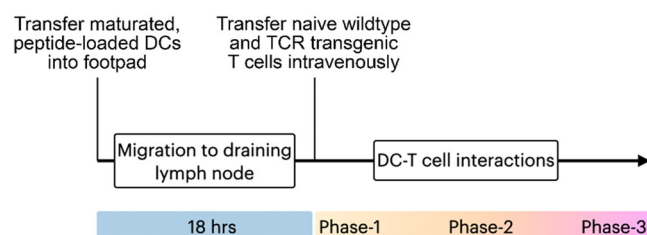
In order to bring together both antigen-presenting DC and naive T cells, successive steps of cell isolation and adoptive transfer via different pathways and at different time points are required (see Fig. 1). The different protocols for isolating both cell types, their different labeling, and intravital imaging to assess the interactions between DC and T cells in the footpad-draining lymph nodes are described in this section.

### 1.3.1 Isolation and transfer of DC from spleen

1. Prepare digestion buffer containing complete RPMI medium (+ FBS, Pen/Strep, L-Gln) + 0.4U/ml Liberase DL (ca. 1ml per spleen is needed).
2. Sacrifice wildtype B10.A mouse and remove the spleen under sterile conditions.

**Table 4.** Software for image analysis

Software	Version	Provider
ZEN black	3.0	Zeiss
Imaris	9.7.2	Oxford Instruments
ImageJ/Fiji	2.3.0	National Institutes of Health
Excel	16.52	Microsoft

**Figure 1.** Experimental outline.

3. Use a sterile syringe with a small needle (e.g., 27G) and inject plenty of digestion buffer directly into the spleen.
4. Incubate at 37°C for 30min.
5. Remove from the incubator and pass the digested spleen through a sterile 70 µm cell strainer using the back of a 5ml syringe plunger.
6. Pellet the cells by centrifugation (400 × g, 4°C, 5 min), remove supernatant, and resuspend in MACS buffer according to the manufacturer's specifications.
7. Perform positive isolation of splenic DC according to the manufacturer's instruction. Depending on the desired purity, magnetic separation may need to be repeated.
8. After cell sorting, resuspend the cells in complete RPMI and induce maturation, e.g., with LPS (100 ng/ml) for 4 h at 37°C. For direct loading of MHC II molecules activate DC in the presence of 1–10 µM pigeon cytochrome C peptide (pPCC). After incubation time, pellet the cells by centrifugation and wash once with PBS. Notably, efficient peptide-loading can be visualized as was shown before [13].
9. At this stage, DC may be treated with different activatory or inhibitory agents to test specific molecular mechanisms in vivo [13]. In this case, the differently treated cells need to be differentially labeled to be able to distinguish them later in vivo. While the range of cytoplasmic staining is limited, additional differential labeling can be achieved by feeding the cells Qdot nanocrystals [14]. Crucially, however, different treatment and thus different activation states may affect migration to the lymph node or intra-nodal distribution after adoptive transfer, and must be carefully controlled.
10. Continue with cell staining protocol (see below).
11. After staining is complete, resuspend the pellet in sterile HBSS for subsequent subcutaneous injection at a concentration of  $2 \times 10^6$  cells per 25–50 µl ( $40\text{--}80 \times 10^6/\text{ml}$ ). Anesthetize the animal using isoflurane (see below), sterilize the footpad using 70% ethanol, and carefully inject 25–50 µl of cell solution into the footpad. Be sure to inject slowly, otherwise the solution can easily spill.
12. You should be able to detect transferred 12–16 h later in the draining popliteal lymph node.

**Note:** In our hands, freshly isolated splenic DC perform best in the experiments described below. However, DC differentiated from bone marrow cells in vitro may constitute a useful



alternative, depending on the scientific question and experimental system.

### 1.3.2 Isolation and transfer of TCR transgenic and wildtype T cells from lymph nodes

13. Sacrifice mice (5C.C7 + B10.A wildtype mouse) and collect as many peripheral lymph nodes as possible under sterile conditions (i.e., popliteal, inguinal, axil, submandibular, etc.).
14. Prepare single-cell solutions separately by passing the lymph nodes through a sterile 70  $\mu$ m cell strainer using the back of a 5ml syringe plunger. Enzymatic tissue digestion is usually not required.
15. Pellet the cells by centrifugation ( $400 \times g$ ,  $4^{\circ}\text{C}$ , 5 min), remove the supernatant, and resuspend in MACS buffer according to the manufacturer's specifications.
16. Perform negative enrichments of naïve T cells according to the manufacturer's instruction. Depending on the desired purity, magnetic separation may need to be repeated.
17. After cell sorting, continue with cell staining protocols (see below).
18. After staining is complete, resuspend cells in sterile HBSS, combine both populations and inject  $2 \times 10^6$  cells in 100–200  $\mu$ l intravenously. Depending on the question and the respective phase of the cell interaction [7, 13], the first T cells can be found in the parafollicular zone already a few minutes after the transfer.

### 1.3.3 Cell staining protocol

19. Prepare working staining solution in HBSS without any serum supplements or contamination. Please refer to the manufacturer's instructions. Optimal working concentrations may vary and need to be established beforehand regarding staining efficiency and cell viability. In our hands, the following concentrations have proven successful [13]:
20. Cell Tracker Blue CTB at 100  $\mu$ M for DC;
21. CMFDA at 1.25  $\mu$ M for TCR transgenic T cells;
22. CMTPX at 1.25  $\mu$ M for wildtype T cells;
23. To stain suspended cells, pellet them first by centrifugation ( $400 \times g$ ,  $4^{\circ}\text{C}$ , 5 min) and wash once with HBSS. Resuspend cells at a concentration of  $1 \times 10^6$ /ml in staining solution and incubate for 30 min at  $37^{\circ}\text{C}$ .
24. Afterward, pellet cells, resuspend in serum-free medium, and incubate for another 30 min at  $37^{\circ}\text{C}$ .
25. Wash once with HBSS.

### 1.3.4 Genetically encoded reporter mouse systems

As an alternative to cell labeling by fluorescent dyes, genetically encoded reporter systems such as CD11c<sup>YFP</sup> [15] or Zbtb46<sup>GFP</sup>

[16] mice may be used to trace DC following transfer, or to study the dynamics of endogenous DC without prior isolation. One advantage of this would be to avoid any toxicity associated with cell isolation or staining. However, this complicates investigating DC with additional genetic modifications such as specific gene knockouts, which will require several rounds of breeding to acquire the desired mouse lines. Note that the excitation maxima of fluorescent proteins and dyes are often quite far apart on the spectrum, so that CMFDA, for example, is not excitable at the 2-photon wavelength optimal for GFP. In this case, the antigen or treatment and intervention must be delivered to the cells by other means, e.g., also via the lymphatic route by injection into the footpad. In contrast to recreating the migration of antigen-bearing DC from the periphery into the lymph node, such a setup would simulate the handling of soluble antigens that accumulate in the lymphatic system and are taken up by resident DC. Functional reporter systems maturation marker such as CD83<sup>GFP</sup> [17] may allow the tracking of cells in different maturation states, however its expression is not restricted to DC. To more specifically target, visualize and track DC, different Cre recombinase-based genetic models are available. These include CD11c<sup>Cre</sup> [18] and Zbtb46<sup>Cre</sup> mice [19] that can be used to broadly label all DC or cDC; Clec9a<sup>Cre</sup> [20], Xcr1<sup>Cre</sup> [21] or Karma<sup>Cre</sup> [22] to more specifically target the cDC1 subset; and CD207<sup>Cre</sup> for targeting LC [23] (see Box 1). By crossing with the appropriate floxed reporter mouse models (e.g., expressing CFP, YFP, GFP, or tdTomato), these Cre-driven lines provide further flexibility in designing appropriate chromatic arrangements for 2-photon imaging. However, it is important to mention that the penetrance of Cre in other cell types has been reported for most of these mouse strains, which needs to be carefully evaluated when using these models [24].

### 1.3.5 Preparation of mouse popliteal lymph node for intravital imaging

26. Anesthetize the mouse using isoflurane vaporized in an O<sub>2</sub>/air-mixture of 80:20 (ca. 4–5 % for induction) and ensure that a sufficient plane of anesthesia is achieved (ca. 1.2–1.5 % for maintenance).
27. Shave the leg of interest (the one into whose footpad the DC were transferred!) using a hair clipper and locally apply hair removal crème for 2–3 min. Be sure to remove the hairs as thoroughly as possible, as stray hairs in the field of view can seriously hamper the experiment.
28. For intravital imaging, researchers usually refer to custom-built microscopy stages that include immobilized clamps, retractors, and usually a 1- or multiple-axis micromanipulator to securely place a cover glass on top of the imaging situs. Here freely available models for 3D printing are helpful as well as model or computer-building supplies. Examples for microscopy stages can be found in the literature [24]. Strap the prepared leg into the holding device and start securing the proximal leg. To do this, make a small skin incision over the greater trochanter and secure it with an immobile clamp.

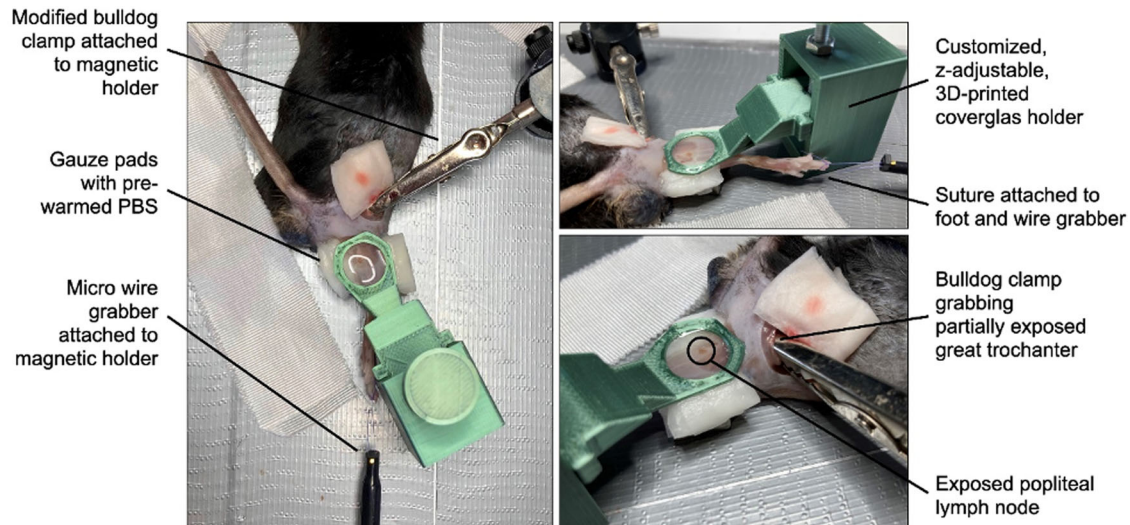


**Figure 2.** Surgical setup for in vivo imaging showing the exposed popliteal lymph node and all necessary holding devices.

This is important to absorb any respiratory movements that may destabilize the imaging. For this, we use small bulldog clamps. Bulldog clamps can be quite strong, which can be controlled by changing the built-in spring. Place a loose suture loop around the midfoot, gently tighten it carefully and stretch the leg so that it lies flat on the base plate (Fig. 2).

29. To expose the popliteal lymph node, make a small skin incision above the popliteal cavity. Be careful not to injure any vessels; if bleeding occurs, use a cautery to stop it. Carefully work your way proximally. The lymph node is hidden in a pocket of fat, often further proximally than you would expect. Look for an “egg-shaped” structure that appears slightly darker than the surrounding fat tissue (Fig. 3). Now, using fine forceps, carefully remove the fat around the lymph node without touching and damaging the lymph node. Be careful when removing the fat, as it is easy to damage the lymphatic network.
30. Place a circle of high vacuum fat around the exposed lymph node and place the preheated buffer over it. Now carefully place the cover glass attached to the micromanipulator and fix its position so that it lies flat on the lymph node. Be sure to avoid exerting pressure on the lymph node, as this impairs microcirculation and leads to tissue damage.

31. Transfer the animal safely into the pre-warmed imaging chamber while maintaining adequate anesthesia. After the transfer, it is recommended to let the animal and tissue rest for 5–10 min to avoid major shifts of the imaging field in lateral or axial directions.
32. Put pre-warmed distilled water on the coverslip, lower the objective and use the epifluorescence function in the “detection mode” of the ZEN software to focus on the lymph node under visual control. If green fluorescent cells have been transferred, you will probably be able to see them through the eyepiece, otherwise the vascularization of the lymph node will often stand out from the highly autofluorescent fat tissue.
33. When the lymph node is in focus, make sure the incubation chamber is closed and all lights are off. In the ZEN software, switch to “detection mode”, set the 2P laser to 930 nm and approx. 90 mW power at a zoom of 1.0, and switch on “live” mode. Use the second harmonic signal at a detection wavelength of approximately 450–460 nm to identify the lymph node capsule and the subcapsular sinus. To visualize the transferred cells, you need to go deeper into the lymph node to reach the parafollicular zone. Switch the wavelength of the 2P laser to 820 nm (to excite the cell stain).

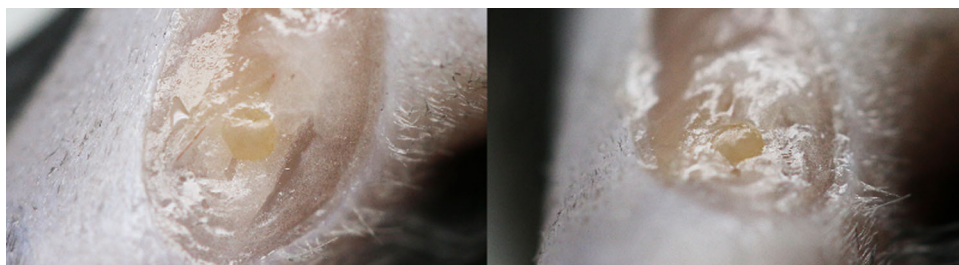


**Figure 3.** Exemplary images of surgically exposed popliteal lymph nodes.



34. Sweep through the tissue until you spot your transferred cells. Once a volume of interest has been identified, adjust the laser power and detector gain to clearly separate individual cells from the background. In general, use as much laser as necessary and as little as possible to avoid damaging the tissue.
35. Define the imaging volume by creating a z-stack by specifying the top and bottom layers. Define the size of the z-stack, we usually use between 3–5  $\mu\text{m}$ , depending on the image volume and the desired axial resolution. **Note:** Most acquisition systems allow automatic or manually programmed correction of the laser power in the Z-axis of the image stack (“Z-correction”). This can be very useful when capturing large and deep volumes, as different laser powers are often required for surface or deeper events and dynamic adjustment is necessary to avoid photodamage.
36. Next, define the frame rate and pixel dwell time by adjusting the acquisition speed and line averaging. A good starting point is a frame rate of about 950 ms with an image resolution of  $512 \times 512$  pixels and a 12-slice Z-stack. Note that the temporal resolution must allow tracking of individual cells from frame to frame: Too slow a sampling may cause the tracking algorithm to lose cells during processing, too fast a sampling may result in more background noise, affecting the segmentation process required for tracking. Recording imaging data for cell tracking in 8-bit is sufficient.
37. Once all parameters are defined, make sure the experiment is set up for time-lapse without pause between frames or stacks, then “Start experiment”.
38. The recording time depends on the research question but should be at least 1–2 h in order to collect sufficient tracking data. Drifting in X/Y or Z may require interrupting the recording to readjust the stack; if this is done quickly, the two resulting images can be combined (often seamlessly) later in post-processing. Note that the water evaporates between the lens and the cover glass, so plan short breaks in recording to refill. The lack of water is noticeable in that the image becomes darker and darker within a few frames until it disappears.
39. After the imaging experiment is finished, sacrifice the animal, and discard appropriately, and transfer the imaging data to the workstation computer for processing.
2. The spot function can then be used to identify individual cells within the imaging volume and track them across images (Fig. 4). To do this, start the “Create Spots” process in automatic mode within a region of interest or across the entire imaging volume, set a size estimate for your spots and use the histogram to define the intensity threshold for what the algorithm will or will not consider a potential event. After spot generation, the tracking algorithm attempts to link individual spots from one image to the next. To do this, set the distance a spot may travel between frames to still be considered a single entity; try the default parameters here first, and re-run both spot generation and spot tracking individually later if the results are not satisfactory.
3. Both spot generation and spot tracking can be inaccurate, in which case manual correction is required; to do this, individual tracks belonging to the same spots can be joined and defined as one. If a frame was omitted during spot generation, the tracks can also be joined by skipping one or two frames without significantly affecting the overall dynamic metrics.
4. The user can specify which parameters are to be calculated and subsequently exported. For example, total velocity or migration stop can be used as an indicator of specific cell-cell interactions, so does cell-cell interaction time. Displacement can be used to distinguish between directional and exploratory movements. Given the large number of parameters that IMARIS can track over time (currently > 80), looking at individual parameters may have limited explanatory value. Dimensionality reduction algorithms can be used here to identify different dynamic behavior patterns [25]. Wind rose plots (sometimes also called hairballs) are suitable for depicting individual migration paths.
5. Next to IMARIS, open-source software alternatives and interesting packages include:
  1. MtrackJ (<https://imagej.net/plugins/mtrackj>),
  2. cellmigRation (<https://github.com/ocbe-uio/cellmigRation/>),
  3. The Baxter Algorithms (<https://github.com/klasma/BaxterAlgorithms>),
  4. CellMigration (<https://github.com/quantixed/CellMigration>)
  5. TrackMate <https://imagej.net/plugins/trackmate>

## 1.4 Data analysis

1. In Imaris, individual subsequent stacks can be combined with the “Add time point” function. Possible homogeneous XYZ shifts can be corrected to a certain degree with the option “Drift correction”: For this purpose, an immobile point of interest must be defined (e.g., strong tissue autofluorescence), we usually use the “Spot” function of Imaris in manual mode to create individual reference spots with corresponding traces across all frames, and use the “Drift correction” mode in the corresponding spot properties.

## 1.5 Top tricks and pitfalls

1. Careful preparation of the lymph node is crucial. Any accidental and even unconscious damage can have a negative impact on the experiment. Special attention should be paid to this when initially learning the technique. It is recommended to practice the technique on a reporter mouse for myeloid cells, especially neutrophils, for example, a  $\text{LysM}^{\text{GFP}}$  mouse [26]. Here, even without visible bleeding, small tissue injuries quickly lead to an infiltration of inflammatory cells, which become visible as a prominent “green” signal in the lymph node parenchyma and in the area of the capsule.

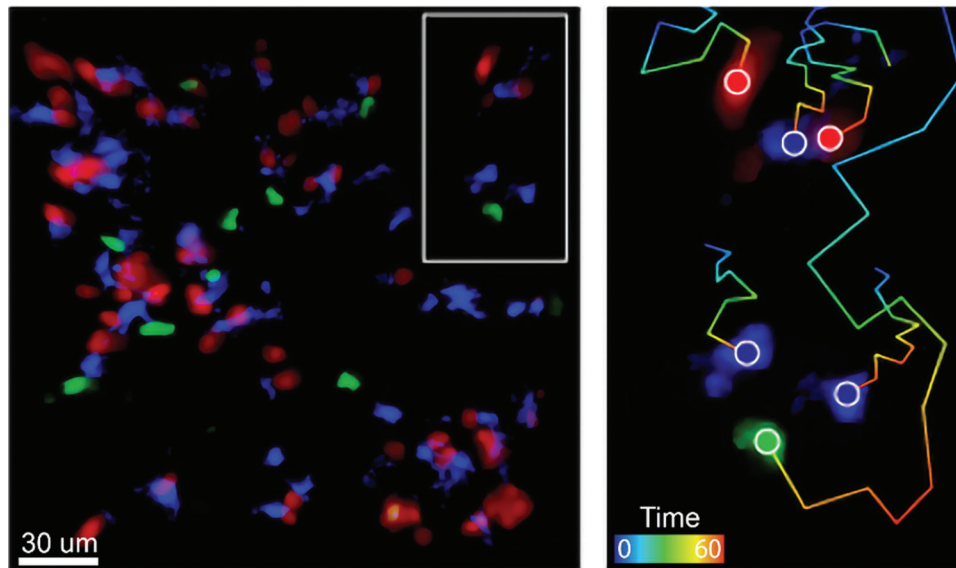


**Figure 4.** Visualization of antigen-specific DC/T cell interactions in vivo. Exemplary still image from an intravital imaging experiment showing antigen-loaded DC (blue; CTB), wildtype T cells (green; CMFDA), and TCR-transgenic T cells (red; CMTPIX). The insert shows example tracking results. Note the exploratory pathway of the wildtype T cell compared to the TCR-transgenic T cells, which stick close to the DC presenting their cognate antigen.

2. Different stages of interactions between T cells and DC have been described [27]. Depending on the scientific question different time points after adoptive transfer of T cells can be used to look at the different stages, e.g., 0–2h for “phase 1”, 12h for “phase 2” or 22h for “phase 3”. Further information on the different cellular dynamics that can be expected are reviewed in [27].
3. Maintaining a physiological environment is key to obtaining usable data. Here, the co-transfer of other stained naive T cells alongside the TCR-transgenic T cells has proven successful. These should - in contrast to the TCR-transgenic cells - not recognize any specific antigen on mature DC and therefore be constantly in an exploratory migration mode. The dynamic behavior and speed of these wild-type cells can be used to assess the overall validity of the experiment [28]: If naive wild-type T cells have an average experimental velocity of at least 8–10  $\mu\text{m}/\text{min}$  [13, 29, 30], this is a good indication that a general physiological milieu is prevalent.
4. To exclude negative effects of the respective cell staining, it is recommended to stain wild-type T cells and TCR transgenic cells with the respective other dye for control experiments.

## 2 Visualization and identification of DC subsets in mouse tissues using Co-Detection by Indexing (CODEX)

### 2.1 Introduction

A heterogeneous mixture of different DC populations and other mononuclear phagocytes (MP) such as monocytes and macrophages is usually present in every tissue. Among these cell

populations, cDC induce potent adaptive immune responses upon antigen encounter and migration to the draining lymph node but also execute tissue-specific immunomodulatory functions [3]. cDC are generally identified as  $\text{CD45}^+\text{CD26}^+\text{CD11c}^+\text{MHCII}^+$  cells and can be subclassified into at least two transcriptionally, developmental, phenotypically, and functionally different subsets, cDC1 and cDC2 (see Box 1). cDC subsets across different tissues display a high degree of phenotypic heterogeneity, which makes efficient identification of bona fide cDC difficult, especially under inflammatory conditions [31–34]. Thus, high-dimensional approaches are imperative for reliable identification of cDC and to better understand the multiple roles of these cells and other DC populations. Several aspects of the cellular microenvironment of DC has been elucidated by conventional fluorescent microscopy approaches. However, these approaches are usually limited to 4–6 colors, hindering i) a proper segregation of cDC subsets and other MP and ii) a broader analysis of the interaction of DC with other cells.

Co-Detection by Indexing (CODEX), a multiplexed tissue imaging technique, allows the visualization of more than 50 antibodies in complete tissue sections [35, 36]. To achieve this, primary antibodies conjugated to specific DNA barcodes are used to stain the sample in a single step. These are subsequently detected by the cyclic addition of small fluorescently labeled DNA oligos complementary to the barcodes of the primary antibodies. In contrast to other multiplexing approaches, the single staining step and the short detection/acquisition times employed by CODEX, lead to better sample preservation and lower autofluorescence.

Here, we describe the use of a CODEX antibody panel to visualize the major anatomical structures of several mouse tissues, identify DC populations, and distinguish them from macrophages and monocytes (Fig. 5). Additionally, an analysis pipeline to

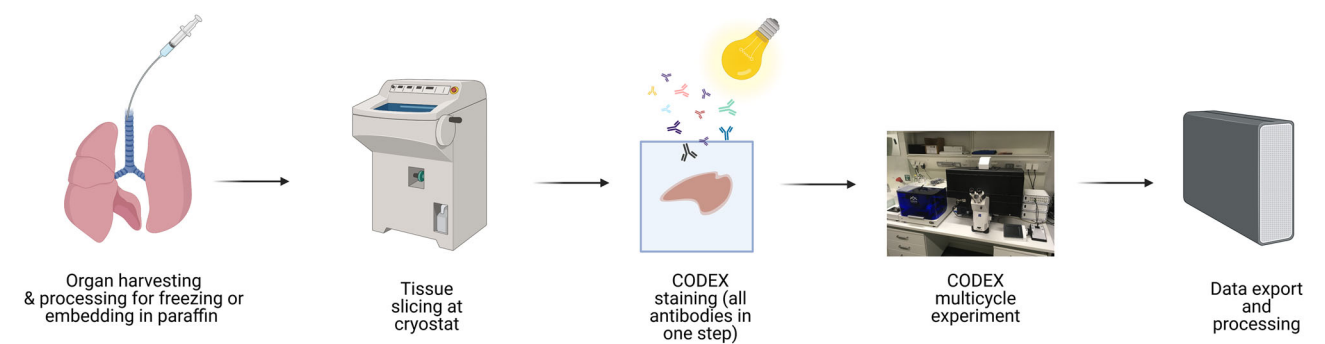


**Figure 5.** CODEX workflow. Organs extracted from euthanized mice are fixed under different conditions before freezing. Frozen sections are prepared and stained with a x-plex CODEX antibody panel in a single step. During staining, samples are photobleached. Antibody detection in tissue sections is performed in a multicycle experiment. After image acquisition, data is exported, processed, and analyzed. Figure created with BioRender.com.

**Table 5.** CODEX antibodies for visualizing DC populations

Antibody	Clone	Provider	Catalogue #	Dilution*
Anti-mouse CD45	30-F11	Biologend	103102	1:200
Anti-mouse CD26	H194-112	Biologend	137802	1:100
Anti-mouse I-A/I-E	M5/114.15.2	Biologend	107602	1:150-1:300
Anti-mouse CD11c	N418	Biologend	117302	1:100-1:200
Anti-mouse/human CD11b	M1/70	Biologend	101202	1:100-1:200
Anti-mouse CD172α	P84	Biologend	144002	1:200
Anti-mouse XCR1	ZET	Biologend	148202	1:50
anti-mouse CD301a	LOM-8.7	Biologend	145602	1:200
Anti-mouse CD301b	URA-1	Biologend	146802	1:50
Anti-mouse CD103	2E7	Thermo Fisher Scientific	14-1031-85	1:100
Anti-mouse F4/80	BM8	Thermo Fisher Scientific	14-4801-85	1:100-1:200
Anti-mouse CD64	X54-5/7.1	Biologend	139302	1:300
Anti-mouse Ly6C	HK1.4	Biologend	128002	1:300
Anti-mouse PDGFRα	APA5	Thermo Fisher Scientific	14-1401-82	1:200
Anti-mouse CD31	MEC13.3	Biologend	102502	1:100-1:200
Anti-mouse SMA	1A4	Biologend	904601	1:150
Anti-mouse EpCAM	F8.8	Biologend	118202	1:250
Anti-mouse CD90.2	30-H12	Biologend	105302	1:200
Anti-mouse/human Ki67	B56	BD Biosciences	550609	1:50-1:200

\* Antibody dilution depends on the efficiency of conjugation

identify cellular neighborhoods and cell–cell interactions is presented. This panel serves as the basis to further investigate DC function in multiple organs under homeostatic and inflammatory conditions.

2.2 Materials

2.2.1 Reagents

Necessary reagents are listed in Tables 5–9.

2.2.2 Equipment

Necessary equipment is listed in Table 10.

2.2.3 Software

Necessary software is listed in Table 11.

2.3 Step-by-step sample preparation

A schematic overview illustrating the key steps for the CODEX workflow described in this section is shown in Fig. 5.

2.3.1 Organ preparation for CODEX multiplexed tissue staining

2.3.1.1 Preparation of mouse lung.

- 1. Anesthetize and euthanize the mice by perfusion with 15 ml cold PBS.

**Table 6.** CODEX DNA barcodes

Barcode & reporter <sup>*</sup>	Fluorophore	Provider	Catalogue #	Conjugated antibody
BX001 – RX001	AF488	Akoya Biosciences	4150001	CD90.2
BX002 – RX002	Atto550	Akoya Biosciences	4250001	CD31
BX004 – RX004	AF488	Akoya Biosciences	5450014	PDGFR $\alpha$
BX006 – RX006	Cy5	Akoya Biosciences	5450027	F4/80
BX013 – RX013	AF488	Akoya Biosciences	5450017	EpCAM
BX014 – RX014	Atto550	Akoya Biosciences	4250003	I-A/I-E
BX016 – RX016	AF488	Akoya Biosciences	5150001	CD172 $\alpha$
BX017 – RX017	Atto550	Akoya Biosciences	5250001	XCR1
BX019 – RX019	AF488	Akoya Biosciences	5450002	CD45
BX021 – RX021	Cy5	Akoya Biosciences	5250004	CD26
BX023 – RX023	Atto550	Akoya Biosciences	5250003	CD301b
BX025 – RX025	AF488	Akoya Biosciences	4150015	CD11b
BX027 – RX027	Cy5	Akoya Biosciences	5350004	CD301a
BX028 – RX028	AF488	Akoya Biosciences	5450008	CD103
BX030 – RX030	Cy5	Akoya Biosciences	4350013	CD11c
BX040 – RX040	AF488	Akoya Biosciences	5450009	Ly6C
BX043 – RX043	AF488	Akoya Biosciences	5450010	SMA
BX046 – RX046	AF488	Akoya Biosciences	5450011	CD64
BX047 – RX047	Atto550	Akoya Biosciences	4250019	Ki67

<sup>\*</sup> Barcode selection should be done considering the expression levels of the selected markers. Refer to section 2.3.4.

**Table 7.** Chemicals required for CODEX staining

Reagents	Use	Provider	Catalogue #
10X CODEX Buffer	Imaging	Akoya Biosciences	7000001
10X sterile PBS	Staining	Roth	9130.2
16% Paraformaldehyde	Tissue preparation and staining	Thermo Fisher Scientific	28908
Acetone	Staining	Sigma Aldrich	650501
Assay Reagent	Imaging	Akoya Biosciences	7000002
Bovine Serum Albumin (BSA)	Staining	Serva	11930
Conjugation Kit	Barcoding	Akoya Biosciences	7000009
DMSO	Imaging	Sigma Aldrich	472301
Fixative	Staining	Akoya Biosciences	7000008
ddH <sub>2</sub> O	Tissue preparation and staining	Personal choice <sup>*</sup>	
EDTA	Staining	Roth	X986.3
G Blocker	Staining	Akoya Biosciences	7000008
Hydration Buffer	Staining	Akoya Biosciences	7000008
Hydrogen Peroxide 30%	Staining	Sigma Aldrich	216763
J Blocker	Staining	Akoya Biosciences	7000008
Methanol	Staining	Sigma Aldrich	34860-1L-R
N Blocker	Staining	Akoya Biosciences	7000008
Nuclear staining	Imaging	Akoya Biosciences	7000013
Poly-L-Lysine 0.1% (w/v)	Coating	Sigma Aldrich	P8920
S Blocker	Staining	Akoya Biosciences	7000008
Sodium Azide (NaN <sub>3</sub> )	Tissue preparation and staining	Sigma Aldrich	71289
Sodium Chloride	Staining	Roth	P029.9
Sodium Hydroxide	Staining	Roth	P031.2
Staining Buffer	Staining	Akoya Biosciences	7000008
Sucrose	Tissue preparation	Sigma Aldrich	84100
Tissue Tek OCT Compound	Tissue preparation	Sakura Finetek	4583

<sup>\*</sup> It is recommended to use a source of high purity ddH<sub>2</sub>O to avoid any source of contamination that could cause artifacts during imaging.

**Table 8.** Buffers required for CODEX staining

Buffer	Use	Composition
Blocking Buffer	Staining	Dilute all blockers 1:40 in staining buffer
Storage Buffer	Sample storage	0.5M NaCl, 5mM EDTA, 0.5% BSA, 0.02% NaN <sub>3</sub> in 1X PBS
Bleaching Buffer	Staining	20mM NaOH, 4.5% H <sub>2</sub> O <sub>2</sub> in 1X PBS

**Table 9.** Consumables required for CODEX

Consumables	Use	Provider	Catalogue #
6-well plates	Staining and storage	Personal choice	
96-well plate pierceable foil	Imaging	Akoya Biosciences	7000007
Black 96-well plates	Imaging	Akoya Biosciences	7000006
Centrifugal filters (50kDa)	Barcoding	Milipore	UFC505024
CODEX Gaskets	Imaging	Akoya Biosciences	7000010
Coverglass staining rack	Staining	Fisher Scientific	72240
Coverslips (22×22 mm, 1.5)	Tissue preparation and staining	Akoya Biosciences	7000005
Cryomolds	Tissue preparation	Personal choice	
Drierite absorbent	Staining	Fisher Scientific	10742071
Serological pipettes	Staining	Personal choice	
Tweezers (bent tip)	Tissue preparation and staining	Fine Science Tools	11251-33

- Infiltrate the lung through the trachea with 1 ml 50% OCT (diluted in PBS) and seal with a piece of thread.
- Carefully remove the lung and transfer it to a falcon tube with 10ml 1.3% PFA (diluted in PBS). Fix at 4°C for 4–6 h.
- Wash the tissue three times with 1× PBS.
- Transfer the lung to a falcon tube with 10% sucrose (prepared in PBS and with 0.1% NaN<sub>3</sub>). Incubate for 1 h at 4°C.
- Replace the 10% sucrose solution with the same volume of 20% sucrose (prepared in PBS and with 0.1% NaN<sub>3</sub>). Incubate for 1 h at 4°C.
- Replace the 20% sucrose solution with the same volume of 30% sucrose (prepared in PBS and with 0.1% NaN<sub>3</sub>). Incubate overnight at 4°C.
- Separate the lobes you want to freeze, remove the excess of liquid with a Kimwipe and transfer to a cryomold containing OCT. Remove bubbles.
- Transfer the mold to a Styrofoam box filled with dry ice. Let freeze.
- Store tissue at –80°C.

### 2.3.1.2 Preparation of mouse liver:

- Anesthetize and euthanize the mice by perfusion with 15 ml cold PBS, followed by 15 ml of cold 4% PFA (prepared in PBS).
- Carefully remove the liver and transfer it to a falcon tube with 10 ml 4% PFA. Fix the tissue overnight at 4°C.
- Wash the tissue three times with 1× PBS.
- Transfer the liver to a falcon tube with 20% sucrose (prepared in PBS and with 0.1% NaN<sub>3</sub>). Incubate for 1 h at 4°C.
- Replace the 20% sucrose solution with the same volume of 30% sucrose (prepared in PBS and with 0.1% NaN<sub>3</sub>). Incubate 24–48 h at 4°C.
- Continue from step 8 of Section 2.3.1.1.

### 2.3.1.3 Preparation of mouse intestine and spleen.

- Carefully collect the intestine and spleen from the euthanized mice (in this case cervical dislocation does not compromise the integrity of the tissue).
- Transfer the spleen to a falcon tube containing 5 ml of 1.3% PFA (prepared in PBS) and fix overnight. In the case of the

**Table 10.** Instruments required for CODEX

Equipment	Use	Provider
Axio Observer Microscope	Imaging	Zeiss
CM3050 S Cryostat	Tissue preparation	Leica Microsystems
CODEX Instrument	Imaging	Akoya Biosciences
LED Pad (30,000 lux)	Staining	Personal choice

**Table 11.** Software used for CODEX image processing and analysis

Software	Use	Reference
CODEX MAV	Image analysis	Akoya Biosciences
CODEX Processor	Image processing	Akoya Biosciences
CytoMAP	Image analysis	Stoltzfus et al., 2020 [37]
Fiji	Image analysis	Schindelin et al., 2012 [38]
ZEN 3.2	Imaging	Zeiss



intestine, all the inner content should be removed before fixation. Transfer the tissue to 4% PFA (prepared in PBS) and fix for 2 h at 4°C.

3. Wash the tissue three times with 1× PBS.
4. Transfer the tissue to a falcon tube with 10% sucrose (prepared in PBS and with 0.1% NaN<sub>3</sub>). Incubate for 1 h at 4°C.
5. Replace the 10% sucrose solution with the same volume of 20% sucrose (prepared in PBS and with 0.1% NaN<sub>3</sub>). Incubate for 1 h at 4°C.
6. Replace the 20% sucrose solution with the same volume of 30% sucrose (prepared in PBS and with 0.1% NaN<sub>3</sub>). Incubate overnight at 4°C.
7. Continue from step 8 of Section 2.3.1.1.

#### 2.3.1.4 Top tricks and pitfalls of tissue preparation for CODEX.

1. To achieve a complete view of the intestine, we recommend doing swiss rolls before fixation.
2. To guarantee the preservation of an inflated structure when collecting the lungs, more than 1 ml of 50% OCT can be used. Additionally, during fixation and sucrose dehydration, it is recommended to use a rotating device, as the lung may float. For the lung, it is recommended to use the left lobe.
3. Before freezing the tissue, it should be equilibrated in OCT for a couple of minutes. For those organs that tend to float (e.g., lung), it is recommended to first freeze the bottom of the tissue using a Styrofoam box filled with ice-cold 70–100% ethanol.

### 2.3.2 Preparation of cryosections for CODEX

#### 2.3.2.1 Preparation of coverslips.

1. Place the coverslips you want to coat in a clean 100 ml glass beaker.
2. Add poly-L-lysine solution until all the coverslips are covered. Gently swirl the beaker to guarantee that the surface of all coverslips is in contact with the liquid.
3. Seal and incubate at room temperature for 24–72 h.
4. Discard the poly-L-lysine and wash the coverslips 8 times (1 min each) with ddH<sub>2</sub>O. Gently agitate the beaker during the washing steps.
5. Carefully transfer the coverslips using the bent tip tweezers to Kimwipe tissues. Let dry.
6. Store them in a sealed petri dish at 4°C for up to 2 months.

#### 2.3.2.2 Sectioning with the cryostat.

1. Equilibrate the tissue blocks and the coverslips inside the cryostat for 30 min.
2. Place the tissue in the sample holder and adjust.
3. Generate sections of a thickness of 3–10 µm. Try to place the section right in the middle of the coverslip.
4. Store at –20°C or –80°C, depending on the storage time.

#### 2.3.2.3 Top tricks and pitfalls.

1. Due to the microscope stage required for CODEX during image acquisition, it is strongly recommended to use the coverslips indicated in this protocol.
2. When washing the coverslips after coating, do not leave them too long in ddH<sub>2</sub>O.
3. Depending on the tissue, the temperature of the cryostat may be adjusted.
4. The actual imaging space is 1.2×1.2 cm. Larger sections should be avoided.
5. Wait at least 24h before proceeding with the staining.

### 2.3.3 CODEX staining of mouse fresh frozen sections

The following two sections are based on modifications implemented by our group of the Akoya CODEX User Manual Guide and the method described by Schürch et al., 2020 [36].

Before starting the staining procedure, prepare a humid chamber. To facilitate the handling of the coverslips, use an empty tip box (20–200 µl). Place a wet tissue on the bottom of the box, fill it with 1–2 cm of ddH<sub>2</sub>O, and put back the support of the tips.

The handling of the coverslips with the tissue sections should be done with the bent tip tweezers.

#### 2.3.3.1 Tissue preparation.

1. Prepare a box (e.g. empty tip box) with a layer of drierite beads. Withdraw tissue sections from the freezer and place them on top of the drierite (tissue facing up) and let dry for 10 min. Alternatively, let the sections dry at room temperature for 30 min.
2. Fill a 50 ml beaker with 10 ml ice-cold acetone. Place the coverslip and incubate for 10 min. If several coverslips will be stained, the staining rack may be used.
3. Immediately transfer the coverslip to the humid chamber. Close and let acetone evaporate for 2 min.
4. In a 6-well plate, add 3 ml of hydration buffer (2 wells per sample). Place the coverslip in the first well, carefully move up and down 3 times with the help of the tweezers, so that the surface is completely covered. Incubate for 2 min.
5. Transfer the coverslip to the next well and incubate for 2 min.
6. In a separate well add 1.6% PFA (prepared in hydration buffer) and transfer the coverslip here. Fix for 10 min.
7. Wash twice in hydration buffer. The solution in the two wells used before can be used for this purpose.

**2.3.3.2 Photobleaching.** The photobleaching protocol described here is based on the method proposed by Du et al., 2019 [39].

1. In a 6-well plate pour 3–5 ml of bleaching solution and transfer the coverslip. Carefully move up and down 3 times with the help of the tweezers. Close the lid of the plate.

2. Switch on the LED lamp and place it on top of the six-well plate. Incubate for 45 min.
3. Pour 3–5 ml of bleaching solution into a new well. Transfer the coverslip to this well.
4. Repeat step 2.
5. In a separate six-well plate, add 5 ml of  $1\times$  PBS to four wells. Wash the coverslip one time in each well for 3 min, for a total of four washing steps.

#### 2.3.3.3 Antibody staining.

1. Add 3 ml of staining solution to one well of a 6-well plate. Transfer the coverslip into this well and incubate 30–60 min. In this time, prepare the antibody cocktail.
2. Prepare blocking buffer as indicated in section 2.2.1. The final volume per coverslip is 200  $\mu$ l.
3. Calculate the volume of antibody needed per sample and subtract this volume to the 200  $\mu$ l of blocking buffer. Dilute antibodies. If the volume of antibodies exceeds 60% of the final volume, proceed to step 4, if not, continue with step 5.
4. If the antibody volume exceeds 60% of the final volume, pipette the antibodies in 50  $\mu$ l of blocking buffer. Transfer the mix to the top of an Amicon 50 kDa filter unit. Spin down at  $12,000 \times g$  for 8 min, and resuspend in blocking buffer to a final volume of 200  $\mu$ l.
5. Retrieve the coverslip from the staining buffer, place it on the humid chamber, and from the corner of the coverslip add 200  $\mu$ l of antibody mix. Close the lid.
6. Incubate for 3 h at room temperature or overnight at 4°C. Protect the chamber from strong vibrations.
7. In a new 6-well plate add 3 ml of staining buffer to 2 wells and 3 ml of 1.6% PFA (prepared in storage solution) to one well.
8. Transfer the coverslip to the first well containing staining buffer. Incubate for 2 min.
9. Move the coverslip to the second well containing staining buffer and incubate as in the previous step.
10. Transfer the coverslip to the well containing PFA. Fix for 10 min. In the meantime, prepare a new 6-well plate with 5 ml of  $1\times$  PBS in each well (3 wells per sample).
11. Wash the coverslip in the first well with  $1\times$  PBS, carefully move up and down approximately three times. Transfer to the second and third wells for a total of three washes.
12. Place a new 6-well plate on ice. Add 5 mL of ice-cold methanol to one well. Transfer the coverslip to this well. Incubate for 5 min.
13. Wash the coverslip as in step 11. PBS does not have to be changed.
14. Add 20  $\mu$ l of cross-linking fixative to 1 ml of  $1\times$  PBS. Transfer the coverslip to the humid chamber and add 200  $\mu$ l of fixative. Close the lid and incubate for 20 min at room temperature.

15. Wash the coverslip as in step 11.
16. Store your samples in 6-well plates containing 5 ml (per well) of storage buffer at 4°C. If proceeding directly with imaging, let the sample equilibrate at least for 30 min at room temperature in storage buffer.

#### 2.3.3.4 Top tricks and pitfalls.

1. In all steps of this section, the tissue should be always facing up.
2. The coverslips break easily and should be handled carefully. If it is the first time, it is recommended to practice the handling with a mock coverslip and an empty six-well plate.
3. Broken coverslips **cannot** be used.
4. During photobleaching bubbles may form. If the tissue dissociates, you can dilute the solution.
5. During photobleaching check occasionally if the coverslips are still in the bottom of the well.
6. Time of bleaching may be adjusted depending on the source of the tissue (e.g. tissue from reporter mice may require longer times).
7. The 6-well plates used during the staining procedure can be reused 5 times. Wash them with ddH<sub>2</sub>O after each use.

#### 2.3.4 Remarks on antibody barcoding

Antibody barcoding is performed using the conjugation kit of Akoya Biosciences, following their instructions. To improve the barcoding efficiency and panel design, the following aspects should be considered:

1. To reduce the number of cycles, thus the time of acquisition, an even number of fluorophores should be selected when designing the panel.
2. Markers with high expression levels should be detected with reporters labeled either with Alexa Fluor (AF) 488 or AF750.
3. The buffer of the antibodies should not contain any additives other than sodium azide. If there are no alternatives than using an antibody containing other additives, the storage buffer has to be exchanged before the barcoding. For this purpose, it is recommended to use 100  $\mu$ g of antibody and to use the BSA Removal Kit of Abcam (ab173231).
4. After conjugation, the antibodies should not be used after 48h.
5. It is recommended to always titrate the conjugated antibodies in the tissue of interest performing a manual addition of reporters.
6. It is possible to conjugate the same antibody to different barcodes and use all of them in the same staining. Likewise, different clones of an antibody targeting the same antigen can be assigned to different barcodes and used to stain a single sample.

**Table 12.** Preparation of reporter solution

Reagent	Dilution	For one cycle (μl)
10X CODEX Buffer	1:10	25
Assay reagent	1:12	21
Nuclear staining	1:300	1
Nuclease-free water		203

### 2.3.5 CODEX imaging

**2.3.5.1 Preparation of reporter plate.** The antibody detection is performed in a multicycle experiment in which the reporters are be pipetted from a source plate.

1. Prepare reporter solution for pipetting the reporters, as indicated in Table 12.
2. For each cycle prepare an amber eppendorf tube. Pipette 250, 245, 240, or 235 μl of reporter solution for detecting 0, 1, 2, or 3 antibodies, respectively, in one cycle. The first and last cycles should be blank (i.e., no reporters added).
3. Dilute the reporters for each cycle 1:50 in the respective amber tube with master mix.
4. Mix by pipetting and transfer 245 μl of reporter mix from the tube to the corresponding well in the black 96-well plate.
5. After transferring the reporter mix to the 96-well plate, seal it with pierceable foil.
6. Store at 4°C for a maximum of 2 weeks.

**2.3.5.2 Imaging.** Before starting the image acquisition, let the sample (in storage buffer) and the reporter plate equilibrate to room temperature for 30min. Start the CODEX Instrument Manager and the ZEN software. The instrument manager will guide you through the preparation steps for the imaging. The basic steps are the following:

1. Check that there is enough 1X CODEX Buffer, DMSO, and ddH<sub>2</sub>O in the respective container.
2. Insert the reporter plate in the machine and prepare the CODEX stage by placing an empty coverslip, followed by a gasket, and the fluidics system.
3. Set the acquisition settings (i.e. targets per cycle and channel, and exposure times), keeping in mind that LED intensity cannot be modified.
4. Prime the system.
5. Insert sample, control for leakage, insert stage into microscope, and perform nuclear staining (1:2000 in 1X CODEX Buffer).
6. Perform a preview scan of your tissue with the lowest magnification.
7. Switch to the preferred objective (20x or 40x) and select regions of interest. When using ZEN 3.2, all the tile regions should have the same dimensions.
8. Determine the focal plane, number of Z-stacks, and autofocus strategy.
9. Verify that the selected settings match your requests.

10. Activate “Auto Save” mode and start acquisition. During the acquisition time refrain from manipulating the system, as this may stop the experiment.
11. After acquisition, clean the system and proceed with data transfer (see Section 2.4). Store the sample in storage buffer at 4°C for maximum of 2 weeks. In this time, it is possible to repeat the acquisition multiple times (e.g., if exposure times have to be adjusted), but no additional antibodies can be added. Furthermore, the samples can be directly used for performing conventional histological stainings such as by hematoxylin and eosin.

#### 2.3.5.3 Top tricks and pitfalls.

1. Avoid bubbles when pipetting the reporters. If unavoidable, try to remove them with a pipet tip.
2. To prevent any dirt that may introduce artifacts, it is recommended to use filter tips to pipette the reporters.
3. Different exposure times can be used for each antibody, but this has to be tested empirically since it may be tissue-dependent.
4. The settings for the UV LED (DAPI) should not be high, as this can potentially bleach the overlapping regions of the tiles.
5. When scanning the tissue and selecting the regions of interest, use the lowest exposure time as possible, as signals may bleach fast.
6. Select a 10–20% tile overlap.
7. The number of z-stacks depends on the thickness of the sections. For the system employed in this protocol, 6–11 z-stacks with a spacing of 1.5 μm were used.
8. To ensure the correct alignment of the images, it is essential to save the X,Y coordinates before starting the acquisition. It is also possible to calibrate the stage of the microscope used, especially if the same imaging needs to be repeated and the exact same coordinates are desired.
9. Every cycle has to include the nuclear staining, as indicated in section 2.3.5.1. It is also possible to add an antibody that stains a membrane protein (e.g. sodium potassium ATPase) in one of the cycles, or perform a membrane staining after the last cycle. This helps to improve the segmentation, described in section 2.4.1.3.
10. Adjustment of the focal plane in every cycle is strongly recommended. As an alternative, several support points can be selected (e.g. per tile, if the tissue is not even).
11. Create a new empty folder for each dataset.

## 2.4 Data processing and analysis

### 2.4.1 Data processing

**2.4.1.1 Data export.** In this step, the raw data is transformed into a format that is recognized by the processor. Additionally, a .json file with the acquisition settings is created.

1. Create a new folder for exporting the data.



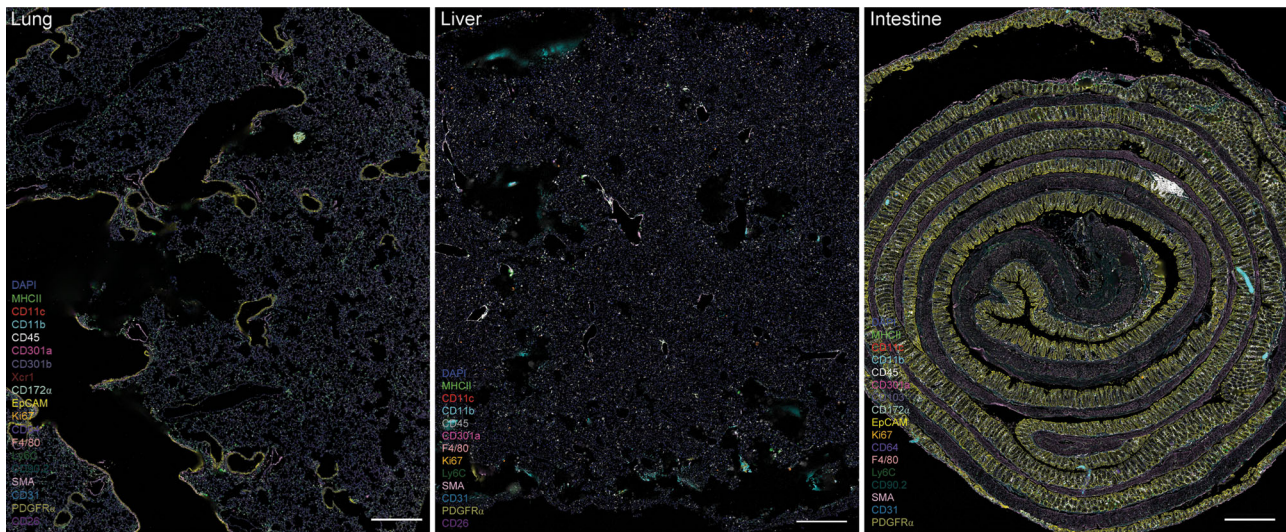


**Figure 6.** Visualization of DC populations in mouse tissues using CODEX. A 19-plex CODEX antibody panel is used to detect DC populations, other mononuclear phagocytes, and stromal cells in mouse lung (left panel), liver (middle panel), and intestine (right panel). Scale bars represent 500  $\mu$ m.

2. In the Instrument Manager verify that the number of images match.
3. Start the transfer.

**2.4.1.2 Data processing.** The data processing is performed using CODEX Processor 1.7.0.6. It will recognize the images generated during the data export and the experimental file. The processing of the images includes (i) background subtraction that uses as a reference the blank cycles, (ii) cycle alignment, (iii) deconvolution, (iv) shading correction, and (v) stitching. The parameters for each of these steps are pre-defined and cannot be modified. However, it is important to highlight that the data generated by the system can be used with other software. Three different examples of post-processing images are shown in Fig. 6.

**2.4.1.3 Cell segmentation.** The CODEX processor also performs the segmentation, although it is not the only option and other open-source software can be used. The CODEX processor uses a watershed algorithm to detect and define the objects in the images. The nuclear staining of one of the cycles should be selected as a reference. For this purpose, neither the first nor the last cycles should be used. Moreover, a membrane marker (from any of the cycles, or a specific membrane marker/staining) can be used to improve the segmentation. The radius of the kernel of each object can be increased or decreased, as well as the cutoff of signal intensities. These parameters should be empirically defined based on the cell density of the tissue analyzed. The final result of the segmentation is a '.csv' and a '.fcs' file.

## 2.4.2 Data analysis

**2.4.2.1 Cell classification.** The .fcs file generated by the processing and segmentation can be used in FlowJo or in CODEX MAV

(Fiji plugin) to perform a supervised cell classification (Fig. 7). The advantage of using CODEX MAV is that the images can be observed next to the .fcs plots. The basic procedure for a supervised cell classification is:

1. Remove unspecific objects using DAPI as a reference: due to the nature of the data, it is possible that objects out of the focal plane or undesired dirt create unspecific signals that are recognized as objects. These objects tend to have low signal intensities; thus, it is possible to easily identify them and remove them from the analysis.
2. Segregate immune and non-immune cells using CD45 signal intensities.
3. Identify macrophages and monocytes using the canonical markers included in the panel. Depending on the tissue this may be done before gating DC, since some markers may be expressed by all MPs.
4. Identify DC and their subpopulations.

**2.4.2.2 Defining cell interactions.** To define cell-cell interactions, the CODEX MAV allows performing a spatial analysis after defining a minimum and maximum distance, which should always consider the characteristics of the system used for acquiring the images. The program counts the number of interactions between different cell types and additionally calculates the likelihood of those interactions computing the Log Odds Ratio. These results can be exported to .csv files for further analyses and presented in a CIRCOS plot [40].

**2.4.2.3 Defining cellular neighborhoods.** Besides analyzing the cell interactions of DC with other MPs and non-immune cells, defining cellular neighborhoods is useful to dissect the complexity of different tissues and determine how the DC compartment

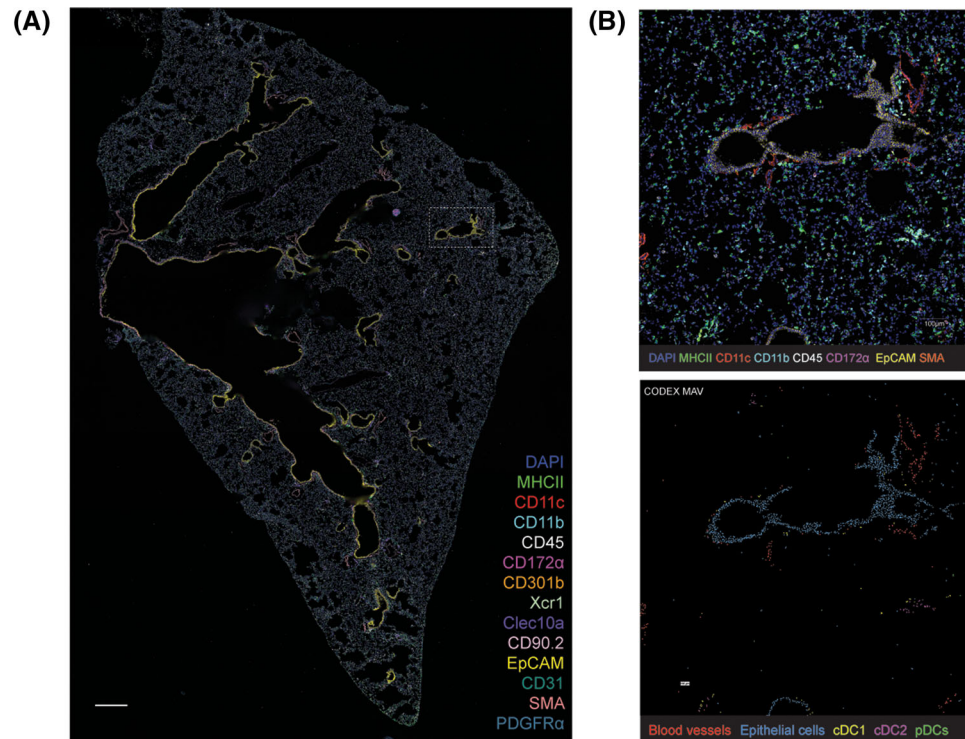


**Figure 7. Identification of DC populations.** A) Full section of the mouse left lung stained with a CODEX 19-plex antibody panel to visualize DC. Scale bar represents 500  $\mu\text{m}$ . B) After processing and cell segmentation, a region of interest from (A) is selected and a supervised or unsupervised cell classification is performed to detect cDC1 and cDC2 (lower panel) and their non-immune surrounding. Scale bar represents 100  $\mu\text{m}$ .

behaves in health and disease. CytoMAP presents a user-friendly tool for this type of analyses [37]. The .csv files generated after cell classification can be opened in CytoMAP and used not only to re-create an overview of the distribution of objects/cells, but also to label them.

Two different approaches can be used: (i) a cell-centered approach in which cellular neighborhoods will be centered around a defined cell type, or ii) a raster scan approach in which the objects will be distributed into regions of a certain radius (Fig. 8). Further characterization of the cell composition of the encountered neighborhoods can be done with algorithms for unsupervised clustering (e.g., k-means). The parameters and the algorithms used should be validated for the different tissues. Nearest Neighbor Analysis and Pearson Correlation can be performed in CytoMAP and may be good alternatives to the LogOddsRatio analysis.

### 3 Detection of human DC subsets by multispectral imaging

#### 3.1 Introduction

The tumor microenvironment (TME) emerged as a key player in the understanding of the tumor-immune cell crosstalk and treatment response [41–43]. While the frequency of immune cells is a strong determinant for survival of cancer patients, other fac-

tors such as their distribution, activation status, and distance to other immune or tumor cells can also be crucial [44, 45]. Therefore, advanced approaches like multiplex immunohistochemistry (mIHC) can facilitate dissolving the spatial organization of the TME [46]. While classical IHC and immunofluorescence (IF) are widely used to detect protein expression in tissue sections, they are limited in the number of detected markers, sensitivity, and antibody host species and are negatively influenced by autofluorescence (AF) or heavily pigmented tissue. The tyramide-signal amplification (TSA)-based Opal mIHC (Fig. 9) using the Vectra 3.0 microscope allows the simultaneous detection of up to six markers on a single tissue section, in addition to DAPI. This enables the investigation of complex immune cell subsets such as DC, which rely on the combination of multiple markers, as well as a functional characterization and distance measurements between different cell types. The enhanced signal amplification combined with the fluorescent-based detection provides a high sensitivity and allows the detection of weakly expressed markers. The stripping-based fluorescent mIHC additionally mediates an independence from the antibody host species and reduces sterical hindrance when staining epitopes that closely colocalize. Upon whole-tissue scanning and acquisition of multispectral images (MSIs), the spectral unmixing is conducted using the inForm software, which also provides the possibility to mark and subtract strong AF from the actual staining signals. Afterward, the trainable tissue segmentation allows a discrete analysis of the stromal vs. tumoral compartment and the exclusion of non-tissue areas.



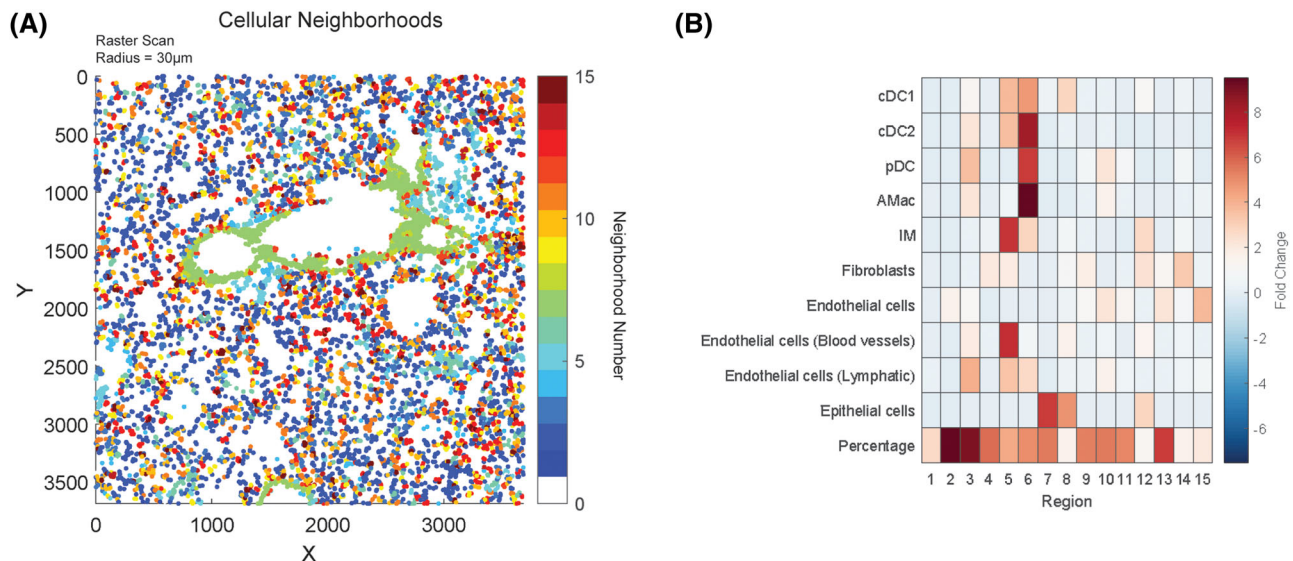


**Figure 8.** Detection of cellular neighborhoods. (A) Upon cell classification a raster scan or a cell-based scan is performed in CytoMAP using a defined radius. (B) The detected regions are subsequently clustered into cellular neighborhoods based on their identity. Heatmap depicts the composition of the regions identified in the selected area of the lung.

The adaptive cell segmentation then integrates not only the DAPI signal, but also phenotyping markers to aid the nuclear segmentation. A self-learning algorithm is then trained by an experienced user to phenotype all markers, allowing to discriminate positive and negative cells not only based on a threshold of signal intensity, but also dependent on its pattern and subcellular localization.

Several research groups successfully harnessed TSA-based mIHC to unravel the tumor-immune cell interaction and correlation to survival and therapy response [47–49]. While this technique enables a high-resolution dissemination of the TME, it is limited to the imaging of a single focus plane and will still require the staining of multiple panels to analyze different immune cell

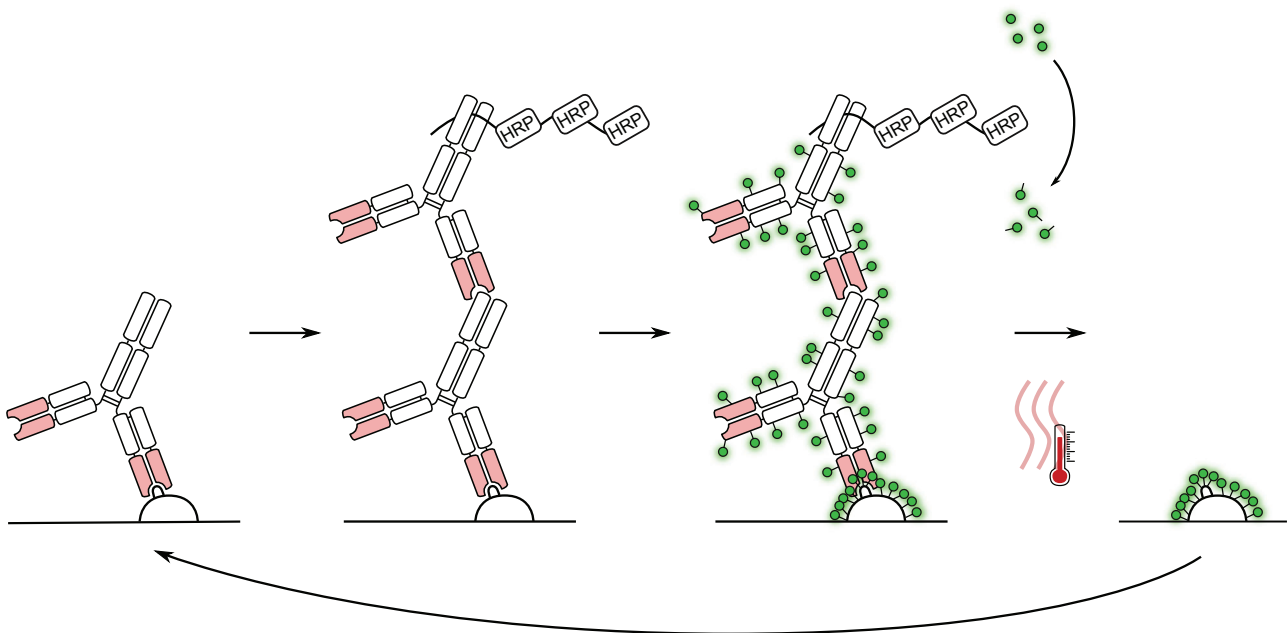


**Figure 9.** Schematic description of one staining round using the TSA-based Opal mIHC method. The primary antibody binds to its target epitope and is then detected by the secondary antibody bound to poly horseradish peroxidase (HRP). The tyramide fluorophore is turned into its reactive state by the HRP and binds to tyrosine residues of proteins in close proximity, including the antibodies. The MWT step removes the complex of primary and secondary antibody, leaving just the covalently bound fluorophore on the tissue. Another round of staining with a different fluorophore can then be applied.

**Table 13.** Primary antibodies

Antibody	Host species	Clone	Manufacturer	Catalog number
BDCA-2	Goat	Polyclonal	R&D Systems	AF1376
CD1c	Mouse	2F4	NovusBiologicals	NBP2-46123
CLEC10A	Rabbit	Polyclonal	Human Protein Atlas	HPA021937
CLEC9A	Rabbit	EPR22324	Abcam	ab223188
IRF7	Mouse	G-8	Santa Cruz	sc-74472
PanCK (manual)	Mouse	AE1/AE3	ThermoFisher	MA5-13156
PanKeratin (automated)	Mouse	AE1/AE3/PCK26	Ventana	05266840001

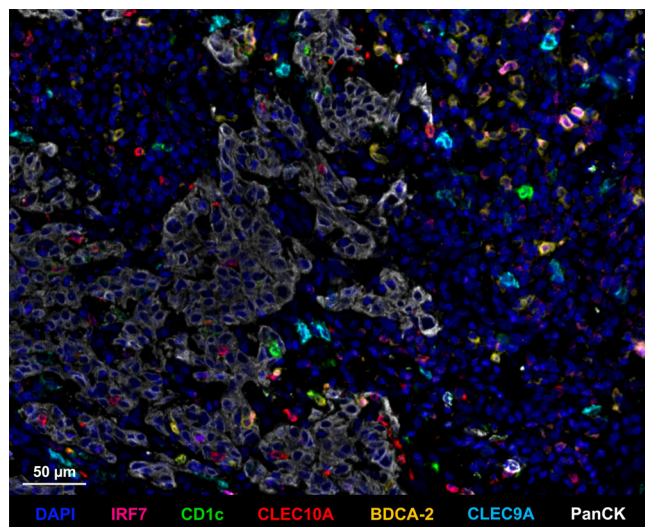


**Figure 10.** Representative multispectral image of a tissue stained for the 7-color human DC subset panel described in this section. A formalin-fixed paraffin-embedded human head and neck squamous cell cancer specimen was stained for IRF7 (magenta), CD1c (green), CLEC10A (red), BDCA-2 (yellow), CLEC9A (cyan), and PanCK (white). Magnification  $\times 200$ , Scale bar 50  $\mu\text{m}$ .

subsets. By pairing fluorescent mIHC with other methods, like 3D imaging, sequential highly multiplexed IF or single cell sequencing, those gaps can be bridged to fully depict the tumor niche and improve our understanding of the TME to guide the prognosis and therapy of cancer patients [50]. While the T cell and macrophage compartments have been thoroughly investigated and various T cell and macrophage panels have been published, comparable panels for DC subsets are lacking. Here, we present a panel comprising the major human DC subsets cDC1 (CLEC9A<sup>+</sup>), cDC2 (CLEC10A<sup>+</sup>CD1c<sup>+</sup>), pDC (BDCA-2<sup>+</sup>) and the pDC activation marker IRF7 [51] as demonstrated in Fig. 10.

## 3.2 Materials

### 3.2.1 Reagents

Necessary reagents are listed in Tables 13–16.

Prepare:

TBS-T: TBS (Tris-buffered saline) + 0.05% Tween 20

**Table 14.** General reagents and materials

Reagent	Manufacturer	Catalog number
4',6-Diamidino-2-phenyl-indol-dihydrochlorid (DAPI)	Sigma	32670-5MG-F
Ab diluent / block	Akoya Biosciences	ARD1001EA
Amplification diluent	Akoya Biosciences	FP1498
Coverslips 24 $\times$ 32 mm	Marienfeld Superior	0101172
Fluoromount-G Mounting Medium	Southern Biotech	0100-01
Opal 520 Reagent Pack	Akoya Biosciences	FP1487001KT
Opal 540 Reagent Pack	Akoya Biosciences	FP1494001KT
Opal 570 Reagent Pack	Akoya Biosciences	FP1488001KT
Opal 620 Reagent Pack	Akoya Biosciences	FP1495001KT
Opal 650 Reagent Pack	Akoya Biosciences	FP1496001KT
Opal 690 Reagent Pack	Akoya Biosciences	FP1497001KT

**Table 15.** Additional reagents for manual staining

Reagent	Manufacturer	Catalog number
AR6 buffer 10x	Akoya Biosciences	AR6001KT
AR9 buffer 10x	Akoya Biosciences	AR9001KT
Ethanol (80 %)	Berkel AHK	7505F
Ethanol (96 %)	Berkel AHK	1641M
Ethanol (absolute)	Carl Roth	K928.5
ImmPRESS® horse radish peroxidase (HRP) Horse Anti-Goat IgG Polymer Detection Kit	Vector Laboratories	MP-7405-15
PAP Pen	Kisker	MKP-1
Sodium chloride	Carl Roth	3957.1
SuperBoost™ Goat anti-Mouse Poly HRP	ThermoFisher	B40961
SuperBoost™ Goat anti-Rabbit Poly HRP	ThermoFisher	B40962
Tris-hydrochloride	Carl Roth	9090.2
Tween 20	SERVA	37470.01
Xylene	Electrophoresis VWR International S.A.S	28975.291

**Table 16.** Additional reagents for automated staining

Reagent	Manufacturer	Catalog number
10x EZ Prep Solution	Ventana	05279771001
10x Reaction Buffer Concentrate	Ventana	05353955001
Benchmark ULTRA CC1	Ventana	05424569001
Benchmark ULTRA CC2	Ventana	05424542001
DISCOVERY anti-HQ HRP	Ventana	07017936001
DISCOVERY anti-Mouse HQ	Ventana	07017782001
OmniMap anti-Goat multimer	Ventana	06607233001
OmniMap anti-Mouse HRP	Ventana	05269652001
OmniMap anti-Rabbit HRP	Ventana	05269679001
Ultra LCS	Ventana	05424534001

**Table 17.** Equipment and software

Equipment / software	Manufacturer
Humid staining chamber	Plano GmbH
inForm Software	Akoya Biosciences
Microwave NN-CF760MEPG	Panasonic Corporation
Orbital shaker	Sustainable Lab Instruments
Phenochart Software	Akoya Biosciences
R and RStudio	Open source
Vectra 3.0 Automated Quantitative Pathology Imaging System	Akoya Biosciences
Vectra software	Akoya Biosciences
Ventana Discovery Ultra	Ventana

### 3.2.2 Equipment and software

Necessary equipment and software is listed in Table 17.

## 3.3 Step-by-step sample preparation

### 3.3.1 Manual staining of a 7-color human DC subset panel

1. Place slides in an incubator set at 60°C for 45min or overnight to melt paraffin.
2. To remove excess paraffin, incubate slides twice for 8min in xylene.
3. Rehydrate tissue in a series of absolute ethanol, 96% ethanol, 80% ethanol, and aqua dest. Incubate slides 5 min each.
4. Prepare 1× AR9 buffer in a plastic cuvette using autoclaved aqua dest.
5. Place slides in plastic cuvette, close the lid loosely, and perform first microwave treatment (MWT) in AR9 in a microwave at 900 W for ~1 min until boiling. Continue MWT at 90 W for 15 min. Allow the slides to cool down for at least 20 min.

6. Wash twice for 2 min in TBS-T.
7. Dry the slides using tissue wipes and a vacuum pump without touching the tissue.
8. Circle the tissue with a hydrophobic barrier pen.
9. Add 150 µl Ab diluent/block on the tissue section within the marked area, move the slide until the whole tissue is covered. Place on the orbital shaker and incubate for 10min.
10. Dilute primary antibodies in Ab diluent/block according to Table 18.
11. Aspirate blocking buffer completely and add 150 µl of diluted antibody solution. Place on the orbital shaker and incubate for 60 min at RT.
12. Wash three times for 2 min in TBS-T.
13. Carefully aspirate TBS-T and add 3–4 drops (~150 µl) of secondary antibody targeted against the host species of the primary antibody, according to Table 18. Move the slide until the whole tissue is covered. Place on the orbital shaker and incubate for 20 min at RT.
14. Wash three times for 2 min in TBS-T.
15. Dilute respective fluorophore in amplification diluent according to Table 18.
16. Aspirate TBS-T and add 150 µl of diluted fluorophore, move until the whole tissue is covered and place on the orbital shaker for 10 min at RT. **Note:** This step should not exceed 10 min of incubation time to ensure optimal staining.
17. Wash three times for 2 min in TBS-T.
18. Prepare 1x AR6 buffer in a plastic cuvette using autoclaved aqua dest.
19. Place slides in plastic cuvette, close the lid loosely, and perform MWT in a microwave at 900W for ~1 min until boiling. Continue MWT at 90 W for 15min. Allow the slides to cool down for at least 20 min.
20. Repeat **steps 6–19** until all epitopes are detected.
21. Wash two times for 2 min in TBS-T.
22. Aspirate TBS-T and add 150 µl of DAPI working solution. Place on the orbital shaker and incubate for 2 min at RT.
23. Wash 2 min in TBS-T followed by 2min in aqua dest.
24. Aspirate aqua dest and add 10 µl of mounting medium. Add coverslip and remove excess medium as well as any air bubbles by gently applying pressure on the coverslip. Let dry at RT and store stained slides at RT (short term) or 4°C (long term).

### 3.3.2 Automated staining of a 7-color human DC subset panel on a Ventana Discovery Ultra

1. Place slide onto a staining chamber in the Discovery Ultra. Verify that the surface of the heating pad is clean and the slide is flush to the contact surface. Up to 30 slides can be stained at once.
2. Apply the following automated staining protocol. Only primary antibodies (except PanKeratin) and fluorophores are added manually (100 µl, diluted in Ab diluent/block and amplification diluent according to Table 19, respectively).

**Table 18.** Manual staining protocol

Antibody	Dilution	Secondary Antibody	Fluorophore	Dilution
IRF7	1:100	Goat anti-mouse Poly HRP	570	1:100
CD1c	1:75	Goat anti-mouse Poly HRP	620	1:100
CLEC10A	1:50	Goat anti-rabbit Poly HRP	520	1:75
BDCA-2	1:125	Horse anti-goat Polymer	690	1:75
CLEC9A	1:200	Goat anti-rabbit Poly HRP	650	1:200
PanCK	1:100	Goat anti-mouse Poly HRP	540	1:800

- Paraffin removal: three cycles of 8 min at 69°C
  - Antigen retrieval: CC1 (pH 9) for 32 min at 95°C
  - Primary antibody incubation: 32 min at 36°C
  - Rinse with reaction buffer
  - Secondary antibody incubation: 12 min at 36°C
  - Rinse with reaction buffer
  - Tertiary antibody incubation (optional: only for CD1c): 12 min at 36°C
  - Rinse with reaction buffer
  - Fluorophore incubation: 8 min at RT
  - Rinse with reaction buffer
  - Antibody denaturation: CC2 (pH 6) for 24min at 100°C
    - Repeat **steps c-k** until all markers are detected.
  - Counterstaining: DAPI at working solution for 8min at RT
- Retrieve the slides from the Discovery Ultra and wash in luke-warm detergent solution until there are no oily residuals. This will depend on the number of slides.
  - Wash in aqua dest for 30 s.
  - Aspirate aqua dest and add 10 µl of mounting medium. Add coverslip and remove excess medium by gently applying pressure on the coverslip. Let dry at RT and store stained slides at RT (short term) or 4°C (long term).

### 3.3.3 Control slides for spectral library

- Create single-fluorophore library slides using the same protocol, but only staining one marker/fluorophore each and skipping the DAPI staining. Perform the MWT steps both before and after the respective marker.
- Prepare one library slide with no fluorophores but only DAPI staining. Perform all MWT steps.
- Create one AF slide with no fluorophores and no DAPI. Perform all MWT steps.

### 3.4 Data analysis

- Adjust exposure times for both 100x and 200x resolution for all channels as described in the user manual. Save the protocol and acquire whole scans at 100x resolution of all slides, including the library slides.
- Define regions of interests on the tissue using the Phenochart software. Choose different representative areas to account for tissue heterogeneity.
- Acquire multispectral images (MSIs) at 200× resolution of all slides.
- Create a spectral library in 'inForm' using a representative MSI of each library slide.
- Unmix fluorophores using the spectral library. Optional: use the AF tool in the AF control slide to remove AF signals.
- Perform trainable tissue segmentation, adaptive cell segmentation, and phenotyping as described in the user manual (Fig. 11). Create a different 'inForm' project for markers that are co-localized, using the same tissue and cell segmentation. **Note:** This facilitates easy phenotype training without the need to train double or triple-positive cells. For the panel described in this protocol, three different projects were created: one with CD1c, CLEC9A, PanCK, and BDCA-2, one with CLEC10A, and one with IRF7.
- Process all images using the batch analysis option and export the cell segmentation data for all three projects.
- Merge single cell segmentation data files and consolidate multiple merged cell segmentation files using the Akoya Biosciences phenoptR add-in in R.
- Calculate densities, proportions, distances, and distribution using the R packages *dplyr* and *spatstat*. Alternatively, the *phenotprReports* add-in provided by Akoya Biosciences allows essential analysis of densities and distance measurements as well as creating a quality of unmixing report.

**Table 19.** Automated staining protocol

Antibody	Dilution	Secondary antibody	Fluorophore	Dilution
IRF7	1:75	OmniMap anti-mouse HRP	570	1:75
CD1c	1:50	Anti-Ms HQ + Anti-HQ HRP	620	1:150
CLEC10A	1:100	OmniMap anti-rabbit HRP	520	1:75
BDCA-2	1:75	OmniMap anti-goat multimer	690	1:75
CLEC9A	1:75	OmniMap anti-rabbit HRP	650	1:350
PanCK	pre-diluted	OmniMap anti-mouse HRP	540	1:400



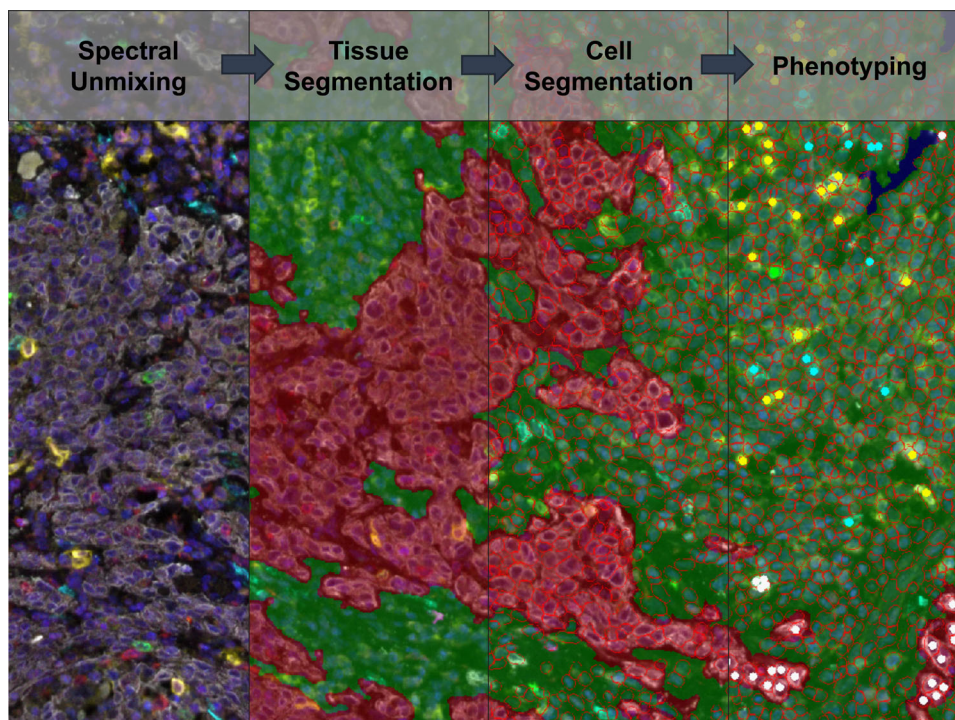


**Figure 11.** Schematic representation of the analysis pipeline including spectral unmixing, tissue segmentation, cell segmentation, and phenotyping. The left panel shows the unmixed image with all stained markers: IRF7 (magenta), CD1c (green), CLEC10A (red), BDCA-2 (yellow), CLEC9A (cyan), and PanCK (white). The tissue segmentation and cell segmentation are depicted in the middle-left and middle-right panel, respectively. Tumoral areas are displayed in red, stromal areas in green and non-tissue areas in blue. In the right panel, phenotyped cells included in one project are shown as dots with the respective color of the marker.

### 3.5 Pitfalls

- Accurate fixation of the tissue is crucial, as under-fixed tissue will create additional AF and background while over-fixed tissue will reduce epitope accessibility. The provided protocol is optimized for standard formalin fixation of 24–48 h at RT. However, the initial AR can be adjusted in strength (temperature) and duration to adjust for improper fixation. For example, extending the AR to 40min at 100°C may enable efficient staining of over-fixed tissue.
- As some epitopes are sensible to heat, the staining order of the included markers is crucial for successful staining.
- Adhesion of the tissue to the slide is important due to extensive cooking procedures. Generic IHC slides might enable tissues, especially those rich in fat, to detach. We recommend using Dako FLEX slides or TOMO slides.
- Antibody and fluorophore dilutions stated in the protocols are meant as a guideline. Final signal intensity may vary depending on antibodies and staining conditions. Balance signal intensity for each marker-fluorophore combination to prevent bleeding and improve spectral unmixing quality. The signal intensity is normalized by the exposure time and can be analyzed in 'inForm'. The target range should be 5–50 "counts".
- Manual staining: make sure to strictly adhere to incubation times for each sample and consider the time it takes to handle

each section. Additionally, account for the time it takes to add the solution to all slides in your experiment. We recommend to not exceed 20 slides per staining.

- Do not use mounting medium containing DAPI as this will increase background DAPI signal and hinder proper cell segmentation.
- Refrain from acquiring MSIs in regions rich in erythrocytes, necrosis or folded tissue, as this will impair cell segmentation and phenotyping.

### 3.6 Top tricks

- Using autoclaved aqua dest for the preparation of TBS-T and AR buffer may reduce background intensity.
- Optimize the nuclear segmentation before moving on to the phenotyping as the segmentation is crucial for a successful phenotyping and the cell segmentation parameters cannot be changed after phenotyping.
- When performing tissue and cell segmentation as well as the phenotyping, use a sufficient number of MSIs from multiple, different patients as the staining intensity, background, AF and DAPI intensity can strongly vary between tissues.
- Apply a grid when imaging large tumor areas to reduce the MSI acquisition time and output data size.



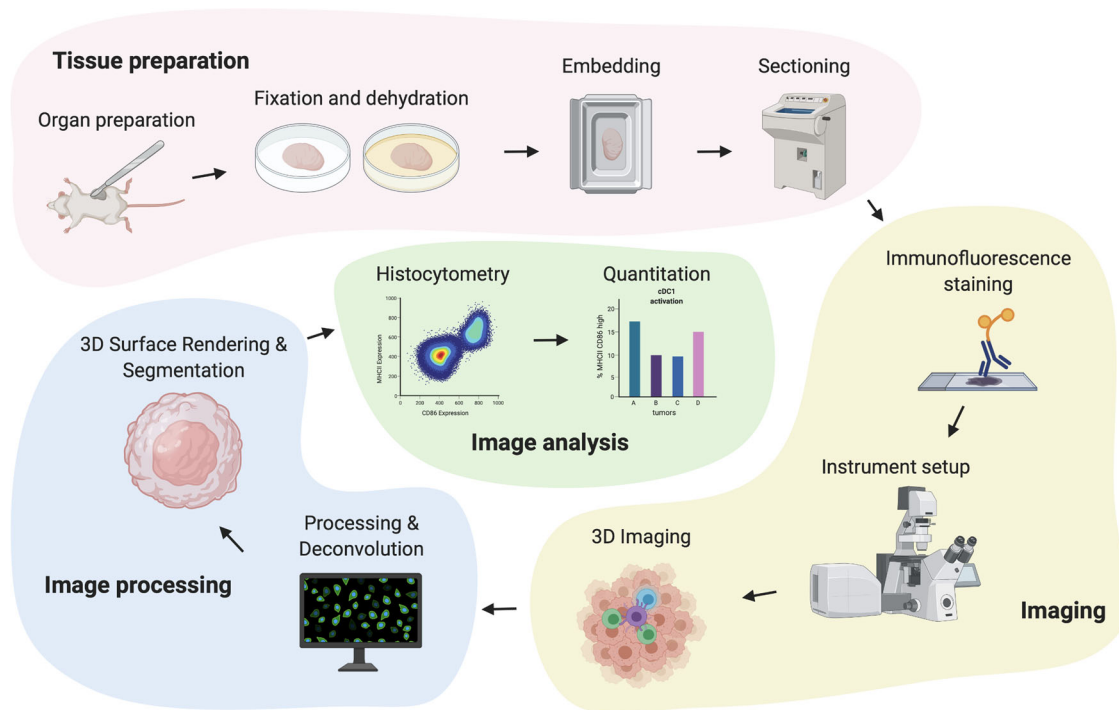


**Figure 12.** Workflow for cDC1 imaging by high-resolution volumetric microscopy, visualization, and analysis. In brief, tissues of interest are first fixed and dehydrated, followed by tissue sectioning. Sections are then blocked, permeabilized, and stained with fluorophore-coupled antibodies followed by confocal microscopy imaging. Next, images are corrected for fluorophore spill-over using dye separation, and deconvoluted to improve contrast and resolution. Finally, 3D cell surface rendering of cDC1 and other cells or tissue structures is performed to enable further quantitative analyses of cell populations and their spatial organization, e.g. by histocytometry. Figure created with BioRender.com.

## 4 Quantitative analysis and visualization of cDC1 in three-dimensional tissue volumes by high-resolution confocal microscopy

### 4.1 Introduction

cDC1 play a key role in immune surveillance, and constitute the key DC subtype for initiation and regulation for antigen-specific CD8<sup>+</sup> T cell responses in lymphoid and non-lymphoid organs. In tumors, cDC1 fulfil a critical role for the orchestration of anti-cancer immunity, which reflects their ability to initiate de novo T cell responses after migration to tumor-draining lymph nodes and the regulation of T cell survival, proliferation, and effector functions at the tumor site [52, 53]. Assessment of cDC1 abundance and functionality in tumor tissue can predict cancer patient survival and help evaluate treatment responses including T cell-targeting immunotherapies [54–61]. All cDC1 selectively express the chemokine receptor XCR1, which can be used as a marker to reliably identify these cells in tissues. The C-type lectin receptor CLEC9A also marks cDC1, although it can also be found on cDC progenitors and at lower levels on plasmacytoid DC. In mice, expression of the integrin  $\alpha$ E (CD103) can be used as an additional marker to identify cDC1 in non-lymphoid organs as well as tumors. In lymph nodes, CD103 expression discriminates migratory cDC1 that immigrated from peripheral tissues via afferent lymphatics from lymph node-resident, CD8 $\alpha$ <sup>+</sup> cDC1. Similar to

mice, XCR1 and CLEC9A can be used to identify human cDC1 in blood, lymphoid and nonlymphoid tissues, alone or in combination with additional cDC1 markers such as BDCA3 or CADM1. Here, we present an imaging-based methodology for the quantitative analysis of cDC1 in mouse and human tissues using multi-phenotypic and functional markers. This methodology entails high-resolution confocal microscopy of large, three-dimensional tissue volumes (Fig. 12), allowing for accurate assessment of cDC1 numbers, morphology, and spatial positioning in the context of intact tissue structures. We further describe detailed procedures for data processing and cell rendering, and provide specific examples of how to make use of 3D imaging data to further characterize cDC1 functional states and their cross-talk with T cells in tissues.

### 4.2 Materials

#### 4.2.1 Reagents

Necessary reagents including primary and secondary antibodies are listed in Tables 20–23.

##### Prepare:

- Blocking buffer: 0.1 M Tris buffer + 0.3% Triton X-100, 1% BSA, and 1% of the respective blocking sera. Adjust pH to 7.4

**Table 20.** Primary and directly-conjugated antibodies for mouse antigens

Antibody	Fluorochrome	Clone	Host	Manufacturer	Catalog No.	Working concentration
Anti-CD3	AF647	17A2	Rat	Biologend	100209	1-2.5 µg/ml
Anti-CD8α	BV421	53-6.7	Rat	Sony Biotechnology	1103765	1-2.5 µg/ml
Anti-CD11b	PE	M1/70	Rat	Biologend	101208	0.4-1 µg/ml
Anti-CD11c	BV421	N418	Hamster	Biologend	117343	2.5 µg/ml
Anti-CD19	FITC	1D3/CD19	Rat	Biologend	152404	2.5 µg/ml
Anti-CD31	BV510	MEC13.3	Rat	BD Biosciences	563089	0.5 µg/ml
Anti-CD80	unconjugated	polyclonal	Goat	R&D Systems	AF740	1-2 µg/ml
Anti-CD86	PE	GL-1	Rat	Biologend	105008	1 µg/ml
Anti-CD103	unconjugated	polyclonal	Goat	R&D Systems	AF1990	1 µg/ml
Anti-Collagen IV	unconjugated	polyclonal	Rabbit	Abcam	ab6586	2 µg/ml
Anti-GFP	AF488	polyclonal	Rabbit	Thermo Fisher	A21311	4 µg/ml
Anti-IRF8	AF488	V3GYWCH	Mouse	Thermo Fisher	53-9852-82	2.5 µg/ml
anti-I-A/I-E	FITC	M5/114.15.2	Rat	Biologend	107606	0.5-1 µg/ml
Anti-TCRβ	AF488	H57-597	Hamster	Biologend	109215	1 µg/ml
Anti-XCR1	BV421	ZET	Rat	Biologend	148216	3 µg per mouse (i.v. injection)

- Surgical instruments and tools: Micro scissors, scalpels, and forceps
- Multi-well plates for harvesting/fixation of organs and tissues
- 15 ml and 50 ml conical tubes

For lung tissue: pre-warmed, melted low melting point agarose (2%/PBS, ~1 ml per lung)

#### 4.2.2 Equipment

Necessary equipment is listed in Table 24.

#### 4.2.3 Software

Software for image analysis is listed in Table 25.

### 4.3 Step-by-step sample preparation

#### 4.3.1 Tissue preparation

##### 4.3.1.1 Preparation of mouse spleen, lymph nodes and solid tumors.

1. Use forceps and micro scissors to carefully dissect the organ or tissue of interest from euthanized mice

2. Transfer samples into a sample tube or a 24-well tissue culture plate containing Antigenfix solution. Use an appropriate volume of Antigenfix to ensure that the tissue is completely submerged during fixation (~1.5 ml for spleen, 1 ml for lymph nodes). In our experience, a fixation time of 4–6 h at 4°C is sufficient for organs such as spleen, lymph nodes, and smaller solid tumors. Larger tissues such as liver or lung should be perfused to ensure optimal fixation and reduce fixation time (see section 4.3.1.2).

3. Wash the fixed tissue twice in PBS.

##### 4.3.1.2 Preparation of mouse liver and lung.

1. In a first step, perfuse mice with 10 ml PBS (using a 26G needle) to eliminate vascular blood content. In a second step, continue perfusion with 10 ml Antigenfix to enable maximal epitope conservation. **Tip:** Optimal perfusion sites are: The right ventricle of the heart for lung perfusion and the portal vein for perfusion of the liver.
2. For preparation of lung tissue, gently inject pre-warmed, melted low melting point agarose into the trachea until lungs are inflated to full capacity (using a 2–5 ml syringe with a 19–21G needle). **Note:** This step is critical to remove air from the airways and preserve the lung architecture during the following fixation and cutting steps.

**Table 21.** Primary and directly-conjugated antibodies for human antigens

Antibody	Fluorochrome	Clone	Host	Manufacturer	Catalog No.	Working concentration
Anti-XCR1	BV421	S15046E	Rat	Biologend	372610	0.5 µg/ml
Anti-CLEC9A	PE	8F9	Mouse	Biologend	353804	1 µg/ml

**Table 22.** Secondary antibodies

Antibody	Fluorochrome	Clone	Host	Manufacturer	Catalog No.	Working concentration
Anti-goat IgG (H+L)	AF680	polyclonal	Donkey	Jackson Immunoresearch	705-625-147	1 µg/ml
Anti-rabbit IgG	BV510	poly4064	Donkey	Biolegend	406419	1 µg/ml

**Table 23.** General reagents and materials

Reagent	Manufacturer	Catalog No.
Acetone	AppliChem	161007
Antigenfix	DiaPath	P0016
Bovine serum albumin	Sigma Aldrich	A9418
Collagenase IV	Thermo Fisher Scientific	LS004188
Coverslips	Omnilab	5161050
DAPI	Biolegend	422801
DNase I	Roche	11284932001
Donkey serum	Merck	D9663-10ML
DRAQ5	Thermo Fisher Scientific	65-0880-96
Flash Phalloidin Green 488	Biolegend	424201
ImmEdge Pen	Thermo Fisher Scientific	NC9545623
Low melting point agarose	Sigma Aldrich	A4018
Microscope slides SuperFrost Plus	Omnilab	5161155
Mouse serum	Thermo Fisher Scientific	10410
Mowiol 4–88	Sigma Aldrich	81381
Osteosoft	Merck	101728
RapiClear	SunJin Lab	RC152001
Sucrose	AppliChem	A2211
Tissue Tek Cryomold	Sakura Finetek	4557
Tissue Tek OCT Compound	Sakura Finetek	4583
Tris	AppliChem	A1379
Triton X-100	AppliChem	A4975

**Table 24.** Equipment for tissue preparation and imaging

Equipment	Model	Manufacturer
Confocal microscope with motorized stage	TCS SP8	Leica Microsystems
Cryostat	CM3050 S	Leica Microsystems
Vibratome	VT1000S	Leica Microsystems

- Place the organ into a tissue plate containing Antigenfix for 4–6 h at 4°C. Ensure that the tissue is completely submerged.
- Wash the fixed tissue twice in PBS.

#### 4.3.1.3 Preparation of mouse bones.

- Collect bones from euthanized mice and cut away the surrounding muscle tissue. Use a paper towel to gently remove remaining tissue attached to the bones.
- Place the bones into a tissue plate containing sufficient Antigenfix solution to submerge the tissue and fix overnight at 4°C.
- Dry the bones on a lint-free wipe to remove excess fixation buffer and place them in Osteosoft for 5–7 days at 4°C.

#### 4.3.1.4 Top tricks and pitfalls.

- To minimize introduction of artefacts, avoid squeezing of samples during their handling
- Make sure to remove any remnants of attached connective tissue or fat from your sample. This will increase stability during the sectioning process.
- Customization of fixation time for organs is crucial for good sectioning results. Under- and over-fixed tissue can tear during the sectioning process.

#### 4.3.2 Preparation of cryosections from mouse organs

- Obtain fixed and washed tissue as described in section 4.3.1.
- Place the tissue in a fresh tube or well containing 30% sucrose in PBS. Incubate at 4°C until the tissue sinks to the bottom of the tube/well (~12 h). This dehydration step is crucial to avoid tissue disruption caused by ice crystals formed during the freezing process and can increase photostability of fluorescent proteins.

**Table 25.** Software for image analysis

Software	Version	Provider
FlowJo	10.8	BD Biosciences
Imaris	9.7.2	Oxford Instruments
Prism	9.2.0	GraphPad
Excel	16.52	Microsoft

3. Place the tissue in an appropriate cryomold and add OCT embedding medium until the tissue is fully covered and a meniscus bulges above the level of the cryomold surface. Freeze at  $-80^{\circ}\text{C}$  for at least 4 h before continuing with the next step. Avoid any air bubbles. **Note:** In order to facilitate the sectioning process, ensure that your samples are located in the center of the cryomold. Consider the desired orientation of the tissue with respect to the sectioning plane.
4. Use a cryostat (e.g., Leica CM3050 S) to cut sections of 30–50  $\mu\text{m}$  thickness, according to the manufacturer's instructions. Transfer sections to a microscopy slide. **Note:** Slides with freshly generated sections should be left to dry at room temperature (RT) for  $\sim 20$  min before proceeding with the staining. Samples can be kept at  $-80^{\circ}\text{C}$  for long-term storage.

#### 4.3.2.1 Top tricks and pitfalls.

- Optimal cutting temperatures vary between tissues. Adjusting the cryostat temperature to your tissue type can improve sectioning results.
- If sectioning lipid-rich tissues, make sure that the part with the highest fat content is the last part to pass the cryostat blade to prevent tearing of the sample.

#### 4.3.3 Immunofluorescence staining of mouse cryosections

1. Rehydrate sections with 0.1 M Tris buffer for 10 min at RT.
2. Circle the sections on the slides with an ImmEdge Pen to create a hydrophobic barrier to prevent spilling of blocking and staining solutions.
3. **Blocking:** in a humidified chamber, incubate sections with 600  $\mu\text{l}$  freshly prepared blocking buffer for at least 2 h at RT. **Note:** Sera in the blocking buffer should correspond to the tissue type (e.g., use mouse serum for blocking mouse tissues) as well as the host species of secondary antibodies to avoid unspecific binding.
4. **Primary staining:** Prepare 300  $\mu\text{l}$  blocking buffer containing the primary antibodies and/or directly labeled antibodies. Incubate in the dark at RT overnight.
5. Discard the staining solution by tilting the slides on tissue paper. Carefully wash the slides three times with 600  $\mu\text{l}$  of 0.1 M Tris buffer.
6. **(Optional) Secondary staining:** prepare 300  $\mu\text{l}$  blocking buffer containing secondary antibodies. Incubate in the dark at RT for at least 6 h.
7. Discard the staining solution. Carefully wash the slides three times with 600  $\mu\text{l}$  of 0.1 M Tris buffer.
8. **Mounting:** Distribute 50  $\mu\text{l}$  of Mowiol as single drops on the slide. Slowly lower a glass coverslip onto the slide. Avoid air bubbles.
9. Let the mounted sample dry in the dark at RT overnight. Afterward, the stained slides should be stored at  $4^{\circ}\text{C}$  protected from

light. In our experience, slides can be imaged up to 10 weeks post staining when using the fluorophores described here.

#### 4.3.3.1 Top tricks and pitfalls.

- It is possible to reduce incubation times for sections thinner than 30–50  $\mu\text{m}$ . We would however advise against the use of thin sections, as these contain insufficient numbers of DC for accurate analysis and complicate reliable identification of tissue structures.
- Lipid autofluorescence can interfere with detection of fluorescent probes and antibodies. Removal of lipids can be achieved by carefully incubating the slides in a cuvette filled with acetone at RT for 20 min. This delipidization step should be performed directly before blocking.
- Throughout the staining process, prevent samples from drying out, as this will reduce staining quality and increase autofluorescence. Work quickly in between steps and make sure that the barrier created with the ImmEdge Pen is intact.
- Mounting reagents vary in their ability to conserve the photostability of fluorescent dyes and proteins and should therefore be evaluated experimentally. In our hands, Mowiol performs well with the fluorophores described here.

#### 4.3.4 Preparation of vibratome sections of mouse tissues

1. Obtain fixed and washed tissue as described in step 3.1.
2. Melt 4% (for bones: 8%) low melting point agarose in PBS and pipette the liquid into the wells of a multi-well tissue plate. Allow the liquid to cool but proceed to the next step before the agarose solidifies. Use forceps to gently embed the organs into the melted agarose.
3. Once solidified, use a scalpel or forceps to dislodge each agar block. **Note:** agar blocks can be used as soon as they have become solid or can be kept at  $4^{\circ}\text{C}$  overnight.
4. Use superglue to attach agar blocks to a vibratome sectioning platform and wait 5 min for the glue to be fully hardened. Meanwhile, fill the vibratome sample chamber with ice-cold PBS.
5. Slice the agar tissue blocks to the desired thickness (200–600  $\mu\text{m}$ ).
6. Transfer the vibratome slices to multi-well plates containing PBS with 0.02% sodium azide, making sure to remove excess agarose. Sections can be directly used for immunofluorescence staining or stored at  $4^{\circ}\text{C}$  for up to 2 weeks.

#### 4.3.4.1 Top tricks and pitfalls.

- Moderate trimming frequency and blade advancement are crucial for successful vibratome sectioning. In our hands, cutting of lung vibratome sections on a Leica VT1000S vibratome works best with a trimming frequency of 85 Hz, a blade advance speed of 0.8 mm/s, and a cutting angle of  $15^{\circ}$ .

- For cutting of soft tissues, using scissors to gently push the tissue towards the cutting edge of the blade can prevent squeezing and deformation of the sample.

#### 4.3.5 Immunofluorescence staining of vibratome sections of mouse tissues

The procedure for staining of vibratome sections follows similar steps as the protocol described for cryosections in section 4.3.3. Due to the larger section volume, blocking, staining, and washing steps are performed in multi-well plates and for longer time periods. Make sure to adjust buffer volumes to well size (e.g., ~500  $\mu$ l buffer is sufficient for staining in 24-well plates).

1. **Blocking:** incubate the tissue with freshly prepared blocking buffer (described above) in the dark at RT for at least 24 h.
2. **Primary staining:** stain the tissue by incubation with a panel of antibodies diluted in blocking buffer in the dark at RT for 48 h.
3. Wash three times for 30 min with 0.1 M Tris buffer.
4. **Secondary staining** (if necessary): stain the tissue by incubation with secondary detection reagents diluted in blocking buffer in the dark at RT for 24 h.
5. Wash three times for 30 min with 0.1 M Tris buffer.
6. If desired, stain nuclei (e.g., using DAPI, 100 nM; or DRAQ5, 10  $\mu$ M) or actin filaments (Phalloidin, 2 U/ml) by incubating the tissue with the diluted reagents for 2 h in the dark at RT. Note that working concentrations of these reagents should be adjusted depending on organ type and section thickness. After staining, wash the samples three times for 30 min with 0.1 M Tris buffer.
7. Before mounting the sample, gently dab the sections on a Kimwipe to eliminate excess washing buffer.
8. **Mounting:** When mounting thick tissue sections, a spacer must be inserted between the microscope slide and the coverslip to prevent compression of the tissue. Create a spacer by cutting double-sided tape into a frame and stick it onto the microscope slide to form a mold. **Tip:** If required, stack the spacers to increase mold heights. Place the vibratome sections in the center of the mold, and cover in Mowiol. Gently cover the tissues with a coverslip. Let the slides dry overnight at RT in the dark. Similar to stained cryosections, stained samples should be stored in the dark at 4 °C, protected from light.

##### 4.3.5.1 Top tricks and pitfalls.

- During mounting, ensure that the mold formed with adhesive tape is airtight to prevent formation of air bubbles.
- Mounting samples in clearing solutions (e.g., RapiClear, Sun-Jin Lab) instead of Mowiol can be helpful to improve imaging depth by increasing tissue transparency and reducing autofluorescence.

#### 4.3.6 Visualization of cDC1 in mouse samples by immunofluorescence

**4.3.6.1 Identification of cDC1 by antibody staining.** cDC1 in mouse organs and tissues can be identified by labeling with antibodies that target cDC1-specific proteins. Here, we list some staining combinations that, in our experience, are useful for the reliable identification of cDC1 and enable their distinction from other cell types.

- **CD103 and MHCII:** In non-lymphoid tissues, staining of the surface marker CD103 together with MHCII can be used to reliably identify cDC1 (Figs. 13A–13C), with the exception of the gut. In lymph nodes, the same marker combination can be used to identify CD103<sup>+</sup> migratory cDC1, whereas resident cDC1 can be identified by additional staining for CD8 $\alpha$ . In our experience, reliable identification of individual cDC1 and their distinction from other DC in dense, DC-rich lymphoid tissues requires implementation of additional cDC1-specific markers or the use of reporter mice.
- **XCR1:** cDC1-specific expression of the chemokine receptor XCR1 makes it an ideal marker for cDC1 identification in tissues. In our experience, currently available clones targeting XCR1 in mice fail on fixed tissue samples. However, staining of cDC1 in vascularized tissues can be achieved by intravenously injecting anti-XCR1 antibodies (3  $\mu$ g per mouse) shortly before sacrificing the animal (Fig. 13D).
- **CD11c and IRF8:** Complementary to the stainings described above, identification of cDC1 can be facilitated by additional staining for CD11c and IRF8. Please note that these markers are also expressed by other DC subsets and/or macrophages and certain T cell populations.

**Note:** In order to distinguish CD103<sup>+</sup> cDC1 from tissue-resident and naive T cells expressing CD103, markers such as CD3 or TCR $\beta$  can be included in the staining panel to exclude T cells from the analysis. Similarly, MHCII<sup>+</sup> macrophages or B cells can be distinguished from cDC1 by additional stainings for CD11b and CD19, respectively.

**4.3.6.2 Functional characterization of cDC1 using immunofluorescence stainings.** Besides localization of cDC1, immunofluorescence and confocal microscopy can further be used to determine the function and activation state of cDC1. For example, expression levels of the surface molecules MHCII, CD80 and CD86 can help to phenotypically identify cDC1 in an activated state and discriminate them from resting DC. Of note, the functional abilities of such activated cDC1 can differ dramatically depending on the nature and environmental context of the activation signal, and should be evaluated in additional experiments [3]. For some cDC1 functional markers, reporter mouse models exist that allow to further interrogate the positioning of functionally distinct cDC1 within tissues (see below).



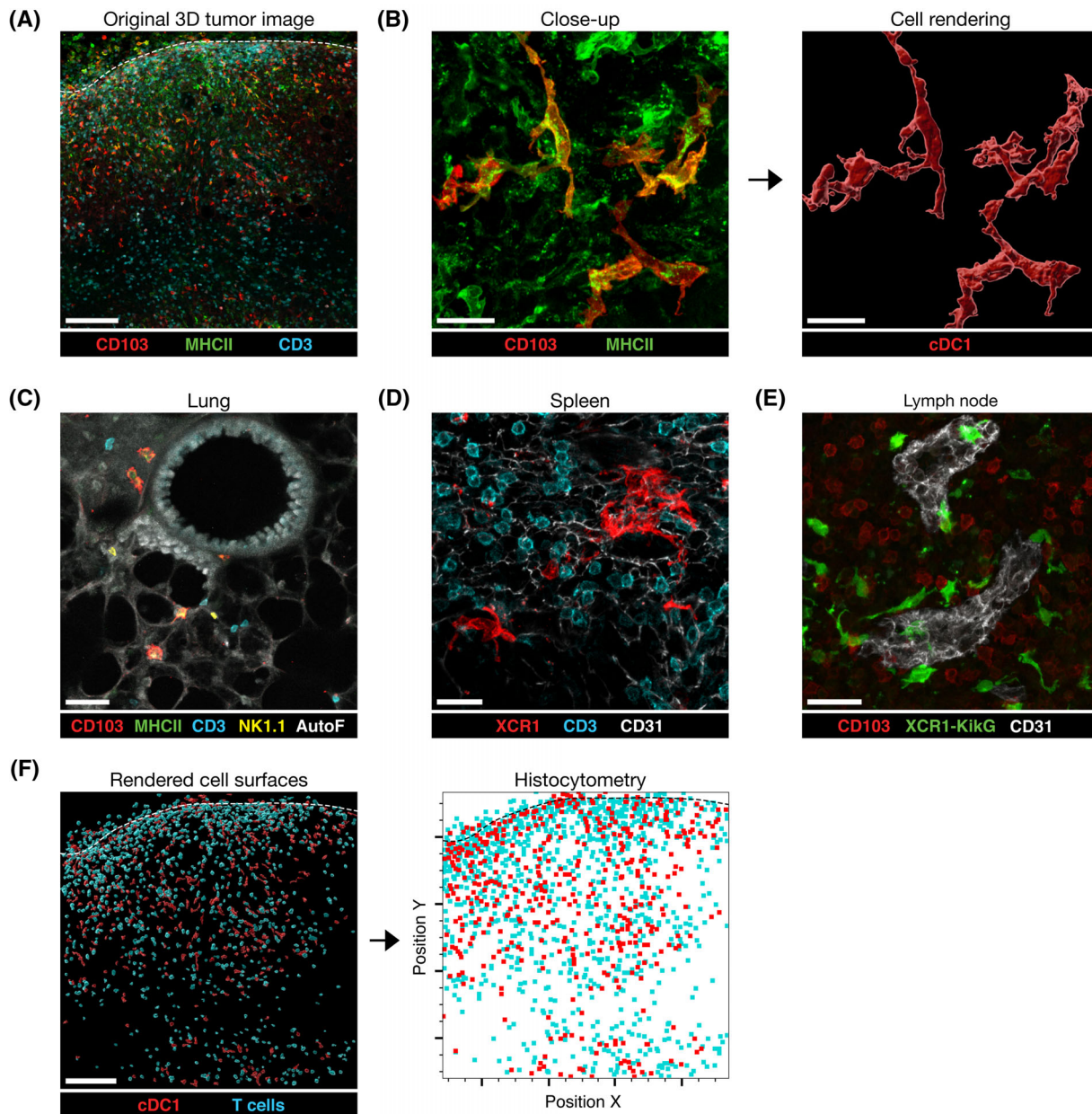


**Figure 13.** cDC1 identification and cell rendering of cDC1. (A) Representative 3D projection of an exemplary region of a 50  $\mu\text{m}$  tumor section stained for CD103 (red), MHCII (green), and CD3 (cyan). The image was obtained using an inverted TCS SP8 confocal microscope (Leica) with an HC PL APO CS2 20 $\times$ /0.75NA objective. Tiled xy stacks were acquired with 1  $\mu\text{m}$  z spacing to provide three-dimensional image volumes of 20  $\mu\text{m}$  depth. Scale bar 150  $\mu\text{m}$ . (B) Close-up showing reconstruction of individual CD103<sup>+</sup>MHCII<sup>+</sup> cDC1 by surface rendering based on CD103 and MHCII channels in Imaris. Acquisition was done using an HC PL APO CORR CS2 63 $\times$ /1.30NA objective, Z stack was acquired with 1  $\mu\text{m}$  spacing and 21  $\mu\text{m}$  depth. Scale bar 20  $\mu\text{m}$ . (C) CD103<sup>+</sup>MHCII<sup>+</sup> cDC1 in a 300  $\mu\text{m}$  lung vibratome section stained with antibodies against various cell populations (CD103, MHCII, CD3, NK1.1). Scale bar 40  $\mu\text{m}$ . (D) Labeling of splenic cDC1 following i.v. injection of a fluorescently labeled anti-XCR1 antibody. Sections were additionally stained for CD3 and CD31 after fixation. Scale bar 20  $\mu\text{m}$ . (E) Identification of Kikume Green (KikG)<sup>+</sup> cDC1 in a lymph node section from an Xcr1<sup>KikGR</sup> mouse. Scale bar 30  $\mu\text{m}$ . (F) Example histocytometric analysis of intratumoral localization for CD103<sup>+</sup>MHCII<sup>+</sup> cDC1 and CD3<sup>+</sup> T cells. Data including positional information from the image shown in (A) were exported into Excel and plotted in FlowJo software.

**4.3.6.3 Identification and functional characterization of cDC1 using reporter mouse lines.** Several transgenic mouse models exist in which fluorescent reporter proteins are expressed under the control of cDC1-specific promoters (Table 26). These models can be used alone or in combination with antibodies to facilitate the identification and visualization of cDC1 in tissues (Fig. 13E).

Note that the reporter signal in such models is influenced by the nature of the fluorescent protein as well as promoter activity, which can vary depending on the tissue environment. In addition, mouse strains with cDC- or cDC1-specific expression of Cre-recombinase (Table 27) can be crossed to Rosa26-stop-fluxed fluorophore reporter strains (e.g., Rosa26<sup>YFP</sup> [62]) to

**Table 26.** Fluorescent reporter mouse lines

Reporter model	Strain	Reference	Comment
Xcr1 <sup>Venus</sup>	Xcr1 <sup>tm2</sup> (Venus)Ksho	[63]	Highly cDC1 specific, no co-staining needed for identification of cDC1.
Xcr1 <sup>DTRVenus</sup>	Xcr1 <sup>tm2</sup> (HBEGF/Venus)Ksho	[63]	Can be used for conditional depletion of cDC1 by diphtheria toxin injection. Reported to yield lower fluorescence intensity.
Xcr1 <sup>KikGr</sup>	Xcr1 <sup>KikGR</sup>	[64]	Highly cDC1 specific, strong signal intensity. Illumination with violet-blue light results in photoconversion of the KikGR protein, enabling spatio-temporal cDC1 tracing in tissues.
Irf8 <sup>Venus</sup>	Irf8 <sup>VENUS</sup> PAC	[65]	IRF8 expression can be used as an additional marker for cDC1 identification. Cells express three additional Irf8 transcripts.

label cDC1. Furthermore, reporter mice for functional markers such as chemokine receptors, cytokines, and chemokines exist that can provide additional information on the migratory capacity of cDC1 and their capability to communicate with other immune or non-immune cells (Table 28).

#### 4.3.7 Identification of cDC1 in human tissues

Staining of cDC1 in human tissues is limited by the availability of cDC1-specific antibodies suitable for formalin-fixed paraffin-embedded (FFPE) samples. In our experience, this issue can be circumvented by fixation of freshly isolated human tissues in Antigenfix followed by sectioning on a cryostat preparation, similar to the above-described protocol for mouse tissues (see sections 4.3.1.1 and 4.3.2). In such sections, cDC1 can be identified

by staining for XCR1 and CLEC9A using the antibodies listed in Table 21.

#### 4.3.8 General remarks on confocal imaging of cDC1

- Obtaining high-resolution volumetric image datasets of larger tissues on a scanning confocal microscope requires long acquisition time per sample. The large file sizes of such data further results in a substantial increase in processing and analysis time. Therefore, the intention of each imaging experiment should be evaluated to determine the appropriate parameters before image acquisition. For global visualization of cDC1 localization throughout a whole tissue section, it is possible to image with a 20x objective and lower resolution settings, which significantly reduces microscopy time. However, in our hands, such

**Table 27.** Cre-expressing mouse strains for cDC1 labelling

Reporter model	Strain	Reference	Comment
Xcr1 <sup>Cre</sup>	Xcr1 <sup>tm1</sup> (iCre)Ciphe Xcr1 <sup>tm1.1</sup> (Cre)Kmm	[21, 22]	Reported to show high frequency of germline recombination, necessitates careful evaluation of Cre-activity in non-cDC1. Partial activity in CD4 <sup>+</sup> T cells.
Karma <sup>Cre</sup> Clec9a <sup>Cre</sup>	Gpr141b <sup>tm2</sup> (iCre)Ciphe Clec9a <sup>tm2.1</sup> (iCre)Crs	[22] [20]	Partial activity in mast cells. Additional expression in cDC-precursors, leading to recombination in cDC2. Low expression and recombination in pDC.

**Table 28.** Fluorescent reporter models for functional characterization of cDC1

Reporter model	Strain	Reference	Comment
IL12p40 <sup>eYFP</sup>	Il12b <sup>tm1.1</sup> Lky	[66]	Can be used as a marker for cDC1 producing the cytokine IL-12, involved in regulation of T cell and NK cell survival and effector function.
Rex3	Cxcl9 <sup>RFP</sup> Cxcl10 <sup>BFP</sup> BAC	[67]	Can be used as a marker for cDC1 producing the chemokines CXCL9 and CXCL10, involved in the recruitment and positioning of CXCR3 <sup>+</sup> lymphocytes
Ccr7 <sup>GFP</sup>	Ccr7 <sup>tm1.1</sup> Dnc	[68]	Can be used to identify migratory cDC1. Counterstain of GFP with anti-GFP can improve signal intensity.

a setup is suboptimal for detailed analysis of cellular phenotype and morphology and the study of cell-cell interactions, especially when investigating cell-dense areas and morphologically complex, heterogeneous cell types such as cDC1. For such detailed analyses, we recommend the use of at least a 40× objective with a high numerical aperture and no more than 1 µm spacing between Z planes.

- Quantitative imaging of fluorescence signals in tissues is best performed using detectors with high sensitivity, ideally with a high quantum efficiency, low dark noise, and a large dynamic range, which will yield the most precise results. We further recommend the use of detectors with the capability to count single photons (i.e., on the Leica microscope used here, Hybrid Detectors) to ensure that the signal registered by the detector is directly proportional to the concentration of the labelled molecule in the sample.

### 4.3.9 Image processing

**4.3.9.1 Tile stitching and dye separation.** Following image acquisition, use the LAS X software (Leica) for image tile stitching and (optional) channel dye separation. Depending on the microscope manufacturer similar software can be used.

**Note:** Dye separation can be used to computationally unmix overlapping spectra and eliminate cross-talk in multiparameter images (also known as compensation). Use this approach when it is impossible to choose dyes with distinct excitation/emission spectra.

**4.3.9.2 Deconvolution (optional).** During any imaging process, light gets diffracted within the imaging system, which produces signal blurring and reduces the effective resolution. Deconvolution is a mathematical process able to mitigate this phenomenon by re-assigning signals to their original position, which helps to improve the accuracy of object surface rendering and cell segmentation. On the Leica microscope used here, deconvolution is enabled by the LIGHTNING tool, which allows for deconvolution of an image immediately after its acquisition. This tool preserves the original sum of signal intensities and the number of photons in the deconvolved image, and can enable distinction of signals as close as 120 nm.

**4.3.9.3 3D surface rendering and cell segmentation with Imaris.** The image analysis software Imaris provides tools for the generation of “object surfaces” based on imaging data, which can be used to model cells and structures in tissues in 3D. Surfaces can not only be used for identification and visualization of individual cells but also act as a container from which all desired statistics can be calculated. For example, surfaces for cDC1 can be used to gather information such as spatial positioning of individual cells within the image (Fig. 13F), distance to other cellular (e.g., T cells) or structural objects (e.g., blood vessels) or signal intensity statistics

for additional fluorescence markers to evaluate protein expression levels. The following list provides tips on the most important steps for the generation of 3D surfaces for cDC1 in Imaris v.9.

- **Source channel:** Object surfaces are computed from a “source channel,” which ideally represents a cell-type specific marker. To generate surfaces for cDC1, it is advisable to use a two-step process by first generating surface objects in channels for CD103 or XCR1, followed by intensity-based exclusion of MHCII<sup>+</sup> objects.
- **Surface detail:** Many cDC1 present a complex morphology with elongated membrane processes. In order to represent these delicate structures in the 3D surfaces, the ‘surface detail’ should be set to <1. **Note:** More detailed surfaces require longer computation time.
- **Object size:** In order to prevent over- or undersegmentation of cDC1, it is crucial to define the maximum size of surface objects (~10 µm for cDC1). The algorithm will automatically segment objects according to this size. In our hands, when following the protocol described here, oversegmentation of CD103<sup>+</sup> cDC1 is <10% for most non-lymphoid organs and tumors.
- **Filtering:** Refinement of cDC1 surfaces can be achieved by deploying additional filters for object characteristics. Small staining artifacts can be excluded by setting a lower threshold for object area and volume. T cells can be excluded from the surface by filtering out CD3<sup>+</sup> and/or MHCII<sup>+</sup> surfaces.
- **Background subtraction:** In tissues with high autofluorescence, the automatic ‘background subtraction’ option can facilitate the identification of cDC1.

**Note:** Careful manual control of object surfaces is vital to validate that the chosen settings are appropriate to generate surfaces representing cDC1 and to exclude that staining artifacts or other cell types are included. One useful quality control is the analysis of markers not to be expected to be found on cDC1 (e.g., CD3).

### 4.3.9.4 Top tricks and pitfalls.

- Accurate 3D surfaces depend on high-quality imaging data. Therefore, antibody concentration and staining should be optimized according to the specific properties of the tissue and the cells of interest. In addition, imaging with high resolution is necessary to provide sufficient details for correct surface generation (preferably a 40× objective or higher, spacing of Z stacks ≤1 µm). Oversampling during acquisition can further help improve image deconvolution.
- Finding the ideal setup for cell segmentation often requires empirical testing of surface rendering parameters for each cell type and tissue. Furthermore, Imaris offers the possibility to manually correct oversegmentation of individual cells by object unification, which can be used for smaller datasets.

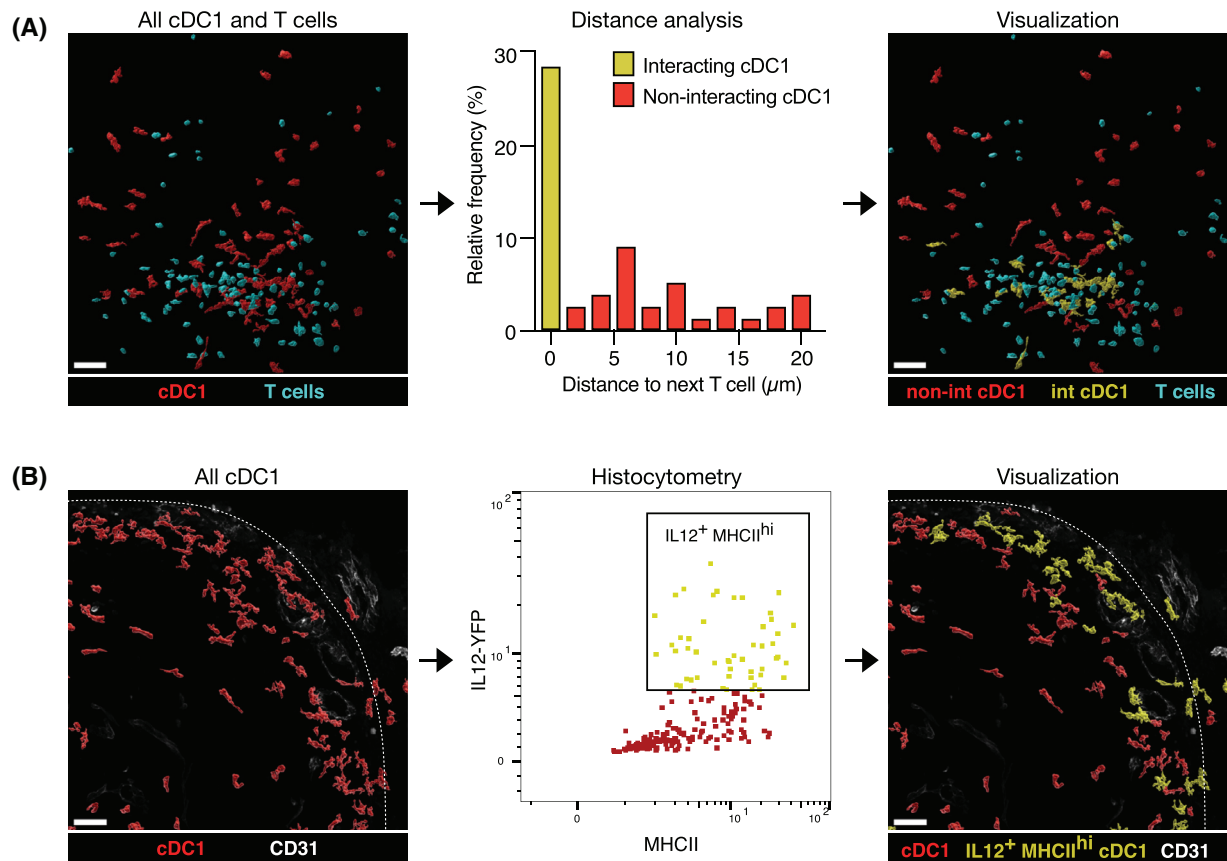


**Figure 14.** Example workflows for spatially-resolved analyses of cDC1. (A) Identification of cDC1 interacting with T cells in an example region of a melanoma tumor. Values for shortest distance between object surfaces for cDC1 and T cells were used to identify cDC1 in close proximity to T cells. In this example, cDC1 with a distance of  $\leq 2 \mu\text{m}$  to the next T cell were classified as “interacting” (int cDC1) and visualized in Imaris. Scale bars 50  $\mu\text{m}$ , original images were obtained using an inverted TCS SP8 confocal microscope (Leica) with an HC PL APO CS2 20x/0.75NA objective. (B) Visualization of IL-12-producing cDC1 in tumors using IL12p40<sup>eYFP</sup> mice. Data for 3D surfaces representing CD103<sup>+</sup>MHCII<sup>+</sup> cDC1 were exported and IL-12<sup>+</sup>MHCII<sup>+</sup> cDC1 were identified by gating on fluorescence intensity channels in FlowJo. Cells were then visualized in Imaris by identifying corresponding surface objects using object IDs.

## 4.4 Image data analysis

### 4.4.1 Quantification of cell–cell interactions

Positional information on rendered cell objects can be used to study physical interactions between different cell populations, which can inform on cell–cell communication. Here, we describe an example workflow to identify cDC1 interacting with T cells in tumor tissue using Imaris v.9 (Fig. 14A).

- Generate object surfaces for cDC1 and T cells in Imaris (see section 4.3).
- In Imaris, activate “Object-object statistics” in the “Edit” tab for both cDC1 and T cell surfaces. Available statistics include “Shortest distance” for each object in one surface to its next neighbor in a second surface (e.g., between a cDC1 and the next T cell) and “Overlapped volume,” which can be used to identify objects in direct contact.
- The “Statistics” tab displays specific statistical values for individual cell objects, which in this example can be used to iden-

tify cDC1 in close proximity to neighboring T cells directly in Imaris. Note that these data can further be exported for additional analyses by other software platforms to help determine statistical significance (e.g., Prism or Excel) or facilitate more complex population gating (see section 4.4.2).

- Use the “Filter” tab for identifying cDC1 in close proximity to T cells, e.g. cells with a shortest distance up to a 2  $\mu\text{m}$  threshold. Copy these objects into a new surface for visualization in Imaris and analysis of additional parameters. In addition to manual thresholding, color-graded visualization of spatial statistics can be achieved using the “Statistics-coded” option in the “Color” tab. This tool can be useful to quickly assess patterns of interacting cells and identify cell clusters in larger datasets.

### 4.4.2 Histocytometry population analysis

For phenotypic analyses of cell populations in multiparameter datasets, it is helpful to implement additional software into the workflow, e.g. FlowJo, which allows for more dynamic, hierarchical population gating. Relevant statistics for such histocytometry



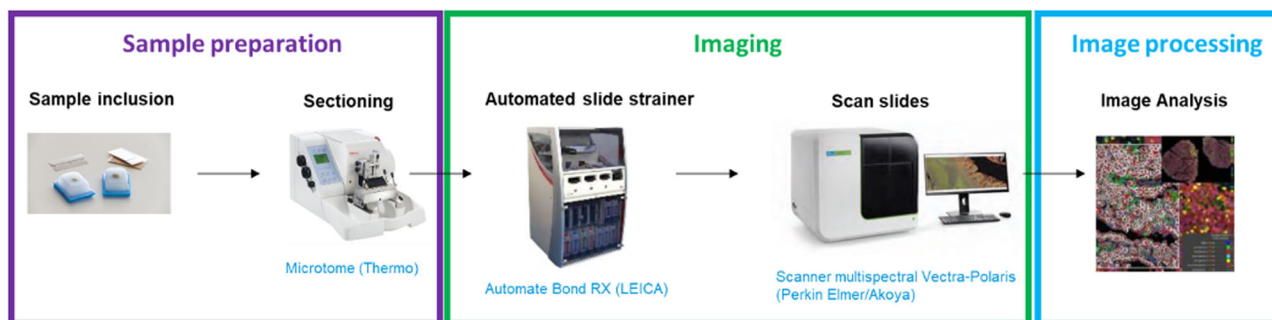


**Figure 15.** Workflow for spatially-resolved functional analyses of cDC1. The protocol includes three main steps: slide preparation, staining/hybridization on a LEICA Bond RX followed by scanning on the scanner Multispectral Vectra Polaris, and finally image analysis using the HALO software.

analyses include object position, sphericity, volume, channel intensity, and object-object distance. For such analyses, compile one Excel file in which each column contains one statistic and every row represents one cell object. Use the statistics names as column headers and export the file in CSV format. Opening these CSV files with FlowJo will generate an FCS file for further analysis. In Imaris, use object surface IDs to identify cells gated in FlowJo. An example for the identification of IL-12-producing cDC1 in tissues by such a workflow is shown in Fig. 14B.

Additional pipelines for histocytometry data analyses of immune cells in tissues are described in references [69–71].

## 5 Immunofluorescence microscopy of cDC1 in human tissues by coupling *in situ* hybridization with antibody staining

### 5.1 Introduction

cDC1 were identified in several tumors [54, 72, 73] and transcriptomic analyses revealed that a high cDC1 infiltration score is associated with a favorable cancer prognosis [54–57]. In patient treated by anti-PD-1, one study has been conducted in metastatic melanoma exploring the cDC1 predictive role in humans and only on very small cohorts. This work demonstrated that the proportion of tumor-associated cDC1 (determined by flow cytometry) is greater in patients with metastatic melanoma responding to anti-PD-1 than in non-responders [56]. This data does not make it possible to assert that cDC1 are necessary for the response to anti-ICP in humans, but provides a first lead that raises the interest of analyzing the functional properties of this population and their implications for the development of new drugs to combine with ICP in order to enhance the proportion of responder patients and overcome the mechanism of resistance. Thus, the underlying mechanisms of positive impact of human cDC1 in patient outcome are not elucidated and the role of each DC subset in human anti-tumor immunity and response to immunotherapy remains elusive. In this context, immunofluorescence can be used not only to determine cDC1 localization in tissues but also to characterize their functionality. For this aim, we developed 3 colors *in situ* visualization protocol combining hybridization and antibody staining

(Fig. 15). We used the *XCR1* and *CD8* probes coupled to an anti-cytokeratin staining to localize  $CD8^+$  T cells and cDC1 inside the tumor parenchyma (cytokeratin<sup>+</sup> cells) and stroma. Then, using a probe directed against *IFN $\lambda$ -1*, we also monitored the expression of this key cytokine inside cDC1 (Fig. 16A and [60]). Of note, our *in situ* hybridization protocol is also compatible with simultaneous detection of proteins expressed at lower levels such as *XCR1*, which can be used to confirm staining specificity of the *CLEC9A* probes (Figs. 16B, 16C).

### 5.2 Materials

#### 5.2.1 Reagents

Necessary reagents are listed in Tables 29–33.

#### 5.2.2 Equipment

Necessary equipment is listed in Table 34.

#### 5.2.3 Software

Necessary software is listed in Table 35.

### 5.3 Step-by-step sample preparation

#### 5.3.1 Preparation of FFPE tumor section

1. Clean all instruments with RNase inhibitor (Thermo Fischer)
2. FFPE tumors were then cut into 4  $\mu$ m sections using the Microtome protocol procedure.
3. Never use the first section because the thickness is not 4  $\mu$ m.
4. Place sections in a cold water bath to remove folds if necessary.
5. Ensure tissue sectioning is smooth and uniform.
6. Cut with a scalpel and put in a water bath at 35°C.
7. Mount the sections onto Microscope slides SuperFrost Plus histological slides.

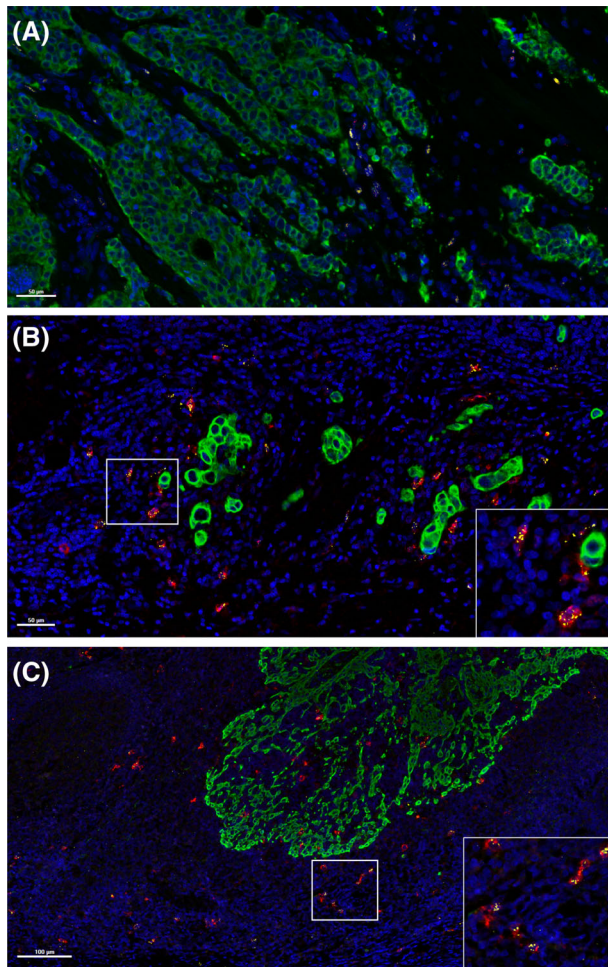


**Figure 16.** Co-detection of CLEC9A transcripts by in situ hybridization (ISH) with cDC1-specific transcripts and proteins in human tissues. (A) Exemplary image of a 4 µm FFPE breast tumor section stained for IFNλ-1 (yellow) and CLEC9A (red) by ISH together with antibody-mediated staining for cytokeratin proteins (green). Nuclei were counterstained with DAPI (blue). (B) Exemplary image of a 4 µm FFPE breast tumor section stained for CLEC9A (yellow) by ISH together with antibody-mediated staining for XCR1 protein (red) and cytokeratin proteins (green). Nuclei were counterstained with DAPI (blue). (C) Exemplary image of a 4 µm FFPE tonsil section stained as in (B). All slides were scanned using the Vectra Polaris automated quantitative pathology imaging system (Perkin Elmer).

8. **Note:** Between each cut/assembly, place the FFPE block on the ice bar.
9. Once the slides are cut, place slides at 37°C for 24 h before storing at 4°C.

**Table 29.** RNAscope probes

RNAscope Probes	Provider	Catalogue #	Dilution	OPAL
IFNλ-1 – Human – C1	ACD	412348	Ready-to use	690
CD8A – Human – C1	ACD	560398	Ready-to use	
CLEC9A – Human – C2	ACD	511558-C2	50x probe for C2	570

### 5.3.2 Manual staining for IFNλ-1 or CD8A and CLEC9A RNAscope staining followed by Cytokeratin immunofluorescent staining

#### 5.3.2.1 Manual IFNλ-1 or CD8 and Clec9a immunofluorescent RNAscope staining.

1. Dry slides in an incubator for 30 min at 60°C
2. Set Hybez oven to 40°C and warm Hybez tray containing wet humidifying paper for 30 min before use
3. To Dewax slides, incubate slides twice in xylene for 5min
4. Rehydrate tissue in two successive baths of 100% ethanol, 5 min each
5. Let the slides dry 5 min at RT
6. Place slides in a distilled water bath for 10 s at 95°C
7. Dilute 10× Target Retrieval Reagents in distilled water and warm for 10 min at 95°C in a water bath.
8. Put slides in 1× Target Retrieval Reagent bath for 15 min at 95°C
9. Wash slides in distilled water bath for 15 s at RT
10. Make a 100% ethanol bath for 10 min at RT
11. Dry slides in an incubator for 2 min at 60°C
12. Draw 2 to 4 times around tissue using the Immedge hydrophobic barrier pen
13. Dry completely few minutes
14. Cover tissue with 3–4 drops of ready-to-use Peroxidase, 10 min at RT
15. Wash slides in distilled water bath for 15s at RT. Dry slides using an absorbent paper without touching the tissue
16. Cover tissue with 3–4 drops of ready-to-use Protease Plus. Incubate 30 min at 40°C in the oven.
17. Wash slides in distilled water bath for 15s at RT. Dry slides using an absorbent paper without touching the tissue
18. Warm probes for 10 min at 40°C. Briefly spin probes and diluted probes C2 (CLEC9A) with the probes C1 (IFNλ-1 or CD8A). Table 36 summarizes the manual optimized immunofluorescence staining conditions for each marker
19. Cover tissue with 450 µl of the mix of probes for 2h at 40°C in the oven.
20. Warm RNAscope 50× wash buffer 10–20 min at 40°C, before preparing the 1× working solution.
21. At the end of the hybridization, wash slides twice with 1× wash buffer. Dry slides using an absorbent paper without touching the tissue
22. Cover tissue with 150 µl of ready to use Amp1 reagent for 30 min at 40°C
23. Wash slides twice with 1× wash buffer. Dry slides using an absorbent paper without touching the tissue

**Table 30.** Primary Antibody

Antibody	Clone	Host	Provider	Catalogue #	Dilution	OPAL
<b>Anti-cytokeratin</b>	AE1/AE3	Mouse	DAKO	M3515	1:200	520

24. Cover tissue with 150 µl of ready to use Amp2 reagent for 30 min at 40°C
25. Wash slides twice with 1× wash buffer. Dry slides using an absorbent paper without touching the tissue
26. Cover tissue with 150 µl of ready to use Amp3 reagent for 30 min at 40°C
27. Wash slides twice with 1× wash buffer. Dry slides using an absorbent paper without touching the tissue
28. Cover tissue with 150 µl of ready to use HRP-C1 reagent for 15 min at 40°C
29. Wash slides twice with 1× wash buffer. Dry slides using an absorbent paper without touching the tissue
30. Cover tissue with 150 µl of OPAL 690 reagent (see Table 36) for 30 min at 40°C
31. Wash slides twice with 1× wash buffer. Dry slides using an absorbent paper without touching the tissue
32. Cover tissue with 150 µl of ready to use HRP Blocker reagent for 30 min at 40°C
33. Wash slides twice with 1× wash buffer. Dry slides using an absorbent paper without touching the tissue
34. Cover tissue with 150 µl of ready to use HRP-C2 reagent for 15 min at 40°C
35. Wash slides twice with 1× wash buffer. Dry slides using an absorbent paper without touching the tissue
36. Cover tissue with 150 µl of OPAL 570 reagent (see Table 36) for 30 min at 40°C
37. Wash slides twice with 1× wash buffer. Dry slides using an absorbent paper without touching the tissue
38. Cover tissue with 150 µl of ready to use HRP Blocker reagent for 30 min at 40°C
39. Wash slides twice with 1× wash buffer. Dry slides using an absorbent paper without
- 5.3.2.2 *Manual cytokeratin immunofluorescent staining.*
40. Cover tissue with 150 µl of ready to use goat serum (Imm-Press kit) for 20 min at RT
41. Cover tissue with 150 µl of cytokeratin antibody working solution (see Table 36) overnight at 4°C

**Table 31.** General reagents

Reagent	Provider	Catalogue #	Dilution
RNAscope® 2.5 LS Hydrogen Peroxide	ACD	322440	Ready-to use
RNAscope® 2.5 LS Protease III	ACD	322440	Ready-to use
RNAscope® 2.5 LS Rinse	ACD	322440	Ready-to use
RNAscope® LS Multiplex AMP 1	ACD	322440	Ready-to use
RNAscope® LS Multiplex AMP 2	ACD	322440	Ready-to use
RNAscope® LS Multiplex AMP 3	ACD	322440	Ready-to use
RNAscope® LS Multiplex HRP C1	ACD	322440	Ready-to use
RNAscope® LS Multiplex HRP C2	ACD	322440	Ready-to use
RNAscope® LS Multiplex HRP Blocker	ACD	322440	Ready-to use
BOND Epitope Retrieval Solution 1	Leica	AR9961	Ready-to use
BOND Epitope Retrieval Solution 2	Leica	AR9640	Ready-to use
BOND Dewax Solution	Leica	AR9222	Ready-to use
BOND Wash Solution 10X Concentrate	Leica	AR9590	1:10 in water
Ethanol	MERCK	Ready-to use	Ready-to use
Xylène	VWR	28975.291	Ready-to use
Formalin solution, neutral buffered, 10%	Sigma-Aldrich	HT501128	Ready-to use
Cryomatrix	ThermoScientific	67690006	Ready-to use
Prolong Gold Antifade	ThermoFisher	P36930	Ready-to use
OPAL 520 REAGENT PACK	AKOYA	FP1487001KT	1:150 in OPAL TSA
OPAL 570 REAGENT PACK	AKOYA	FP1488001KT	1:150 in OPAL TSA
OPAL 620 REAGENT PACK	AKOYA	FP1495001KT	1:150 in OPAL TSA
Antibody Diluent / Block	AKOYA	ARD1001EA	Ready-to use
1X Plus Amplification Diluent	AKOYA	FP1498	Ready-to use
SPECTRAL DAPI	AKOYA	FP1490	2 drops/~1ml of TBS
Opal Polymer HRP Ms + Rb	AKOYA	ARH1001EA	Ready-to use
TBS 10X	SIGMA	T5912	1:10 in water

**Table 32.** Additional Automated Reagents

Reagents	Provider	Catalogue #	Dilution
RNAscope® 2.5 LS Hydrogen Peroxide	ACD	322440	Ready-to use
RNAscope® 2.5 LS Protease III	ACD	322440	Ready-to use
RNAscope® 2.5 LS Rinse	ACD	322440	Ready-to use
RNAscope® LS Multiplex AMP 1	ACD	322440	Ready-to use
RNAscope® LS Multiplex AMP 2	ACD	322440	Ready-to use
RNAscope® LS Multiplex AMP 3	ACD	322440	Ready-to use
RNAscope® LS Multiplex HRP C1	ACD	322440	Ready-to use
RNAscope® LS Multiplex HRP C2	ACD	322440	Ready-to use
RNAscope® LS Multiplex HRP Blocker	ACD	322440	Ready-to use
BOND Epitope Retrieval Solution 1	Leica	AR9961	Ready-to use
BOND Epitope Retrieval Solution 2	Leica	AR9640	Ready-to use
BOND Dewax Solution	Leica	AR9222	Ready-to use
BOND Wash Solution 10X Concentrate	Leica	AR9590	1:10 in water
Antibody Diluent / Block	AKOYA	ARD1001EA	Ready-to use
1X Plus Amplification Diluent	AKOYA	FP1498	Ready-to use
Opal Polymer HRP Ms + Rb	AKOYA	ARH1001EA	Ready-to use

42. Wash slides 3 times with TBST wash buffer. Dry slides using an absorbent paper without touching the tissue

**Table 33.** General expendables

Expendables	Provider
Immedge Hydrophobic pen	DAKO
Microscope slides SuperFrost Plus	Omnilab
Cover Glass 24×50 mm	Fisher Scientific
BOND 30ml Open containers	Leica
BOND 7ml Open containers*	Leica
BOND Research Detection System	Leica

**Table 34.** Equipment

Equipment	Provider
Microtome	THERMO
BOND RX System Automated slide stainer	LEICA Biosystem
Scanner Multispectral Vectra-Polaris	Perkin Elmer / AKOYA

**Table 35.** Software

Software	Provider
QuPath	Open web platform
HALO	Indica Lab

**Table 36.** Staining conditions for manual slide staining

RNAscope probes	Dilution	Secondary antibody	OPAL	Dilution
IFN $\lambda$ -1 – Human – C1	Ready to use	HRP-C1 ready to use	690	1:300
CD8A – Human – C1	Ready to use	HRP-C1 ready to use	690	1:300
CLEC9A – Human – C2	50x in C1 probe	HRP-C2 ready to use	570	1:300
Anti-cytokeratin	1:200	ImmPress anti-mouse HRP	520	1:150

43. Cover tissue with 150  $\mu$ l of ready to use goat anti-mouse HRP conjugated antibody (ImmPress kit) for 10min at RT
44. Wash slides 3 times with TBST wash buffer. Dry slides using an absorbent paper without touching the tissue
45. Cover tissue with 150  $\mu$ l of OPAL 520 reagent (see Table 29) for 10 min at RT
46. Wash slides 3 times with TBST wash buffer. Dry slides using an absorbent paper without touching the tissue
47. Wash slides with distilled water
48. Cover tissue with 3–4 drops of DAPI for 30s at RT
49. Wash slides with TBST wash buffer then with distilled water
50. Remove DAPI and immediately place 1 to 2 drops of Prolong Gold Antifade
51. Carefully place a glass coverslip over the tissue section.
52. Let slides dry, 30 min to overnight at RT in the dark
53. Store slides in the dark at 4°C
54. Clean the slide with alcohol before using the Vectra Polaris automated quantitative pathology imaging system (Perkin Elmer)

### 5.3.3 Automated slide staining

1. Put the slides in an oven at 60°C for 20 min
2. Put all the reagent and the slides on the Leica's rack. Table 37 summarizes the automated optimized immunofluorescence staining conditions for each marker
3. Put the slides on the Leica's rack and carefully place covertile over the tissue section.



**Table 37.** Conditions for automated immunofluorescence staining

RNAscope Probes	Dilution	Secondary antibody	OPAL	Dilution
IFN $\lambda$ -1 – Human – C1	Ready to use	HRP-C1 ready to use	690	1:150
CD8A – Human – C1	Ready to use	HRP-C1 ready to use	690	1:150
CLEC9A – Human – C2	50x in C1 probe	HRP-C2 ready to use	570	1:150
Anti-cytokeratin	1:200	ImmPress anti-mouse HRP	520	1:150

**Table 38.** Protocol steps

Protocol Step	Reagent	Incubation time (min)	Temperature (°C)
1	BOND Epitope Retrieval Solution 2	15	95
2	Bond Wash solution	5	RT
3	RNAscope® 2.5 LS Hydrogen Peroxide	10	RT
4	Bond Wash solution	5	RT
5	RNAscope® 2.5 LS Protease III	30	40
6	Hybridation IFN $\lambda$ -1 or CD8A/CLEC9A Probes	120	42
7	Bond Wash solution	9	42
8	RNAscope® LS Multiplex AMP 1	31	42
9	Bond Wash solution	6	RT
10	RNAscope® 2.5 LS Rinse	10	RT
11	RNAscope® LS Multiplex AMP 2	31	42
12	Bond Wash solution	6	RT
13	RNAscope® 2.5 LS Rinse	10	RT
14	Bond Wash solution	3	RT
15	RNAscope® LS Multiplex AMP 3	26	42
16	Bond Wash solution	5	RT
17	RNAscope® LS Multiplex HRP C1	16	42
18	Bond Wash solution	5	RT
19	OPAL 690	31	RT
20	Bond Wash solution	4	RT
21	RNAscope® LS Multiplex HRP Blocker	16	42
22	Bond Wash solution	4	RT
23	RNAscope® LS Multiplex HRP C2	16	42
24	Bond Wash solution	4	RT
25	OPAL 570	31	RT
26	Bond Wash solution	4	RT
27	RNAscope® LS Multiplex HRP Blocker	16	42
28	Bond Wash solution	12	RT
29	Antibody Diluent / Block	20	RT
30	Anti-cytokeratin	60	RT
31	Bond Wash solution	1	RT
32	Opal Polymer HRP Ms + Rb	15	RT
33	Bond Wash solution	1	RT
34	OPAL 520	10	RT
33	Bond Wash solution	2	RT
34	SPECTRAL DAPI	5	RT
35	Deionized	5	RT

4. Select the Leica Bond™ Dewax and Bond™ Wash steps before running the defined protocol as in Table 38:
5. After the staining, carefully wash the slides with distilled water
6. Let the slides wet at RT in a dark place, protect from light
7. Distribute 50  $\mu$ l of prolong gold antifade on the slide
8. Slowly lower a glass coverslip onto the slide. Try to avoid air bubbles
9. Let the slides wet at RT or at 4°C before performing the scan analysis
10. Afterward, the stained slides should be stored at 4°C protected from light
11. Clean the slide with alcohol before using the Vectra Polaris automated quantitative pathology imaging system (Perkin Elmer).

### 5.3.3.1 Top tricks and pitfalls.

- Manual staining: It is important to let all reagents equilibrate at RT
- Manual staining: do not let sections dry out between incubation steps. Make sure that the barrier is intact and that all solutions cover completely the tissue section. Work quickly
- Manual staining: It is important to keep tray warm during assay and keep the oven wet
- It is crucial to optimize the staining and imaging processes on each different tissue as auto-fluorescence will be different depending on the tissue type. Do not keep slides for more than one month. Stain as soon as possible.
- It is very important to cut tissue in RNase free conditions.
- To have the best staining it is important to use freshly cut sections (not older than approximately 1 month)

**Note:** It is in principle possible to combine in situ hybridization with antibody stainings for proteins of lower abundance than cytokeratins, including cDC1-specific proteins such as XCR1 (Figs. 16B, 16C). The validity of such stainings needs to be carefully validated even for antibodies known to work well in other staining protocols. One useful quality control is to test the validity and sensitivity of such antibody stainings by co-staining for RNA transcripts encoding for the protein of interest.

## 5.4 Data analysis

The multispectral imaging system enables the identification and downstream quantification of multiple overlapping biomarkers without the autofluorescence interference as signals are unmixed from one another.

- Using QuPath, we design a 1 mm grid on the whole slide scan and randomly selected eight regions of interest per slide
- We performed a tissue quality verification in the defined regions of interest, or re-generate eight regions
- We made a code attribution to each identified area and manually count *CLEC9A* and *IFN $\gamma$ -1* double or single positive cells with HALO software
- If events observed are rare, quantification can be done manually as described in Hubert *et al.* [60], however algorithm exists for automatic counting using the HALO software.

## 6 Quantitative image analysis of host-pathogen interactions in an in vitro 3D human lung/DC model

### 6.1 Introduction

3D *in vitro* models that recapitulate the *in vivo* lung tissue architecture and physiology are crucial to study immune-related (patho-)mechanisms during human diseases. This became even more evident with the emergence of SARS-CoV-2 in late 2019, which has given rise to an unprecedented global health crisis with

significant economical and societal consequences. Studies within sophisticated cell culture models might contribute to finding alternative treatment options for severe COVID-19 [74–77]. While different approaches to *in vitro* human lung models have already been developed [78–80], the role of DC and other immune cells is often neglected [8]. Previously described 3D models are already far superior to 2D monolayer cultures, as the differentiation in apical, basal and lateral cell structures allows to investigate tissue reactions to a plethora of chemicals and molecular gradients [74, 75]. Nevertheless, existing 3D models for epithelial respiratory tissues are still not optimal as they commonly lack immune cells; which precludes the analysis of innate immune cell activation and the interplay of these cells with non-immune tissue cells to explore potential targets for immunotherapies, e.g., upon *in vitro* infection using SARS-CoV-2-clinical specimen [74–76]. Here, we describe the setup of an optimized protocol for long-term 3D co-cultures of human primary respiratory epithelial cells and APC including MoDC, BDCA1<sup>+</sup> blood-derived DC, and macrophages (Fig. 17). In this system, primary epithelial cells from the upper (normal human bronchial epithelium, NHBE) or lower (small-airway epithelium, SAE) part of the airway tree are embedded in a birch-based, animal-free cellulose-like hydrogel (Growdex<sup>®</sup>), that mimics the extracellular matrix in which cells are surrounded *in vivo*. Besides that, Growdex<sup>®</sup> also accelerates cell proliferation and differentiation rates compared to rat-tail collagen, as we have previously shown [82]. Physiological conditions of parental tissues are recreated by establishing an air-liquid interface (ALI) culture seeding cells in Transwell filters. This results in differentiation of basal cells, ciliated cells and mucus-producing goblet cells [82]. Such Transwell-ALI-grown, highly differentiated epithelia can be equipped with DC and other APC to explore their response to infection with viruses, bacteria, or fungi and within these co-cultures many read-out parameters are feasible. For example, from one infected or control sample, we can measure trans-epithelial electrical resistance (TEER) to acquire tissue integrity, cytokines, and anaphylatoxins from basolateral supernatants. Most importantly, we can perform live or fixed cell imaging approaches, for instance 3D visualization of host-pathogen interactions, which are vital to characterize cellular processes, such as cell migration and differentiation. This highly differentiated lung and/or APC model has already been successfully used to study the cross-talk between viruses and cells of the airway in *A. fumigatus* [83, 84] and SARS-CoV-2 [73, 75] infected respiratory tissue.

### 6.2 Materials

#### 6.2.1 Reagents

Necessary reagents are listed in Tables 39–41.

#### 6.2.2 Equipment

Necessary equipment is listed in Table 42.

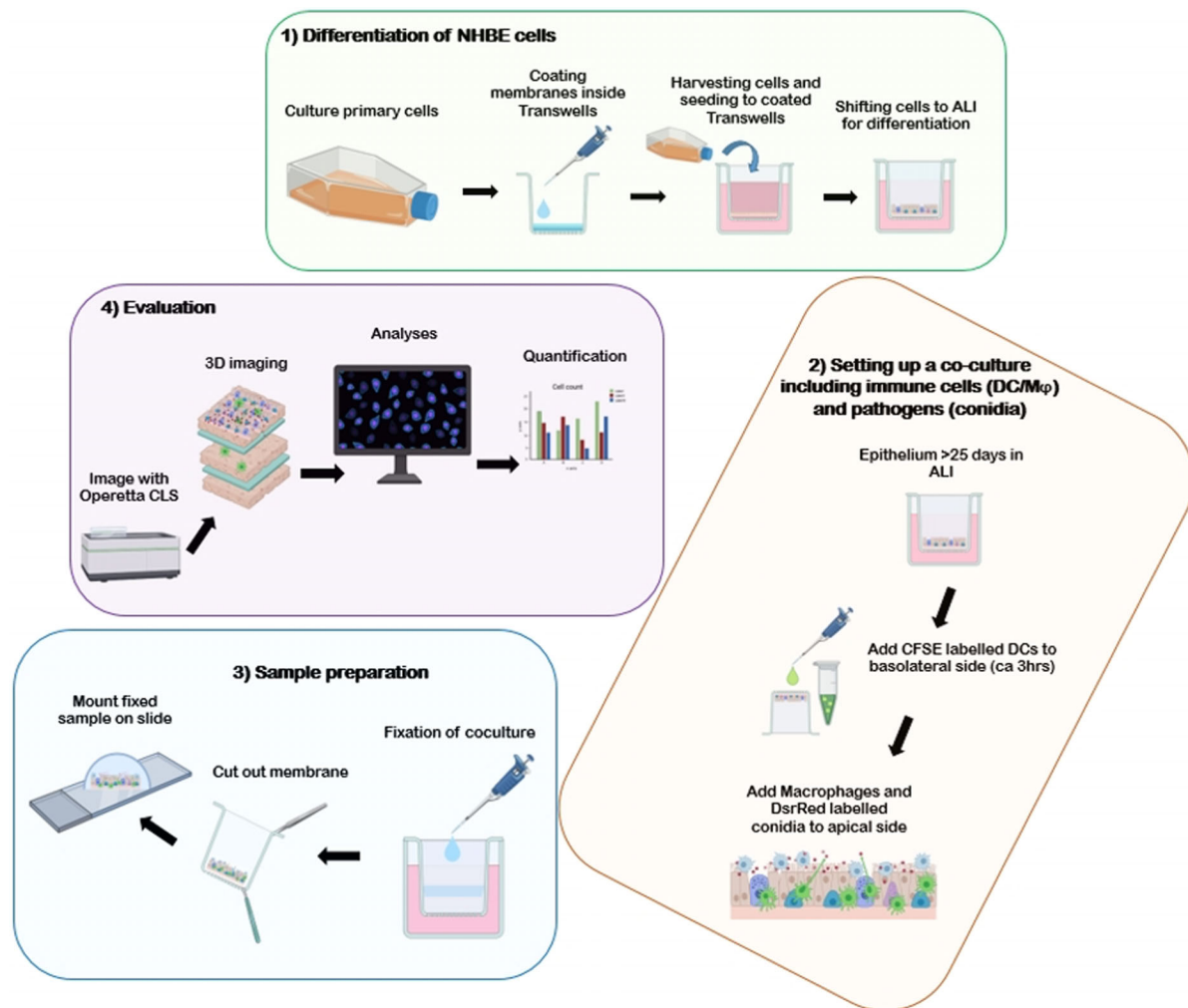


**Figure 17.** Overview of the key steps of Operetta CLS imaging and analyses using Harmony Software of infected epithelial/DC co-cultures. Figure created with BioRender.com.

**Table 39.** Antibodies

Antibody	Fluorochrome	Host	Provider	Catalogue #	Dilution
Acetylated Tubulin	Alexa 647	mouse-a-human	Abcam	ab218591	1:50
C3	Alexa 488	mouse-a-human	Dako/Agilent	F020102-2	1:50
CD11b	Alexa 488	mouse-a-human	BioLegend	301304	1:50
CD11c	Alexa 488	mouse-a-human	BioLegend	301601	1:50
CD14	PE	mouse-a-human	BioLegend	301801	1:50
CD19	APC	mouse-a-human	BioLegend	302201	1:50
CD209	PE	mouse-a-human	BD Pharmingen	5512165	1:50
CD3	Alexa 488	mouse-a-human	BioLegend	300406	1:50
CD83	APC	mouse-a-human	BD Pharmingen	551073	1:50
CD83	BV510	mouse-a-human	BD Pharmingen	563223	1:200
CD83	Alexa 647	mouse-a-human	BioLegend	305312	1:50
Ghost Dye	BV510	–	Tonbo Biosciences	13-870	1:500
Hoechst 33342	UV	–	Cell Signaling	4082	1:1000
Mucin5AC	Alexa 555	mouse-a-human	Abcam	ab218714	1:50
Phalloidin	Alexa 647	mouse-a-human	Abcam	ab176759	1:50
SARS-CoV-2-N	Alexa 594	Rabbit mAb	Sinobiological	40150-R019	1:50
SARS-CoV-2-S1	Alexa 594	Rabbit mAb	Sinobiological	40150-R007	1:50
WGA	Alexa 488	–	Biotium	29022	1:250

**Table 40.** General reagents

Reagent	Provider	Catalogue #
Animal component-free cell dissociation kit	STEMCELL, Cologne, Germany	05426
Carboxyfluorescein succinimidyl ester (CFSE)	Sigma Aldrich, St Louis, MO, USA	SCT110
CD1c (BDCA-1)+ Dendritic Cell Isolation Kit, human	Miltenyi Biotec	130-119475
CD14+ IMAG Beads, human	BD Biosciences	557769
Cytofix Fixation Buffer	BD Biosciences	554655
Dulbecco's Phosphate Buffered Saline	Sigma Aldrich, St Louis, MO, USA	D8537-1L
GrowDase®	a) UPM Biochemicals, b) Helsinki, Finland	c) 900102001 d)
GrowDex-T® stock solution	UPM Biochemicals, Helsinki, Finland	e) 200103002
GM-CSF	MACS Milenyi Biotec	130-093-862
Heparin Solution	STEMCELL, Cologne, Germany	07980
Hydrocortisone Solution	STEMCELL, Cologne, Germany	07925
IL-4 CC	PromoKine	C-61401
L-Glutamine solution	Sigma-Aldrich	G7513
Mowiol	Carl Roth	9002-89-5
NHBE cells	Lonza, Cologne, Germany	CC-2540-S
Perm/Wash Buffer for intracellular staining	BD Biosciences	554723
PneumaCult™-ALI Basal Medium	STEMCELL, Cologne, Germany	05002
PneumaCult™-ALI 10 × supplement	STEMCELL, Cologne, Germany	05003
PneumaCult™-ALI 100 × Maintenance supplement	STEMCELL, Cologne, Germany	05006
PneumaCult™-Ex Plus Basal Medium	STEMCELL, Cologne, Germany	05041
PneumaCult™-Ex Plus 50 × Supplement	STEMCELL, Cologne, Germany	05042

**Table 41.** Expendables

Expendables	Provider	Catalogue #
BD Imagnet	BD Biosciences	552311
Coverslips	Omnilab	5161050
Microscope slides SuperFrost Plus	Omnilab	5161155
Costar 6 Well Clear TC-Treated Multiple Well Plates	Costar	3506
Density gradient media: Ficoll-Paque Premium	GE Healthcare Bio-Sciences	17-5442-03
Microscope slides SuperFrost Plus	Omnilab	5161155
Transwell permeable supports, 6,5mm Insert for 24 well plates	Merck, Corning Costar	CLS3399

**Table 42.** Equipment

Equipment	Provider
Operetta CLS™	Perkin Elmer Cellular Technologies Germany GmbH, Hamburg, Germany
FACS Verse™	BD Biosciences

**Table 43.** Software

Software	Version	Provider
FlowJo	10.8	BD BioSciences
Harmony	4.9	Perkin Elmer Cellular Technologies Germany GmbH, Hamburg, Germany
Prism	9.2.0	GraphPad

## 6.2.3 Software

Necessary Software is listed in Table 43.

## 6.3 Step-by-step sample preparation

### 6.3.1 Epithelial/DC co-cultures for immunofluorescence stainings

#### 6.3.1.1 Reagent Setup Epithelial Cells.

1. Complete PneumaCult™-Ex Plus Medium: Thaw PneumaCult™-Ex Plus 50× Supplement at room temperature (15–25°C). Add 2ml 50× Supplement and 100 µl Hydrocortisone stock solution to 98ml of PneumaCult™-Ex Plus Basal Medium.
2. PneumaCult™-ALI Complete Base Medium: Thaw PneumaCult™-ALI 10× Supplement at room temperature (15–25°C). Mix gently without vortexing and add it to PneumaCult™-ALI Basal Medium 1:10.
3. PneumaCult™-ALI Maintenance Medium: Thaw PneumaCult™-Maintenance Supplement (100×) at room temperature (15–25°C). Add the following components to



49.15 ml PneumaCult™-ALI Complete Base medium; 500 µl PneumaCult™-ALI Maintenance Supplement; 100 µl Heparin Solution; 250 µl Hydrocortisone stock solution.

4. GrowDex-T Solution for seeding NHBE cells: Pre-warm Complete PneumaCult™-Ex Plus Medium in the water bath at 37°C. For the preparation of GrowDex® coating solution, the number of Transwell inserts needed has to be calculated first. To seed NHBE/SAE cells upside-down into Transwell inserts, a 0.5% GrowDex® solution was used. Thus, for preparing 1 ml of 0.5% GrowDex®, 333 µl of 1.5% stock solution is gently mixed with 567 µl of pre-warmed cell culture medium. The number of needed cells ( $1 \times 10^5$  per Transwell) is spun down and re-suspended in 100 µl of PneumaCult™-Ex Plus medium. The 100 µl of cell suspension is added to the GrowDex® solution by pipetting gently up and down.

#### 6.3.1.2 Top tricks and pitfalls.

- Mix components gently by pipetting up and down and avoid air bubbles as much as possible.
- During the preparation of the reagents and for all the following steps work under sterile conditions.
- All the prepared media can be stored for up to 2 weeks at a temperature of 2–8°C.

#### 6.3.1.3 Seeding of Primary Epithelial Lung Cells to Cell culture flask: Expansion Phase.

1. Prepare 100 ml of Complete PneumaCult™-Ex Plus medium;
2. Pre-heat 25 ml of the medium at 37°C;
3. Thaw primary respiratory cells at 37°C;
4. After thawing, immediately transfer cells to pre-warmed growth medium (Complete PneumaCult™-Ex Plus) in the cell culture flask (T75). Ideally  $0.5\text{--}1 \times 10^6$  cells should be seeded in a T75 cell culture flask to reach a confluence of 80% after 3 days;
5. Rinse the cryovial with 500 µl of pre-warmed growth medium and transfer it to the cell culture flask. Rinse the vial again to make sure that all cells have been transferred;
6. Incubate the flask at 37°C at 5% CO<sub>2</sub> until cells expand to the 80% confluence, which normally takes 3 days;
7. On day 2 of the expansion phase, 10 ml of the medium in the flask is exchanged with fresh and pre-heated growth medium.

#### 6.3.1.4 Top tricks and pitfalls.

- Pre-heat medium at 37°C for a minimum of 30 min before using it;
- NEVER thaw cells for more than 2 min at 37°C. When they are on 37°C frequently check on them and use them as soon as the ice is melted;
- Incubate the flask in the incubator in a lying, and not standing, position, so that cells can adhere to one side of it;

- The older the cell passage, the longer the expansion time will take. For example, with a passage > 4, a confluence of 80% will be reached after approximately 4 days. Overall, the use of cells from the first three passages is recommended because they can be frozen and further expanded, without losing any of the cellular features;
- When changing the medium, consider that cells are attaching to the bottom of the lying flask. Put the flask in a standing position under the hood and aspirate the medium in the furthest corner from where cells are adhering, in order to avoid scraping them.

#### 6.3.1.5 Harvesting of NHBE/SAE cells from T75 Cell Culture Flasks.

1. Prepare and pre-heated Complete PneumaCult™-Ex Plus Medium and D-PBS (without Mg<sup>2+</sup> and Ca<sup>2+</sup>);
2. Aspirate the medium from the T75 flask;
3. Wash the cells with 5ml pre-warmed D-PBS;
4. Aspirate the D-PBS and add 6ml of ACF Enzymatic Dissociation Solution;
5. Incubate at 37°C for 7–8min until cells start to detach from the bottom of the flask
6. Add 6ml of CF Enzymatic Inhibition Solution and mix by gently moving the flask;
7. Collect the cells in a 15 ml falcon using a 10ml serological pipette;
8. Centrifuge the Falcon at 1400RPM ( $350 \times g$ ) for 5min;
9. Aspirate the supernatant and resuspend in pre-warmed Complete PneumaCult™-Ex Plus Medium;
10. Count the cells using a Neubauer chamber or an automated cell counter;
11. Between  $1 \times 10^7$  and  $1.3 \times 10^7$  cells are harvested from the T75 cell culture flask after the first expansion cycle;
12. A total of  $1 \times 10^6$  cells are seeded in a new T75 cell culture flask for a new expansion cycle (*repeat from 3.1.2, thawing excluded*), frozen (*see 3.1.4*) or seed the harvested cells on Transwells (*see 3.1.5*).

#### 6.3.1.6 Top tricks and pitfalls.

- When you count cells and divide your culture in cells to be frozen/expanded and seeded, consider that for each Transwell insert you need  $1 \times 10^5$ .

#### 6.3.1.7 Freezing of non-seeded cells.

1. Cells that are not used immediately for further culture can be frozen up to passage 4, without losing any cellular features (ciliogenesis, proliferative capacities, mucus production);
2. The calculated cell number that will be seeded on the Transwell or be further expanded in a cell culture flask is divided from the one that will be frozen. Both of them are centrifuged at 1220RPM ( $350 \times g$ ) for 5 min;

- For cells that will be frozen the supernatant is aspirated and the pellet is directly resuspended using 500  $\mu$ l of Recovery cell culture freezing medium per 1 million cells;
- Cells are transferred to properly labeled cryovials in a freezing container for cell preservation to ensure a controlled-rate freezing. Cells are first put at  $-80^{\circ}\text{C}$  and, the next day they are switched to  $-150^{\circ}\text{C}$ .

#### 6.3.1.8 Seeding of NHBE/SAE cells onto Transwells.

- 100  $\mu$ l of 0.5% Growdex® solution are used (*Read Reagent Setup*) for each Transwell;
- Re-suspend cells in pre-warmed ( $37^{\circ}\text{C}$ ) Complete PneumaCult™-Ex Plus Basal Medium;
- Mix 1% Growdex® solution at a 1:1 ratio with cells;
- 100  $\mu$ l of 0.5% GrowDex®/cell mixture are added to the Transwell membrane;
- When cells are freshly seeded to Transwells, they undergo an expansion phase during the first 3–4 days. For this, cells have to be cultured under submerged conditions, meaning not only 500  $\mu$ l of PneumaCult™-Ex Plus Basal Medium is added to the basolateral chambers, but 100  $\mu$ l of medium is added additionally inside the Transwells (apical side);
- Change the medium every second day;
- Shift cells to ALI when a confluency of 80% is reached, which is usually reached after about 3 days.

#### 6.3.1.9 Top tricks and pitfalls.

- Calculation for 10 Transwells:  $1 \times 10^6$  cells are re-suspended in 100  $\mu$ l of prewarmed medium, cells are added to 333  $\mu$ l GrowDex® stock solution (1.5%) and 567  $\mu$ l diluent (medium);
- On each Transwell, 100  $\mu$ l of 0.5% GrowDex® containing  $1 \times 10^5$  cells are seeded.

#### 6.3.1.10 Shifting to ALI.

- Prepare and pre-heat at  $37^{\circ}\text{C}$  PneumaCult™-ALI Maintenance medium, considering that for every Transwell 500  $\mu$ l of medium are needed;
- Aspirate the medium at both sides of the membrane and shift the Transwells to new wells, containing ALI medium instead of growth medium.
- Change the medium every second day.

#### 6.3.1.11 Top tricks and pitfalls.

- Epithelial cells grown on rat-tail collagen are ready to be used in further experiments at day 21, while Growdex® containing cultures are ready to be used after 15 days;
- If you want to keep cells in culture for a longer time, carefully aspirate the mucus once a week using a 100  $\mu$ l tip.

### 6.3.2 Isolation of monocytes and MoDC differentiation or optionally: Preparation of DC directly from human blood

**6.3.2.1 Generation of Human MoDC from Whole Blood.** This procedure was described by us in detail in the Journal of Visualized Experiments in 2016 > Link: <https://doi.org/10.3791/54968>.

#### 6.3.2.2 Isolation of BDCA-1<sup>+</sup> DC from Whole Blood.

- BDCA-1<sup>+</sup> DC were isolated directly from blood collection bags using the human CD1c (BDCA-1)<sup>+</sup> DC Isolation Kit (Miltenyi)
- PBMCs are isolated as described in <https://doi.org/10.3791/54968>;
- BDCA-1<sup>+</sup> DC are isolated according to the protocol provided by Miltenyi as described
- under <https://www.miltenyibiotec.com/upload/assets/IM0020760.PDF>.

#### 6.3.2.3 CFSE Labeling of DC.

- Spin DC @1000 rpm, 5 min,  $4^{\circ}\text{C}$
- Re-suspend at  $5 \times 10^6$  cells/ml in PBS containing 2.5  $\mu\text{M}$  CFDA-SE (carboxyfluorescein diacetate succinimidyl ester)
- Incubate at  $37^{\circ}\text{C}$  for 10 min to allow cell permeation of CFDA-SE and conversion to CFSE (carboxyfluorescein succinimidyl ester) by intracellular esterases, that forms covalent dye-protein conjugates resulting in live cells with an intracellular fluorescent label;
- Add equal volume of culture media containing serum (quenching) to the cells/CFSE solution for 5min
- Wash twice with culture media
- Cells are now fluorescently labeled.

#### 6.3.2.4 Top tricks and pitfalls.

- Cytotoxic side effects of CFSE labeling may arise at higher labeling concentrations and/or longer incubation times. Therefore, CFSE staining is performed with relatively low concentrations in short-term incubation, from 0.5  $\mu\text{M}$  (low fluorescence intensity) to 5  $\mu\text{M}$  (high fluorescence intensity).
- CFSE is amine group reactive > Avoid buffers containing primary amines during the CFSE labeling step.

### 6.3.3 Epithelial/DC co-cultures

- Use fully differentiated NHBE/SAE tissues in ALI for co-culturing with DC or other immune cells
- Flip fully differentiated ALI cultures under a hood using a forceps and place it into a 6-well plate to have the basolateral filter-side facing up
- Add  $5 \times 10^5$  CFSE-labeled MoDC or BDCA-1<sup>+</sup> cDC in 100  $\mu$ l PneumaCult™-ALI to the basolateral side of the Transwell

filter, close lid of the 6-well plate carefully and make sure the lid is not touching the seeded drop

4. Incubate for 2–3 h at 37°C/5%CO<sub>2</sub>
5. After the incubation time, carefully take the six-well plate under a hood
6. Place the epithelial/DC co-cultures back into a 24-well plate with DC on the basolateral side in 700 µl PneumaCult™-ALI medium (submerged) and apical side of epithelia at air phase ('normal' orientation)
7. Co-cultures are now ready for being challenged with pathogens (e.g., a dsRed strain of *Aspergillus fumigatus*, see [83]).

#### 6.3.3.1 Top tricks and pitfalls.

- Take special care for closing the six-well plate when cells are seeded upside-down on the Transwells or when DC are added to the basolateral side of the cells. Make sure the lid is not touching the liquid drop on the inverted Transwells.

### 6.3.4 Immunofluorescence (IF) staining of Epithelial/DC co-cultures and pathogens

#### 6.3.4.1 DC and pathogens: IF for imaging.

1. DC can be labeled with CFSE to perform live cell analysis such as migration (see 3.6.5. *Migration analysis*) or determine viral/DC co-localization within epithelial tissues using fixed cells (see 3.5.1 *Useful parameters for monitoring pathogen interactions in epithelial/DC co-cultures*).
2. For pathogen detection with image analysis, fluorescently labeled pathogens or virus-like particles (for live cell approaches) can be used, e.g., dsRed *Aspergillus fumigatus*, mCherry-tagged SARS-CoV-2 or HIV-1
3. Instead of labeling DC using CFSE, other DC markers (extra- and intracellular) can be applied to monitor DC activation/maturation (e.g., CD40, CD80, CD86, CD83, or CCR7) or intracellular localization of ingested particles (e.g., Rab5, Rab7, CD71, EEA-1, Lamp-1), dependent on the research question. **Note:** for these analyses, tissues have to be fixed following treatment/infection (see. 3.4.2 *IF of fully differentiated epithelia*)

#### 6.3.4.2 IF of fully differentiated epithelia.

1. After infection the cells are fixed over night at 4°C using the Cytofix fixation buffer (100 µl apical, 700 µl basolateral)
2. Following fixation, the filter is washed once using sterile-filtered D-PBS
3. The Transwell filter is cut into two halves by using a sharp scalpel to evaluate more than 2 to 3 markers per filter.
4. By using forceps, each half is removed from the Transwell clip and transferred upside down into 1× Perm/Wash solution

(50 µl drop on a parafilm) for 30 min (room temperature (RT)) to permeabilize the cells.

5. Dilute the primary antibodies or dyes within a mastermix in the Perm/Wash solution at the working concentrations stated above (in the Reagents list). To distinguish the different types of cells in the differentiated tissue, we suggest using conjugated antibodies against Mucin5Ac and acetylated tubulin, which will respectively stain goblet and ciliated cells, allowing the measurement of cell-specific effects of pathogen exposure;
6. Primary antibodies and dyes that can be used in our co-culture system are: *Epithelial cells* – e.g., acetylated tubulin, MUC5AC, MUC16, Occludin, ZO-1, phalloidin, KRT5; *DC* – e.g., CD11c, CD1a, C-type lectins (DC-SIGN, DEC-205, CD207/Langerin), CD83, CD86, CD80, CD40, CCR5, CCR7; *Viruses*: SARS-CoV-2-S1, SARS-CoV-2-N, HIV-1-KC57, mCherry-tagged HIV or VLPs; *Fungi*: dsRed-*Aspergillus fumigatus*
7. Each half of the filter is put into 50 µl of Ab mastermix after permeabilization;
8. Incubate 3 h at RT in a humidified chamber on a parafilm;
9. Wash 1×5 min using Perm/Wash;
10. Wash 2×5 min using sterile-filtered D-PBS;
11. Put a drop of Mowiol mounting medium on a microscope slide. Place the 3D culture facing upwards on the microscope slide and add one further drop of mounting medium on top of the 3D culture. Cover the 3D culture with a cover glass while taking care not to create air bubbles, then seal with nail varnish or tape. If using nail varnish, leave to dry for 10–30 min at room temperature.
12. The sample is now ready for imaging by HCS using the Operetta CLS (Perkin Elmer)

#### 6.3.4.3 Top tricks and pitfalls.

- Cutting the Transwell filter in two halves needs experience and training. If untrained, first, perform just one staining using the whole filter. When becoming familiar with the handling of the filter, try cutting the filters in two halves for getting the most information out of one filter.
- Take care not to flip the filter membrane when putting it into the antibody mastermix on the parafilm.
- Longer incubation times of fluorescently labeled antibodies are needed (at least 3 h at room temperature) due to the thickness of the fully differentiated epithelia.
- During this step, take care that the antibody solution does not evaporate, in case add 1× Perm/Wash buffer during the incubation time.

### 6.3.5 Imaging of host-pathogen interactions using the Operetta CLS™

The Operetta CLS™ high-content analysis system (HCS) provides a unique combination of technologies allowing a fast and gentle

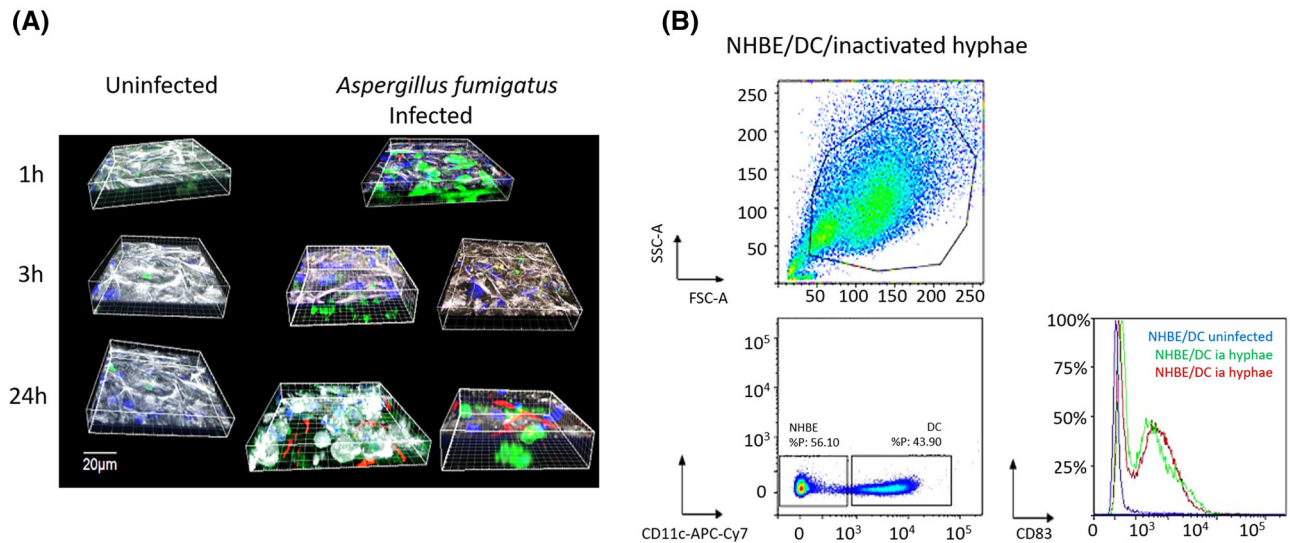


**Figure 18.** Analysis of DC in the human 3D co-culture model. (A) 3D illustration of DC/Aspergillus interactions. On the left, uninfected control cells over time are depicted to exclude unspecific migration of DC to the apical side of the epithelium. Right: Basolaterally added, CFSE-labeled DC (green) are co-localizing with dsRed Aspergilli already after 3 h (yellow dots) and DC can be found alongside fungal hyphae due to destruction of the epithelia (white) by fungal toxins after 24 h. (B) Flow cytometric analysis of DC isolated from the co-culture model. Cells were released from the scaffold by GrowDase treatment and subsequently analyzed for maturation. Only live cells were gated (upper panel), then CD11c-negative cells excluded (lower panel, left) and DC maturation upon exposure to inactivated fungal hyphae analyzed using a CD83-BV510 labeled antibody (lower panel, right). An overlay of control cells (blue) and fungus-treated cells (green and red) is depicted.

imaging process due to LED light source and confocal spinning disk technology. It enables efficient background rejection, live cell analyses and 3D imaging of deep tissues (as our Transwell-grown epithelial/DC co-culture model). Moreover, rapid high throughput analyses can be performed, if using the multiwell plate format. This is—of course—not possible with our Transwell-grown epithelial/DC co-culture model, but for DC monolayers this is a very convenient method to do rapid and unbiased quantitative and confocal image analysis of up to 10 parameters (brightfield, digital phase contrast, 8 fluorescent markers) in, e.g., a 96-well format. Thus, it is a very versatile tool allowing not only high content screening, but also more demanding applications, such as fixed- and live-cell assays, complex cell models or FRET.

**General remark:** While this protocol specifically refers to Operetta CLS and Harmony software for imaging and data analysis, a similar workflow could be implemented and reproduced in other platforms for confocal images analysis (such as Amira, Imaris, ZEN, LAS X, FIJI, and ImageJ).

#### 6.3.5.1 Useful parameters for monitoring pathogen interactions in epithelial/DC co-cultures.

1. To evaluate the functionality of the inserted DC into the co-culture system upon pathogenic challenge, several parameters can be used:
  - 1a. Monitoring co-localization of CFSE-labeled DC (green) with e.g. dsRed *Aspergillus fumigatus* (red) > overlay (= co-localization) appears yellow; in this case, the epithelium is stained using occludin to analyze tissue integrity or destruc-

tion mediated by the pathogen (Fig. 18A). Here, the interaction of the pathogen with DC within the tissue co-culture is assessed using the Operetta CLS system. For this, a time course is performed, in Fig. 18A below, interactions were monitored after 1, 3, and 24 h. Transwells are infected and the reaction is stopped at indicated times using 4% paraformaldehyde. After fixation, co-cultures are permeabilized (Cell Permeabilization Buffer, Biolegend) and counterstained using an occludin Ab for visualizing epithelial cells as described (see 3.4.2). Microscopic analysis creating XYZ stacks is performed by defining the fluorescence used (CFSE, dsRed, Höchst for nuclei, Alexa647 for occluding) and first and bottom plane of the stack. After characterizing the height of the stack, the run is started and the image analyzed using XYZ analysis and 3D analysis (Fig. 18A). Useful parameters to measure here are, e.g., whether DC sense the pathogen added, when the sensing starts, if pathogens are internalized and processed, quantifying pathogens ingested by DC, or if pathogens cause maturation of DC (see 1c). For example, in this experiment we found by image analysis that DC within the epithelial tissue already interact with pathogenic fungi after 1 h, with even more co-localization after 3 h and most interactions of DC with fungal hyphae after 24 h and destruction of epithelia by fungal toxins (Fig. 18A). Files can be easily exported and analyzed on other platforms for image analysis (e.g. Imaris, ImageJ, FIJI, Huygens, ZEN, LAS X).

- 1b. Maturation and activation of pathogen-exposed DC can be monitored using characteristic markers, e.g. CD83, CD86, HLA-DR, CCR7, DC-SIGN (CD209), CD11b, CD11c. Analysis is performed by either confocal imaging using fluorescent markers other than the ones already in use. For these analyses, it is more



convenient to use unlabeled DC instead of CFSE-labeled DC to save one fluorescent channel. They are applied to the system and then a combination of, e.g., CD83-APC, CD86-Alexa488, CCR7-Alexa700, CD11c-BV510 can be added to characterize the DC phenotype. Staining and analysis are performed on fixed cells as described in 3.4.2 and 3.5.1 (1a).

- 1c. *Alternatively*: Epithelial cells and DC can be released from the birch-based scaffold by using GrowDase® (= cellulose, UPM Biomedicals) for degradation of GrowDex®. Thereby, enzymes specifically degrade cellulose to soluble glucose without affecting cells. This is a huge advantage compared to the use of rat-tail collagen, because the degradation of the collagen scaffold by collagenase also affects—of course—human cells. Detailed down-stream analyses of DC following GrowDase® degradation, like flow cytometric analysis or immunohistochemistry and SEM are also possible after GrowDase treatment (Fig. 18). To distinguish DC from epithelial cells, markers not expressed on epithelial cells, e.g., CD11c, are used for gating strategies, and in addition, maturation and activation markers can be applied (Fig. 18B).
- 1d. *Alternatively*: Uninfected and infected co-cultures can be lysed for RNA isolation and further for down-stream qPCR analyses.
- 1e. Not only DC, but also changes in the epithelia can be analyzed within this system, e.g., changes in mucus composition using either confocal imaging or proteomic analyses of collected mucus, tissue destruction by TEER (trans-epithelial electrical resistance) measurements or confocal imaging (see Fig. 18A, 24 h time-point *Aspergillus*-infected).
- 1f. Moreover, basolateral supernatants (or subnatants) can be used for examination of cytokine and anaphylatoxin release by Luminex or qPCR measurements, or for determination of viral load (virus released into the subnatant).

#### 6.3.5.2 Image analysis of slides using Harmony™ on Operetta CLS™.

1. After switching on the Operetta CLS™ and the Harmony PC, a log in into Harmony™ software is required.
2. The Harmony software is built up in 4 tabs (Setup, Measurement, Image Analysis, Evaluation) and no other software is needed for quantitative analysis in high throughput or from slides.
3. Tab 1 *SETUP*: Use the setup tab to load or define an experiment, including, plate format (slide, slide holder for up to 4 slides, 96- to 1536-well format), objective type, optical mode (non-confocal/confocal), binning, temperature on/off, CO<sub>2</sub> on/off, channel and exposure settings, plate and well layout, stack, time series, and online jobs. An exact description of the experimental setup can be found in the Operetta CLS Application Guide, chapter 2 for experimental setup and chapter 1.5 for optical modes;
4. Perform a test measurement under the Setup tab to test current experiment settings and correct within the Setup tab, if

necessary. The test measurement is used to check for compatibility of combined plate type and objective.

**Note:** Setup experiments can be saved as a template and recalled at next use.

5. Tab 2 *MEASUREMENT*: Use this tab to run the experiment (Fig. 19A). The “Run experiment” tab is the second tab. After pushing the START button, the measurement progress is indicated by color of wells, fields and stack planes (orange) in real-time.
6. Tab 3 *IMAGE ANALYSIS*: This tab is used for automated image analysis for image detection and quantitation. An example for image analysis of DC co-localizing with dsRed *Aspergillus terreus* is given in section 6.3.6.
7. Tab 4 *EVALUATION*: This tab can be used for evaluating measurements and depicting these graphically (Fig. 19B)
8. Place your slide into the slide holder, with the apical side facing down
9. In the Setup tab, exposure times, stack etc. are set using the 5xAIR to give an overview of the whole Transwell filter
10. For more detailed analysis of DC-pathogen interactions within a mucosal tissue, the 40xWATER or 63xWATER objectives are used (see Fig. 18A).

#### 6.3.5.3 Top tricks and pitfalls.

- Smaller plate formats can be programmed in the Setup tab. Please ensure to adhere to the plate format specifications provided by the manufacturer.
- Values from the evaluation tab can easily be exported to Excel or GraphPad
- Sometimes it is difficult to finding the correct plane. TIP: using the 5xAIR objective, the whole filter containing epithelial cells and DC can be monitored > after taking a test image, right-mouse click on the test image and select ‘Background for well’ > this helps to find the ROI, if then choosing an objective with higher magnification, e.g. 40x or 63x water immersion objectives

### 6.4 Combined Image and Data analysis using the Harmony software

The Harmony™ high-content imaging and analysis software allows an easy set-up of assays, automation of experiments, image acquisition and data analysis. Additionally, the software contains a full range of incorporated ready-made-solutions (RMS) enabling analysis of most common assays, e.g. cell viability, apoptosis, cell cycle, cell proliferation, cytoskeletal rearrangement, receptor translocation, spot analysis, cell migration etc. that can be adapted to the individual applications.

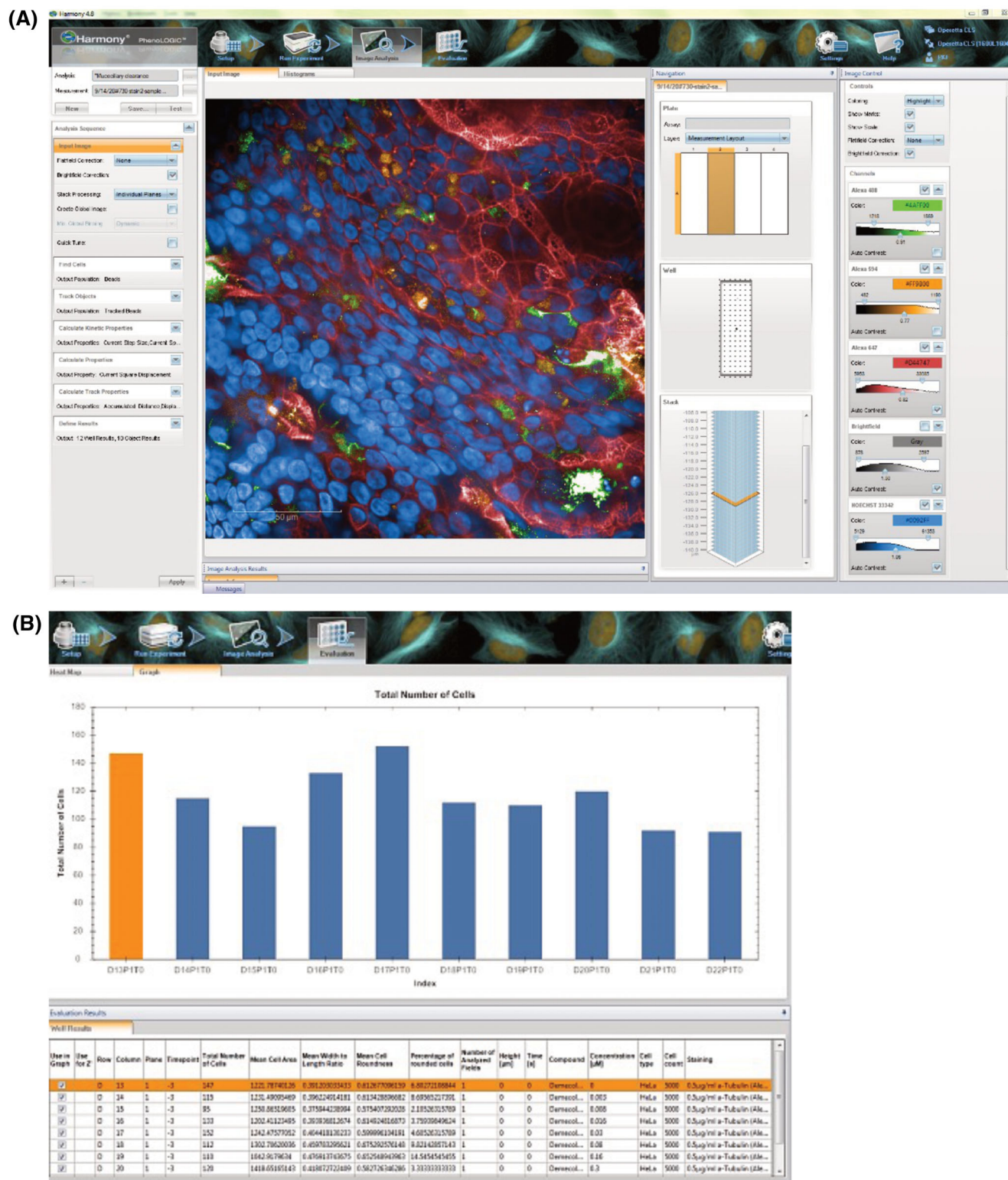


**Figure 19.** Setup of image analysis using the Harmony software. (A) Exemplary illustration of the 'Run experiment' tab to start the experiment and follow its progress. (B) Graphical depiction of exemplary measurements in the 'Evaluation' tab.

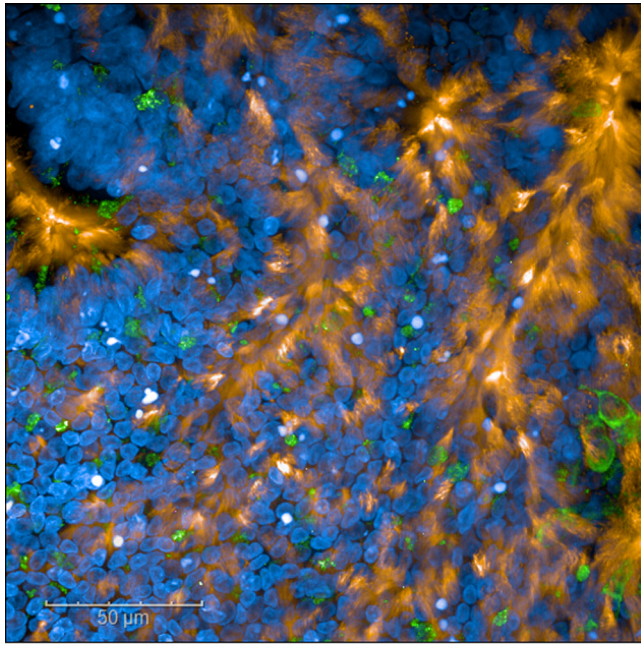


**Figure 20.** Analyzing epithelial cell types in co-cultures. To distinguish between goblet and ciliated cells within differentiated normal human bronchial epithelial cell cultures, cells were stained using acetylated tubulin for ciliated cells (orange) and MUC5AC for goblet cells (green). In addition, nuclei were visualized with Hoechst. Images were taken using the Operetta CLS system and the 40x water objective.

**Note:** All confocal imaging files can be easily exported to other platforms for downstream analysis (such as ImageJ, Imaris, Huygens, ZEN, LAS X, FIJI).

#### 6.4.1 Discrimination of cells within co-cultures

To study the various cell types within the co-culture system, specific markers can be used for cell type identification

Examples for antibodies useful for the identification of epithelial cell types are:

Acetylated tubulin (for ciliated cells), MUC5AC (mucus-producing cells) and KRT5 (basal cells); see also Fig. 20. Furthermore, DC within the system can in addition be assessed by using characteristic markers dependent on the DC subset (e.g., CD1a, CD11c, DC-SIGN).

#### 6.4.2 Live/Dead cell analysis

The 'RMS Live/Dead Cell Counting' is an easy way to quantify the percentage of cells in your assay that are responding to cytotoxic compounds, pathogens or secreted toxins from pathogens. The RMS identifies nuclei in the building block 'Find nuclei' of the Harmony software and within this region detects the amount of dead cell stain. Building blocks for this analysis are already integrated in the RMS Live/Dead Cell Counting. Further building blocks can be incorporated in the analysis depending on the user-

specific experiment, e.g. to evaluate live or dead DC, a building block using a specific DC marker can be added in between the nuclei and dead cell stain building block. The ROI can be determined by adding the fluorochrome-coupled DC-specific antibodies (e.g., CD11c for all DC).

How to create Live Cell Analysis:

1. Determine the best method for nuclear detection and tune parameters for including all nuclei on the view, adjust the intensity threshold if needed.
2. Select DC within the epithelial/DC co-cultures by choosing the fluorescence of the DC marker in a next building block, e.g. use building block 'find cytoplasm' and choose Alexa488 (i.e., the label of the CD11c antibody) > this is the region of the DC within the tissue model
3. Select dead stain marker in the next building block (e.g., LIVE/DEAD dyes (ThermoFisher), BOBO-3, GhostDye, etc.) and choose Alexa488 as ROI > this enables calculation of live/dead DC upon treatment/infection also within a 3D tissue model containing in addition epithelial cells.

#### 6.4.3 XYZ- and 3D view of pathogen-DC interactions

**XYZ View:** The XYZ-view displays the layers of a stack measurement in a special viewer of the Harmony software, where sectional planes in x, y- and z-direction are illustrated. The X-Y or top view of the stack is the large one in the middle, X-Z view at the top (= front view), and Y-Z (right side view) at the left (Fig. 21A).

The XYZ-view is created by:

1. Loading a suitable stack measurement
2. Selecting multiple planes from a single well
3. Processing the stack using either MAXIMUM PROJECTION (2D analysis) or 3D ANALYSIS: the XYZ view is calculated, which may take several minutes dependent on the data processed
4. Opening the XYZ View tab, that allows dragging the viewpoint in one of the three sections of the view. The other sectional planes are updated accordingly

**3D View:** Here the selected planes of a stack are used for 3D calculation of an image (Fig. 18A and Fig. 21B).

Instead of single images or maximum projection, a whole 3D image is generated. The 3D-view is created by:

1. Loading a suitable stack measurement
2. Selecting multiple planes from a single well to define the 3D image cube
3. The Z-resolution depends on the stack size
4. 3D calculation can take some time



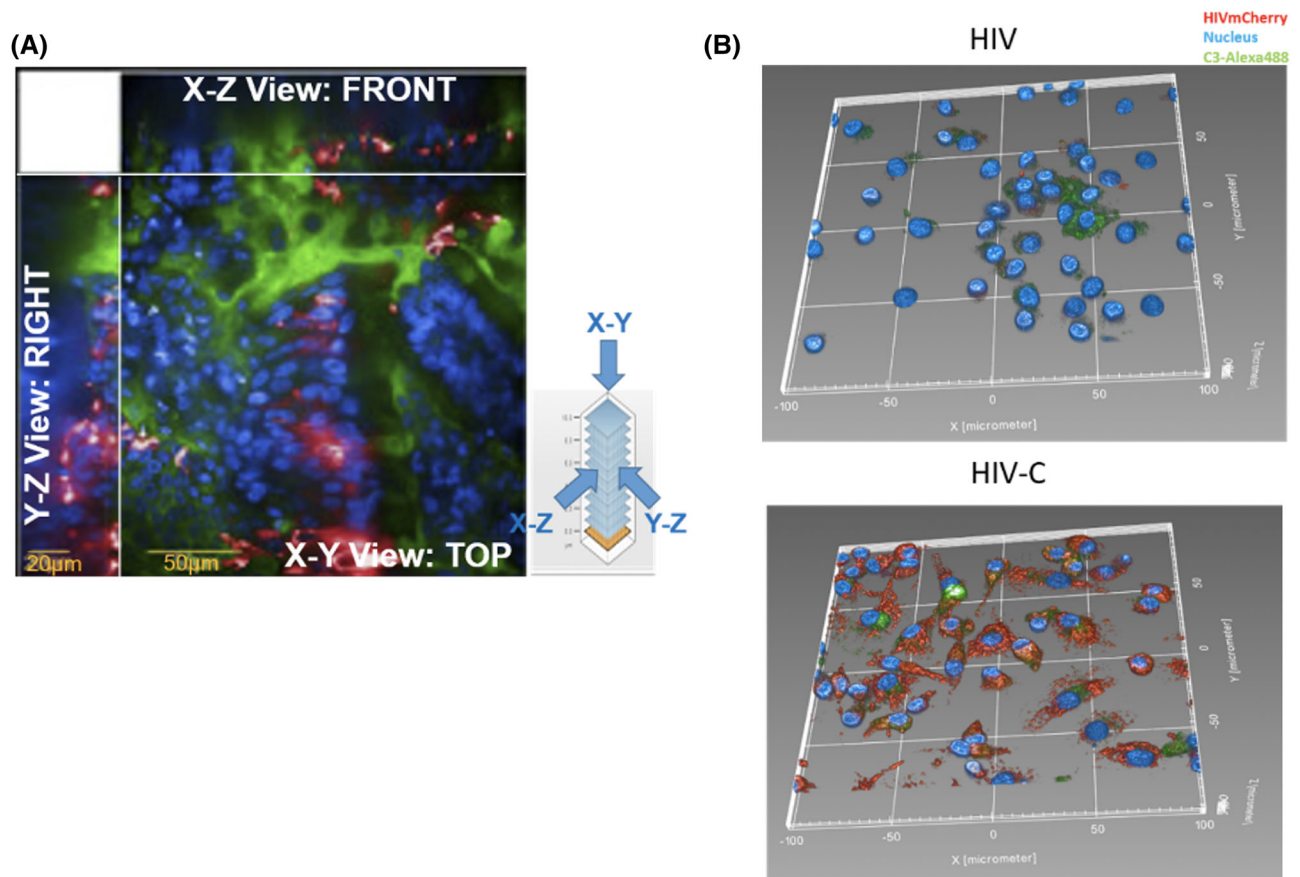


**Figure 21.** Analyzing virus-infected co-cultures. (A) XYZ View of virus-infected epithelial/DC co-cultures. Blue: nuclei (Hoechst), green: cilia (acetylated tubulin), red: SARS-CoV-2 (B) 3D analysis of DC infected with non-opsonized HIV-1 (left) or HIV-C (right). HCS revealed that mCherry tagged HIV-C (red, right) strongly infects DC and the virus is localized in both cytoplasm and endosomal compartments (not shown). In contrast, non-opsonized HIV-1 caused a low-productive infection of DC and the virus was only found in endosomal compartments (red, left). In addition, intracellular C3 was stained (C3-Alexa488, green) and the nucleus using Hoechst (blue).

#### 6.4.4 Top tricks and pitfalls

- By these 2 analysis modes pathogen-DC interactions can be monitored within a thick epithelial layer more closely and it can be determined using appropriate markers or treatment methods (4°C vs. 37°C), if the pathogen is internalized or solely bound to the surface of the cells.
- XYZ analysis cannot be combined with DPC
- 3D analysis cannot be combined with tracking objects, global images and DPC
- In 3D mode a powerful graphic card is required, otherwise the processing can be slow and software may even crash.

#### 6.4.5 Spot Analysis

This analysis is a valuable tool for enabling detection and quantification of spots (viruses, peroxisomes, endosomes etc.) in DC. If using a second appropriate marker, e.g., cytoplasmic or endosomal, the localization of the virus can be assessed by this method. For this, standalone building blocks in the Harmony software are

combined, that can be saved and recalled, if performing spot analysis more often. Thus, a user-specific RMS is generated this way. This analysis was already recently published by our group [74, 85].

How to build a RMS spot analysis is shown below, using HIV-1-infected DC as example:

1. Create a blank analysis sequence in the image analysis tab
2. Find Nuclei (choose nuclear stain)
3. Find Cytoplasm (choose cytoplasmic or endoplasmic stain, dependent on the read-out)
4. Remove Cells at the image borders to include only fully visible objects
5. Find spots (e.g., choose the mCherry channel for mCherry-tagged HIV-1) of the selected cell population
6. Report useful quality control parameters
7. Report single cell results
8. Run analysis
9. Determine spots co-localizing with a cytoplasmic or endoplasmic marker to quantify HIV-1 internalized in intracellular compartments or cytoplasmic HIV-1 particles



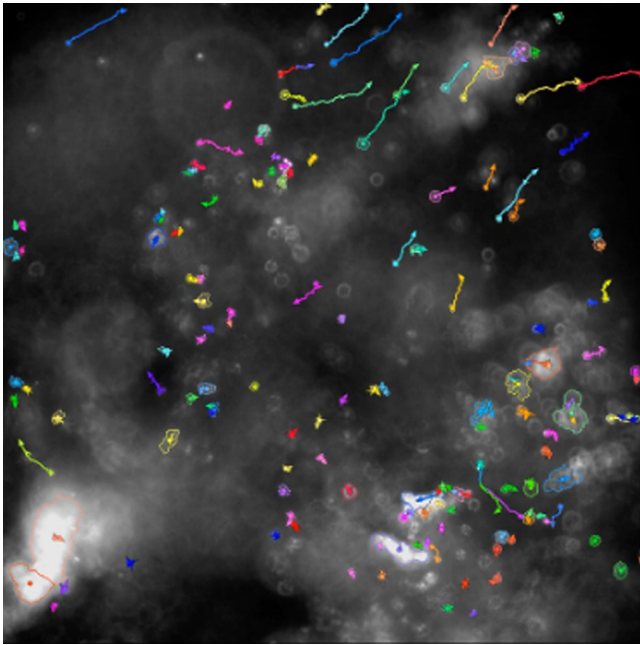


**Figure 22.** Analysis of DC migration. The image shows the tracking of CFSE-labeled DC migrating within the epithelial barrier model using the CellMigration-1 RMS within the Harmony Software.

10. Illustration of co-localized spots can be depicted within Harmony software.

#### 6.4.6 Migration Analysis (RMS, Harmony software) of DC

Due to much more complex shape of 3D objects compared to 2D, more morphology properties are necessary. Therefore, the set of measures within the Harmony software is designed to also enable identification of object orientation to evaluate the direction of migration. DC migration after pathogen recognition at entry sites plays a major role to initiating adaptive immune responses within the proximate lymph node. DC migration following pathogen exposure towards a chemokine-coated open area (e.g., CCL19 and/or CCL21) that separates the cell layer from background can be monitored using the Harmony CellMigration-1 RMS. Unstimulated and infected CFSE-labeled DC can be tracked over time and quantified within the open area (Fig. 22).

The procedure for live cell imaging is as follows:

1. The co-culture is infected with (optional: mCherry-tagged or dsRed-tagged) pathogens or VLPs.
2. The Transwell filter is cut out and transferred to a CCL19/21-coated glass bottom dish.
3. Live cell imaging of migrating CFSE-labeled DC within the epithelial barrier model and towards CCR7 ligands is monitored using the temperature and CO<sub>2</sub> option (TCO) at 37°C/5% CO<sub>2</sub> and time series measurements. Time points are processed as fast as possible or a fixed interval.

4. Live cell imaging is performed overnight and one large measurement including various time points is generated.
5. In the image analysis mode, all time points are chosen for creating a time window.
6. Objects are tracked over time within the time window, which allows calculating DC migration (speed in  $\mu\text{m/s}$ ) following pathogen exposure compared to mock-treated DC or LPS-loaded DC (Fig. 22).

Alternatively, emigrated unlabeled DC can be collected, transferred to slides or 96-well plates (Cell Carrier Ultra, Perkin Elmer) and in addition stained using markers associated with DC activation, maturation or infection (see section 6.3.4).

**Note:** The subsequent analysis of emigrated DC for markers associated with DC activation, maturation or response to infection can be performed by different analyses techniques such as flow cytometry (see Fig. 18).

**Acknowledgements:** This collection represents key protocols routinely used by the authors, which hopefully will be useful to others in the field. Notably, a number of other methods for microscopy-based analysis of DC are used by other colleagues, and we have tried to mention them wherever possible. We apologize to colleagues whose work we have not included.

Section 4:

This work was supported by the Deutsche Forschungsgemeinschaft (DFG, German Research Foundation - project numbers 442405234; 424926990; 449174900 and 61704785), the German Cancer Aid (DKH, 70113847) and the Elite Network of Bavaria, Bavarian State Ministry of Science and the Arts (N-LW-2016-370) to J.P.B.; a DFG Emmy Noether Grant (Schr 1444/1-1) and an ERC Starting Grant (ERC-2016-STG-715182) to B.U.S.

Section 5:

This work was supported by funding from INSERM, INCA (PLBIO INCa), ANRS, ARC, Ligue contre le Cancer (Régionale Auvergne-Rhône-Alpes et Saône-et-Loire, Comité de la Savoie); We would like to thank our financial supports: the Région Auvergne-Rhône-Alpes and the ANR, the SIRIC project (LYRIC, grant no. INCa\_4664), and the LABEX DEVweCAN (ANR-10-LABX-0061) of the University of Lyon.

**Conflict of interest:** The authors declare no commercial or financial conflict of interest.

**Author contributions:** Section 1: Lijian Li and Stefan Uderhardt; lead author Stefan Uderhardt

Section 2: David A. Bejarano and Andreas Schlitzer; lead author Andreas Schlitzer

Section 3: Luise Rupp and Marc Schmitz; lead author Marc Schmitz

Section 4: Philippa Meiser, Felix Bayerl, Anna-Marie Pedde, Barbara U. Schraml and Jan P. Böttcher; lead author Jan P. Böttcher

Section 5: Anne-Claire Doffin\*, Elisa Gobbini\*, Margaux Hubert and Jenny Valladeau-Guilemond; \*contributed equally, lead author Jenny Valladeau-Guilemond

Section 6: Giulia Bertacchi, Viktoria Zaderer, Wilfried Posch and Doris Wilflingseder; lead author Doris Wilflingseder

**Data availability statement:** The data used to exemplify key protocol steps in this study are available from the section lead authors upon reasonable request.

**Peer review:** The peer review history for this article is available at <https://publons.com/publon/10.1002/eji.202249923>

## References

- Guilliams, M., Ginhoux, F., Jakubzick, C., Naik, S. H., Onai, N., Schraml, B. U., Segura, E. et al., Dendritic cells, monocytes and macrophages: a unified nomenclature based on ontogeny. *Nat. Rev. Immunol.* 2014.14: 571–578.
- Nutt, S. L. and Chopin, M., Transcriptional Networks Driving Dendritic Cell Differentiation and Function. *Immunity.* 2020. 52: 942–956.
- Cabeza-Cabrerizo, M., Cardoso, A., Minutti, C. M., Pereira da Costa, M. and Reis e Sousa, C., Dendritic Cells Revisited. *Annu. Rev. Immunol.* 2021. 39:131–166.
- Dalod, M. and S. Scheu. Dendritic cell functions in vivo: A user's guide to current and next-generation mutant mouse models. *Eur. J. Immunol.* 2022. 0:1–38.
- Kastenmüller, W., Gerner, M. Y. and Germain, R. N., The in situ dynamics of dendritic cell interactions. *Eur. J. Immunol.* 2010. 40: 2103–2106.
- Uderhardt, S., Martins, A. J., Tsang, J. S., Lämmermann, T. and Germain, R. N., Resident Macrophages Cloak Tissue Microlesions to Prevent Neutrophil-Driven Inflammatory Damage. *Cell.* 2019. 177: 541–555. e17.
- Mempel, T. R., Henrickson, S. E. and Von Andrian, U. H., T-cell priming by dendritic cells in lymph nodes occurs in three distinct phases. *Nature.* 2004. 427: 154–159.
- Seder, R. A., Paul, W. E., Davis, M. M. and Fazekas de St Groth, B., The presence of interleukin 4 during in vitro priming determines the lymphokine-producing potential of CD4+ T cells from T cell receptor transgenic mice. *J. Exp. Med.* 1992, 176: 1091–1098.
- Barnden, M. J., Allison, J., Heath, W. R. and Carbone, F. R., Defective TCR expression in transgenic mice constructed using cDNA-based alpha- and beta-chain genes under the control of heterologous regulatory elements. *Immunol. Cell Biol.* 1998. 76: 34–40.
- Pircher, H., Moskophidis, D., Rohrer, U., Bürki, K., Hengartner, H. and Zinkernagel, R. M., Viral escape by selection of cytotoxic T cell-resistant virus variants in vivo. *Nature.* 1990. 346: 629–633.
- Victoria, G. D., Schwickert, T. A., Fooksman, D. R., Kamphorst, A. O., Meyer-Hermann, M., Dustin, M. L. and Nussenzweig, M. C., Germinal center dynamics revealed by multiphoton microscopy with a photoactivatable fluorescent reporter. *Cell.* 2010. 143: 592–605.
- Medaglia, C., Giladi, A., Stoler-Barak, L., De Giovanni, M., Salame, T. M., Biram, A., David, E. et al., Spatial reconstruction of immune niches by combining photoactivatable reporters and scRNA-seq. *Science.* 2017. 358: 1622–1626.
- van Panhuys, N., Klauschen, F. and Germain, R. N., T-cell-receptor-dependent signal intensity dominantly controls CD4(+) T cell polarization In Vivo. *Immunity.* 2014. 41: 63–74.
- Muccioli, M., Pate, M., Omosebi, O. and Benencia, F., Generation and labeling of murine bone marrow-derived dendritic cells with Qdot nanocrystals for tracking studies. *J. Vis. Exp.* 2011. 52: 2785.
- Lindquist, R. L., Shakhar, G., Dudziak, D., Wardemann, H., Eisenreich, T., Dustin, M. L. and Nussenzweig, M. C., Visualizing dendritic cell networks in vivo. *Nat. Immunol.* 2004. 5: 1243–1250.
- Satpathy, A. T., Wumesh, K. C., Albring, J. C., Edelson, B. T., Kretzer, N. M., Bhattacharya, D., Murphy, T. L. et al., Zbtb46 expression distinguishes classical dendritic cells and their committed progenitors from other immune lineages. *J. Exp. Med.* 2012. 209: 1135–1152.
- Lechmann, M., Shuman, N., Wakeham, A. and Mak, T. W., The CD83 reporter mouse elucidates the activity of the CD83 promoter in B, T, and dendritic cell populations in vivo. *Proc. Natl. Acad. Sci. U. S. A.* 2008. 105: 11887–11892.
- Stranges, P. B., Watson, J., Cooper, C. J., Choisy-Rossi, C.-M., Stonebraker, A. C., Beighton, R. A., Hartig, H. et al., Elimination of antigen-presenting cells and autoreactive T cells by Fas contributes to prevention of autoimmunity. *Immunity.* 2007. 26: 629–641.
- Loschko, J., Schreiber, H. A., Rieke, G. J., Esterházy, D., Meredith, M. M., Pedicord, V. A., Yao, K.-H. et al., Absence of MHC class II on cDCs results in microbial-dependent intestinal inflammation. *J. Exp. Med.* 2016. 213: 517–534.
- Schraml, B. U., van Blijswijk, J., Zelenay, S., Whitney, P. G., Filby, A., Acton, S. E., Rogers, N. C. et al., Genetic tracing via DNGR-1 expression history defines dendritic cells as a hematopoietic lineage. *Cell.* 2013. 154: 843–858.
- Ferris, S. T., Durai, V., Wu, R., Theisen, D. J., Ward, J. P., Bern, M. D., Davidson, J. T. et al., cDC1 prime and are licensed by CD4+ T cells to induce anti-tumour immunity. *Nature.* 2020. 584: 624–629.
- Mattiuz, R., Wohn, C., Ghilas, S., Ambrosini, M., Alexandre, Y. O., Sanchez, C., Fries, A. et al., Novel Cre-Expressing Mouse Strains Permitting to Selectively Track and Edit Type 1 Conventional Dendritic Cells Facilitate Disentangling Their Complexity in vivo. *Front. Immunol.* 2018. 9: 2805.
- Zahner, S. P., Kel, J. M., Martina, C. A. E., Brouwers-Haspels, I., van Roon, M. A. and Clausen, B. E., Conditional deletion of TGF- $\beta$ R1 using Langerin-Cre mice results in Langerhans cell deficiency and reduced contact hypersensitivity. *J. Immunol.* 2011. 187: 5069–5076.
- Murooka, T. T. and Mempel, T. R., Multiphoton Intravital Microscopy to Study Lymphocyte Motility in Lymph Nodes. *Integrin and Cell Adhesion Molecules: Methods and Protocols.* 2012. 757: 247–257.
- Crainiciuc, G., Palomino-Segura, M., Molina-Moreno, M., Sicilia, J., Aragones, D. G., Li, J. L. Y., Madurga, R. et al., Behavioural immune landscapes of inflammation. *Nature.* 2022. 601: 415–421.
- Faust, N., Varas, F., Kelly, L. M., Heck, S. and Graf, T., Insertion of enhanced green fluorescent protein into the lysozyme gene creates mice with green fluorescent granulocytes and macrophages. *Am. J. Blood Res.* 2000. 96: 719–726.
- Bousso, P., T-cell activation by dendritic cells in the lymph node: lessons from the movies. *Nat Rev Immunol.* 2008. 8: 675–684.
- Textor, J., Peixoto, A., Henrickson, S. E., Sinn, M., von Andrian, U. H. and Westermann, J., Defining the quantitative limits of intravital two-photon lymphocyte tracking. *Proc. Natl. Acad. Sci. U. S. A.* 2011. 108: 12401–12406.
- Miller, M. J., Safrina, O., Parker, I. and Cahalan, M. D., Imaging the single cell dynamics of CD4+ T cell activation by dendritic cells in lymph nodes. *J. Exp. Med.* 2004. 200: 847–856.

- 30 Mempel, T. R., Pittet, M. J., Khazaie, K., Weninger, W., Weissleder, R., von Boehmer, H. and von Andrian, U. H., Regulatory T cells reversibly suppress cytotoxic T cell function independent of effector differentiation. *Immunity*. 2006. 25: 129–141.
- 31 Liu, Z., Gu, Y., Chakarov, S., Bleriot, C., Kwok, I., Chen, X., Shin, A. et al., Fate mapping via Ms4a3-expression history traces monocyte-derived cells. *Cell* 2019. 178: 1509–1525. e1519.
- 32 Schlitzer, A., Sivakamasundari, V., Chen, J., Sumatoh, H. R., Schreuder, J., Lum, J., Malleret, B. et al., Identification of cDC1- and cDC2-committed DC progenitors reveals early lineage priming at the common DC progenitor stage in the bone marrow. *Nat. Immunol.* 2015. 16: 718–728.
- 33 Becher, B., Schlitzer, A., Chen, J., Mair, F., Sumatoh, H. R., Teng, K. W., Low, D., Ruedl, C. et al., High-dimensional analysis of the murine myeloid cell system. *Nat. Immunol.* 2014. 15: 1181–1189.
- 34 Schlitzer, A., McGovern, N., Teo, P., Zelante, T., Atarashi, K., Low, D., Ho, A. W. et al., IRF4 transcription factor-dependent CD11b<sup>+</sup> dendritic cells in human and mouse control mucosal IL-17 cytokine responses. *Immunity*. 2013. 38: 970–83.
- 35 Goltsev, Y., Samusik, N., Kennedy-Darling, J., Bhate, S., Hale, M., Vazquez, G., Black, S. and Nolan, G. P., Deep Profiling of Mouse Splenic Architecture with CODEX Multiplexed Imaging. *Cell*. 2018. 174: 968–981. e15.
- 36 Schürch, C. M., Bhate, S. S., Barlow, G. L., Phillips, D. J., Noti, L., Zlobec, I., Chu, P. et al., Coordinated Cellular Neighborhoods Orchestrate Antitumoral Immunity at the Colorectal Cancer Invasive Front. *Cell*. 2020. 182: 1341–1359. e19.
- 37 Stoltzfus, C. R., Filipek, J., Gern, B. H., Olin, B. E., Leal, J. M., Wu, Y., Lyons-Cohen, M. R. et al., CytoMAP: A Spatial Analysis Toolbox Reveals Features of Myeloid Cell Organization in Lymphoid Tissues. *Cell Rep.* 2020. 31: 107523.
- 38 Schindelin, J., Arganda-Carreras, I., Frise, E., Kaynig, V., Longair, M., Pietzsch, T., Preibisch, S. et al., Fiji: an open-source platform for biological-image analysis. *Nat. Methods* 2012. 9: 676–682.
- 39 Du, Z., Lin, J. R., Rashid, R., Maliga, Z., Wang, S., Aster, J. C., Izar, B. et al., Qualifying antibodies for image-based immune profiling and multiplexed tissue imaging. *Nat. Protoc.* 2019. 14: 2900–2930.
- 40 Krzywinski, M., Schein, J., Birol, I., Connors, J., Gascoyne, R., Horsman, D., Jones, S. J. et al., Circos: An information aesthetic for comparative genomics. *Genome. Res.* 2009. 19: 1639–1645.
- 41 Fridman, W. H., Zitvogel, L., Sautès-Fridman, C., Kroemer, G., The immune contexture in cancer prognosis and treatment. *Nat. Rev. Clin. Oncol.* 2017. 14: 717–734.
- 42 Binnewies, M., Roberts, E. W., Kersten, K., Chan, V., Fearon, D. F., Merad, M., Coussens, L. M., et al., Understanding the tumor immune microenvironment (TIME) for effective therapy. *Nat. Med.* 2018. 24: 541–550.
- 43 Bruni, D., Angell, H. K., Galon, J., The immune contexture and Immunoscore in cancer prognosis and therapeutic efficacy. *Nat. Rev. Cancer* 2020. 20: 662–680.
- 44 Massi, D., Rulli, E., Cossa, M., Valeri, B., Rodolfo, M., Merelli, B., De Logu, F. et al., The density and spatial tissue distribution of CD8<sup>+</sup> and CD163<sup>+</sup> immune cells predict response and outcome in melanoma patients receiving MAPK inhibitors. *J. Immunother. Cancer*. 2019. 7: 308.
- 45 Parra, E. R., Zhai, J., Tamegnon, A., Zhou, N., Pandurengan, R. K., Barreto, C., Jiang, M. et al., Identification of distinct immune landscapes using an automated nine-color multiplex immunofluorescence staining panel and image analysis in paraffin tumor tissues. *Sci. Rep.* 2021. 11: 4530.
- 46 Hofman, P., Badoual, C., Henderson, F., Berland, L., Hamila, M., Long-Mira, E., Lassalle, S. et al., Multiplexed Immunohistochemistry for Molecular and Immune Profiling in Lung Cancer—Just About Ready for Prime-Time? *Cancers*. 2019. 11: 283.
- 47 Huang, Y. K., Wang, M., Sun, Y., Di Costanzo, N., Mitchell, C., Achuthan, A., Hamilton, J. A. et al., Macrophage spatial heterogeneity in gastric cancer defined by multiplex immunohistochemistry. *Nat. Commun.* 2019. 10: 3928.
- 48 Berry, S., Giraldo, N. A., Green, B. F., Cottrell, T. R., Stein, J. E., Engle, E. L., Xu, H. et al., Analysis of multispectral imaging with the AstroPath platform informs efficacy of PD-1 blockade. *Science*. 2021. 372: eaba2609.
- 49 Edwards, J., Wilmott, J. S., Madore, J., Gide, T. N., Quek, C., Tasker, A., Ferguson, A. et al., CD103<sup>+</sup> Tumor-Resident CD8<sup>+</sup> T Cells Are Associated with Improved Survival in Immunotherapy-Naïve Melanoma Patients and Expand Significantly During Anti-PD-1 Treatment. *Clin. Cancer Res.* 2018. 24: 3036–3045.
- 50 Allam, M., Cai, S. and Coskun, A. F., Multiplex bioimaging of single-cell spatial profiles for precision cancer diagnostics and therapeutics. *npj Precis. Onc.* 2020. 4: 1–14.
- 51 Kießler, M., Plesca, I., Sommer, U., Wehner, R., Wilczkowski, F., Müller, L., Tunger, A. et al., Tumor-infiltrating plasmacytoid dendritic cells are associated with survival in human colon cancer. *J. Immunother. Cancer* 2021. 9: e001813.
- 52 Böttcher, J. P. and Reis e Sousa, C., The Role of Type 1 Conventional Dendritic Cells in Cancer Immunity. *Trends Cancer* 2018. 4: 784–792.
- 53 Wculek, S. K., Cueto, F. J., Mujal, A. M., Melero, I., Krummel, M. F. and Sancho, D., Dendritic cells in cancer immunology and immunotherapy. *Nat. Rev. Immunol.* 2020. 20: 7–24.
- 54 Broz, M. L., Binnewies, M., Boldajipour, B., Nelson, A. E., Pollack, J. L., Erle, D. J., Barczak, A. et al., Dissecting the tumor myeloid compartment reveals rare activating antigen-presenting cells critical for T cell immunity. *Cancer Cell* 2014. 26: 638–652.
- 55 Böttcher, J. P., Bonavita, E., Chakravarty, P., Blees, H., Cabeza-Cabrero, M., Sammiceli, S., Rogers, N. C. et al., NK Cells Stimulate Recruitment of cDC1 into the Tumor Microenvironment Promoting Cancer Immune Control. *Cell*. 2018. 172: 1022–1037. e14.
- 56 Barry, K. C., Hsu, J., Broz, M. L., Cueto, F. J., Binnewies, M., Combes, A. J., Nelson, A. E. et al., A natural killer-dendritic cell axis defines checkpoint therapy-responsive tumor microenvironments. *Nat. Med.* 2018. 24: 1178–1191.
- 57 Michea, P., Noël, F., Zakine, E., Czerwinski, U., Sirven, P., Abouzid, O., Goudot, C. et al., Adjustment of dendritic cells to the breast-cancer microenvironment is subset specific. *Nat. Immunol.* 2018. 19: 885–897.
- 58 Spranger, S., Dai, D., Horton, B. and Gajewski, T. F., Tumor-Residing Batf3 Dendritic Cells Are Required for Effector T Cell Trafficking and Adoptive T Cell Therapy. *Cancer Cell* 2017. 31: 711–723. e4.
- 59 Chow, M. T., Ozga, A. J., Servis, R. L., Frederick, D. T., Lo, J. A., Fisher, D. E., Freeman, G. J. et al., Intratumoral Activity of the CXCR3 Chemokine System Is Required for the Efficacy of Anti-PD-1 Therapy. *Immunity*. 2019. 50: 1498–1512. e5.
- 60 Hubert, M., Gobbini, E., Couillault, C., Manh, T.-P. V., Doffin, A.-C., Berthet, J., Rodriguez, C. et al., IFN-III is selectively produced by cDC1 and predicts good clinical outcome in breast cancer. *Sci. Immunol.* 2020. 5: eaav3942.
- 61 Zilionis, R., Engblom, C., Pfirschke, C., Savova, V., Zemmour, D., Saatioglu, H. D., Krishnan, I. et al., Single-Cell Transcriptomics of Human and Mouse Lung Cancers Reveals Conserved Myeloid Populations across Individuals and Species. *Immunity*. 2019. 50: 1317–1334. e10.
- 62 Srinivas, S., Watanabe, T., Lin, C. S., William, C. M., Tanabe, Y., Jessell, T. M., Costantini, F., Cre reporter strains produced by targeted insertion of EYFP and ECFP into the ROSA26 locus. *BMC Dev. Biol.* 2001. 1: 4.
- 63 Yamazaki, C., Sugiyama, M., Ohta, T., Hemmi, H., Hamada, E., Sasaki, I., Fukuda, Y. et al., Critical roles of a dendritic cell subset expressing a chemokine receptor, XCR1. *J. Immunol.* 2013. 190: 6071–6082.



- 64 Kitano, M., Yamazaki, C., Takumi, A., Ikeno, T., Hemmi, H., Takahashi, N., Shimizu, K. et al., Imaging of the cross-presenting dendritic cell subsets in the skin-draining lymph node. *Proc. Natl. Acad. Sci. USA*. 2016. **113**: 1044–1049.
- 65 Schönheit, J., Kuhl, C., Gebhardt, M. L., Klett, F. F., Riemke, P., Scheller, M., Huang, G. et al., PU.1 level-directed chromatin structure remodeling at the *Irf8* gene drives dendritic cell commitment. *Cell Rep.* 2013. **3**: 1617–1628.
- 66 Reinhardt, R. L., Hong, S., Kang, S.-J., Wang, Z.-E., Locksley, R. M., Visualization of IL-12/23p40 in vivo reveals immunostimulatory dendritic cell migrants that promote Th1 differentiation. *J. Immunol.* 2006. **177**: 1618–1627.
- 67 Groom, J. R., Richmond, J., Murooka, T. T., Sorensen, E. W., Sung, J. H., Bankert, K., von Andrian, U. H. et al., CXCR3 chemokine receptor-ligand interactions in the lymph node optimize CD4<sup>+</sup> T helper 1 cell differentiation. *Immunity*. 2012. **37**: 1091–1103.
- 68 Nakano, H., Burgents, J. E., Nakano, K., Whitehead, G. S., Cheong, C., Bortner, C. D. and Cook, D. N., Migratory properties of pulmonary dendritic cells are determined by their developmental lineage. *Mucosal. Immunol.* 2013; **6**:678–691.
- 69 Gerner, M. Y., Kastenmüller, W., Ifrim, I., Kabat, J. and Germain, R. N., Histo-cytometry: a method for highly multiplex quantitative tissue imaging analysis applied to dendritic cell subset microanatomy in lymph nodes. *Immunity*. 2012. **37**: 364–376.
- 70 Li, W., Germain, R. N., Gerner, M. Y., Multiplex, quantitative cellular analysis in large tissue volumes with clearing-enhanced 3D microscopy (Ce3D). *Proc. Natl. Acad. Sci. USA*. 2017. **114**: E7321–E7330.
- 71 Li, W., Germain, R. N. and Gerner, M. Y., High-dimensional cell-level analysis of tissues with Ce3D multiplex volume imaging. *Nat. Protoc.* 2019. **165**: 1–29.
- 72 Laoui, D., Keirsse, J., Morias, Y., Van Overmeire, E., Geeraerts, X., Elkrim, Y., Kiss, M. et al., The tumour microenvironment harbours ontogenically distinct dendritic cell populations with opposing effects on tumour immunity. *Nat. Commun.* 2016. **7**: 13720.
- 73 Lavin, Y., Kobayashi, S., Leader, A., Amir, E. D., Elefant, N., Bigenwald, C., Remark, R. et al., Innate Immune Landscape in Early Lung Adenocarcinoma by Paired Single-Cell Analyses. *Cell*. 2017. **169**: 750–765. e17.
- 74 Posch, W., Vosper, J., Noureen, A., Zaderer, V., Witting, C., Bertacchi, G., Gstir, R. et al., CSaR inhibition of nonimmune cells suppresses inflammation and maintains epithelial integrity in SARS-CoV-2-infected primary human airway epithelia. *J. Allergy Clin. Immunol.* 2021. **147**: 2083–2097. e6.
- 75 Posch, W., Lass-Flörl, C. and Wilflingseder, D., SARS-CoV-2-infected primary human airway epithelia illustrate mucus hypersecretion. *J. Allergy Clin. Immunol.* 2021. **148**: 909.
- 76 Posch, W., Vosper, J., Zaderer, V., Noureen, A., Constant, S., Bellmann-Weiler, R., Lass-Flörl, C. et al., ColdZyme Maintains Integrity in SARS-CoV-2-Infected Airway Epithelia. *mBio* 2021. **12**: e00904-21.
- 77 Lafon, E., Diem, G., Witting, C., Zaderer, V., Bellmann-Weiler, R. M., Reindl, M., Bauer, A. et al., Potent SARS-CoV-2-Specific T Cell Immunity and Low Anaphylatoxin Levels Correlate With Mild Disease Progression in COVID-19 Patients. *Front. Immunol.* 2021. **12**: 684014.
- 78 Chen, Y. W., Huang, S. X., de Carvalho, A. L. R. T., Ho, S. H., Islam, M. N., Volpi, S., Notarangelo, L. D. et al., A three-dimensional model of human lung development and disease from pluripotent stem cells. *Nat. Cell. Biol.* 2017. **19**: 542–549.
- 79 Bucchieri, F., Pitruzzella, A., Fucarino, A., Gammazza, A. M., Bavisotto, C. C., Marcianò, V., Cajozzo, M. et al., Functional characterization of a novel 3D model of the epithelial-mesenchymal trophic unit. *Exp. Lung. Res.* 2017. **43**: 82–92.
- 80 Tomašek, I., Horwell, C. J., Damby, D. E., Barošová, H., Geers, C., Petri-Fink, A., Rothen-Rutishauser, B. et al., Combined exposure of diesel exhaust particles and respirable Soufrière Hills volcanic ash causes a (pro-)inflammatory response in an in vitro multicellular epithelial tissue barrier model. *Part. Fibre Toxicol.* 2016. **13**: 67.
- 81 Osswald, A., Hedrich, V. and Sommergruber, W., 3D-3 Tumor Models in Drug Discovery for Analysis of Immune Cell Infiltration. *Methods Mol. Biol.* 2019. **1953**: 151–162.
- 82 Zaderer, V., Hermann, M., Lass-Flörl, C., Posch, W. and Wilflingseder, D., Turning the World Upside-Down in Cellulose for Improved Culturing and Imaging of Respiratory Challenges within a Human 3D Model. *Mol. Cells* 2019. **8**: 1292.
- 83 Chandorkar, P., Posch, W., Zaderer, V., Blatzer, M., Steger, M., Ammann, C. G., Binder, U. et al., Fast-track development of an in vitro 3D lung/immune cell model to study *Aspergillus* infections. *Sci. Rep.* 2017. **7**: 11644.
- 84 Luvanda, M. K., Posch, W., Noureen, A., Lafon, E., Zaderer, V., Lass-Flörl, C. and Wilflingseder, D., Dexamethasone Creates a Suppressive Microenvironment and Promotes *Aspergillus fumigatus* Invasion in a Human 3D Epithelial/Immune Respiratory Model. *J. Fungi*. 2021. **7**: 221.
- 85 Schönfeld, M., Knackmuss, U., Chandorkar, P., Hörtnagl, P., Hope, T. J., Moris, A., Bellmann-Weiler, R. et al., Co- but not Sequential Infection of DCs Boosts Their HIV-Specific CTL-Stimulatory Capacity. *Front. Immunol.* 2019. **10**: 1123.

**Abbreviations:** AF: Alexa Fluor · AF: autofluorescence · ALI: air-liquid interface · APC: antigen-presenting cells · BSA: Bovine Serum Albumin · CODEX: Co-Detection by Indexing · CSFE: Carboxyfluorescein succinimidyl ester · CTB: Cell Tracker Blue · DC: dendritic cells · DFG: Deutsche Forschungsgemeinschaft · FFPE: formalin-fixed paraffin-embedded · HBSS: Hank's buffered saline · HCS: high-content analysis system · HRP: horseradish peroxidase · IF: immunofluorescence · LC: Langerhans cells · mIHC: multiplex immunohistochemistry · MoDC: Monocyte-derived DC · MP: mononuclear phagocytes · MSIs: multispectral images · NDDs: Non-descanned detectors · NHBE: normal human bronchial epithelium · pDC: Plasmacytoid DC · RMS: ready-made-solutions · RT: room temperature · SAE: small-airway epithelium · TEER: trans-epithelial electrical resistance · TME: Tumor microenvironment · TBS: Tris-buffered saline · TSA: tyramide-signal amplification

**Full correspondence:** Jan P. Böttcher, Institute of Molecular Immunology, School of Medicine, Klinikum Rechts der Isar, Technical University of Munich (TUM), Ismaninger Str. 22, Munich, 81675 Germany. Email: j.boettcher@tum.de

Received: 24/3/2022

Revised: 7/11/2022

Accepted: 14/11/2022

Accepted article online: 18/11/2022